

Numerical analysis and comparison of distorted fingerprints from the same source

Bruce Comber

**This thesis is submitted pursuant to a Master of
Information Science (Research) at the University of
Canberra**

February 2012

Abstract

There has been significant recent criticism of conclusions of identity based on the subjective methods of visual comparison of fingermarks and fingerprints. This has led to much discussion and research directed at devising purely objective methods of fingerprint identification.

The aim of this research project is to develop a metric that will provide an objective test of the conclusion reached by a fingerprint examiner. The metric assumes that the examiner has carried out the usual visual comparison of a fingermark (left at a crime scene, and which will usually be distorted) and a fingerprint (in an official file) and has concluded that the two impressions were made by the same finger. The data used by the examiner, namely the selected minutiae (particular distinguishing features of the fingermark) are fed into the metric, which then estimates the deviation from what would be expected if, the fingermark and the official fingerprint were made by the same finger.

The model uses “within-source” distributions (each generated by systematically measuring distortions of impressions from the same finger) and “between-source” distributions (based on images not from the same finger). The outcome of a test depends on the location of the calculated output in relation to these distributions.

Preliminary results distinguish clearly between within-source and between-source comparison responses, thus enabling an objective test of an examiner’s conclusion of identity. Such a test can be used to support the examiner’s conclusion or, alternatively, indicate to the examiner that variations in the observed minutiae positions cannot be explained by normal

skin distortion. This could arise if poor minutiae marking has been applied by the examiner or if the fingermarks are actually not from the same source. The proposed approach therefore serves as an objective quality control mechanism.

Acknowledgements

My family have endured my endless dedication, ensuing frustration and resultant non-communicative self, due to this research. They have accepted this whilst not gaining any benefit from it. Their tolerance was not well stated to me but is appreciated. Without their support, this would not be possible. Thanks to Geoff Comber (Dad) for welcome suggestions and further proof reading. I trust this “modelling assignment” is better than my last!

Professor Michael Wagner of the University of Canberra (Faculty of Information, Science & Engineering) as the primary supervisor provided much needed direction as to the application of multivariate normal distributions, feedback generally on concepts and progress on the research.

Professor Chris Lennard of the University of Canberra (Faculty of Applied Science) as the second supervisor was invaluable in providing feedback in relation to the scientific validity of the approach and comprehensive feedback on the thesis layout and his ability to translate my words and ideas concisely and clearly stated sentences.

Professor Christophe Champod of the University of Lausanne provided valued comments on the proposal and between-source data collection.

Elizabeth Brooks of the Australian Federal Police (Biological Criminalistics) was always available for proof reading pages of complete rubbish, speaking the blunt truth, support and encouragement to see the research completed.

Carolyn McLaren (PhD Student, University of Canberra, Faculty of Applied Science)

provided excellent feedback on the method of data analysis.

The Australian Federal Police allowed me time to attend the university to complete requisite coursework and spend an allocation of time to complete the research over a four-year period.

Contents

Acknowledgements	vii
Table of Figures	xiii
List of Tables	xvii
1. Introduction	1
1.1 A brief history of the fingerprint identification science.....	1
1.2 Friction ridge skin growth and development	3
1.3 Deposition of latent fingermarks	7
1.4 Development of the fingerprint identification methodology	9
1.5 Present situation	13
2. Challenges and responses	15
2.1 Introduction.....	15
2.2 Knowledge gap	17
2.3 Research contributions.....	18
2.4 This project	24
2.5 Research objectives.....	26
2.6 Hypothesis.....	26
3. Materials and methodology	29
3.1 Introduction.....	29
3.2 Equipment	30
3.3 Software	31
3.4 Choice of finger movements for within-source data collection.....	34
3.5 Application and chosen range of force	36
3.5.1 Finger, surface and movement relationships	36
3.5.2 Rationale for the choice of range of applied finger force in sample collection.....	38
3.6 Acquisition and processing of images; within-source images	43
3.6.1 Recording of images.....	44
3.6.2 Correction of foreshortening	46
3.6.3 Correction of non-linear systemic distortion	47
3.6.4 Image processing summary	50
3.7 Acquisition and processing of images– between-source images	51
3.8 Comparison of images and generation of data.....	53
3.8.1 Method for marking of minutiae	54
3.8.2 Collection of within-source data.....	60
3.8.3 Collection of between-source data.....	61
3.8.4 Order of minutiae examined.....	63
3.8.5 Selection of minutiae for measurement.....	64
3.8.6 Measurements from selected minutiae	67
3.9 Errors generated by using digital images for measurement.....	70
3.9.1 Potential error for distance measurements	72
3.9.2 Potential error for angle measurement.....	74
3.9.3 Error summary	77

3.7 Data extraction	79
3.7.1 Within-source data	79
3.7.2 Between-source data	81
3.7.3 Test case data	82
4. Data analysis and results.....	85
4.1 Introduction.....	85
4.2 Use of normal distributions.....	87
4.2 Use of multivariate normal distributions	88
4.2.1 Use of mean vectors and covariance matrices for calculating multivariate probability densities	89
4.3 The need for a generic mean vector and covariance matrix	91
4.4 Approach taken for data collection	93
4.5 Within-source data	93
4.5.1 Compliance with the requirements for the use of normal distribution density functions..	94
4.5.2 Compliance with the requirements for the use of multivariate normal distributions	100
4.6 Generation of the generic mean vector and covariance matrix.....	102
4.7 The effect of multiple variables on the resultant probability density	106
4.8 Establishing regression functions for within- and between-source test response probability densities	108
Number of minutiae	112
Probability density of within-source	112
4.8.1 Between-source probability densities for all minutiae.....	115
4.8.2 Within-source probability densities for varied numbers of minutiae	118
4.9 Model testing against within- and between-source cases	121
4.9.1 Between-source comparisons.....	122
4.9.2 Within-source subject comparisons	122
4.9.3 Within-source case comparisons	122
4.9.4 Results of comparisons	123
4.10 Testing model sensitivity	124
4.10.1 Test 1: Movement of one minutia by 10 pixels	125
4.10.2 Test 2: Movement of all minutiae by varied amounts.....	126
4.10.3 Test 3: Variation as a result of repeated manual plotting	127
4.10.4 Test 4: Swapping minutiae placement order.....	129
5. Discussion & conclusion	133
5.1 Limitations	133
5.1.1 Training data obtained on a flat surface.....	133
5.1.2 Measurements in the digital environment	134
5.1.3 Minimal variables used	136
5.1.4 Manual marking of minutiae positions.....	136
5.1.5 Variation in ridge structure	138

5.1.6 Cases with few features	140
5.1.7 Use of close friction ridge detail	140
5.2 Assumptions.....	142
5.2.1 Skin stretch.....	142
5.2.2 Proximal minutiae and amount of stretch variation.....	142
5.2.3 Variations in distortion	143
5.3 Discussion	143
5.3.1 Generic mean and covariance matrix elements	143
5.3.2 Straight impressions in training data collection	144
5.3.3 Interpretation of results.....	145
5.4 Conclusion	148
5.5 Further work.....	149
6. Bibliography	151
7. Appendices	155
7.1 INI file.....	155
7.2 V++ Scripts	155
7.2.1 Process images.....	155
7.2.2 Get NAFIS sub images	157
7.2.3 Create Distance Map.....	158
7.2.4 get 2 coords for 10 minutiae matlab output training data.....	160
7.2.5 get 2 coords for all minutiae matlab output training data2	164
7.2.6 get 2 coords for all minutiae matlab output training data2 test case	167
7.2.7 Draw numbers for flags.....	170
7.2.8 Acquire image of finger for pressure test	172
7.2.9 get finger contact area.....	174
7.2.10 move random direction fixed amount.....	175
7.2.11 move one flag.....	176
7.2.12 swap two flags.....	177
7.3 Matlab scripts.....	178
7.3.1 csv input from V++ 2 no abs_18 values	178
7.3.2 all minutiae data input from max minutiae file 18	179
7.4.0 Data	180
7.4.1 Sample marked image and coordinate data collected	180
7.4.2 Sample distance map and values.....	181
7.4.3 Sample data extracted from a reference image and related movement images.....	182
7.4.4 Sample of the difference data calculated from the reference and movement images	183
7.4.5 Sample of covariance values returned from Matlab	184

7.4.6 Sample of mean values returned from Matlab.....	185
7.4.7 Descriptive statistics on means and variances from finger data	186
7.4.8 Generic values for means and variances from finger data	186
7.4.9 Example of test within-source and another within-source image.....	187
7.4.10 Example of test within-source and other within-source data	188
7.4.11 Example of probabilities calculated for a within-source comparison for varied numbers of minutiae	189
7.4.12 Example of test within-source and between-source images.....	190
7.4.13 Example of test within-source and between-source data	190
7.4.14 Example of probabilities calculated for a between-source comparison for varied numbers of minutiae	191
7.5 DVD contents.....	192
7.5.1 Data collection	192
7.5.2 Miscellaneous	193
7.5.3 Scripts.....	194

Table of Figures

Figure 1	Cross section of friction ridged skin	5
Figure 2	Examples of fingerprint features	9
Figure 3	Regions a, b & c of a finger as defined by Cappelli et al.	20
Figure 4	Continuous features as used by Neumann et al (2006).	22
Figure 5	Features extracted by Neumann et al.	24
Figure 6	File copier application in Visual Basic.	32
Figure 7	Images of friction ridged skin contact at forces of 0.3kp and 1.2kp.	39
Figure 8	Measurement of pressure on skin with an increase of force applied	41
Figure 9	Measurement of pressure on skin with an increase of force applied.	42
Figure 10	Camera and prism arrangement	44
Figure 11	Schematic diagram of the friction ridged skin contacting the prism	45
Figure 12	Example of an acquired image of the friction ridge skin contact area	45
Figure 13	Schematic diagram showing the cause of foreshortening in an acquired image	46
Figure 14	Method of foreshortening correction	47
Figure 15	Image acquired of the 1mm-scale graph paper	48
Figure 16	Graph paper image and the target image	49
Figure 17	Graph paper image corrected for systemic non-linear distortion	49
Figure 18	Acquired and processed images	51
Figure 19	Screen capture of a NAFIS comparison	52
Figure 20	Extracted images of search image (left) and candidate image (right).	53
Figure 21	Sample images: reference (normal) and distorted	54
Figure 22	Two images of the same finger showing a difference in available minutiae.	55
Figure 23	Diagram showing the method for placing flags on ridge endings	56
Figure 24	Diagram showing the method for placing flags on bifurcations	57
Figure 25	Diagram showing the method for placing flags on dots	58
Figure 26	Diagram of showing a difference in the placement of a minutia.	59
Figure 27	Example of an AFIS nominated minutia and manual flagging.	60
Figure 28	A distance map for the left index finger and corresponding pixel values.	64
Figure 29	Figure 29 Marked minutiae for a left index fingerprint and coordinate data.	66
Figure 30	Section of image BC_LL_ref displayed in V++.	66
Figure 31	Schematic diagram of a minutia (M) and the two nearest minutiae (N1 and N2).	67
Figure 32	Plotting of the change in minutiae position; within-source.	68
Figure 33	Plotting of the change in minutiae position; between-source.	69

Figure 34	Marking a point inside a pixel's area.	71
Figure 35	Measurement of distance between two minutiae (M1 and M2).	72
Figure 36	Potential maximum error described as a percentage of the distances measured.	73
Figure 37	Limitations of angle measurement in the Cartesian plane.	74
Figure 38	The relationship between distance in pixels and number of possible angles.	75
Figure 39	The amount of error in angle measurement using pixels as units.	76
Figure 40	The amount of error due to angle measurement using three pixel locations.	77
Figure 41	The distribution of means of Distance 1 and Distance 2 values.	78
Figure 42	A bifurcation as marked by different fingerprint examiners (Neumann C. , 2007).	79
Figure 43	The extracted data for within-source variation.	81
Figure 44	The process to develop the model in this project.	86
Figure 45	Normal distribution density curve.	87
Figure 46	The test case vector, mean vector and covariance matrix for one minutia.	90
Figure 47	The test case vector, mean vector and covariance matrix for n minutiae.	90
Figure 48	Distribution of D1diff for all finger movements and reference images.	98
Figure 49	Distribution of D2 diff for all finger movements and reference images.	98
Figure 50	Distribution of Adiff for all finger movements and reference images.	99
Figure 51	Scatter plot showing the relationship between variables D1diff and D2diff.	100
Figure 52	Scatter plot showing the relationship between variables Adiff and D1diff.	101
Figure 53	Scatter plot showing the relationship between variables Adiff and D2diff.	101
Figure 54	Probability density of multiple events of the same occurrence.	107
Figure 55	Probability density of multiple events where an occurrence is varied	108
Figure 56	Comparison of a left index finger and the correctly nominated candidate.	109
Figure 57	Comparison of a left index finger and an incorrectly nominated candidate.	111
Figure 58	The function describing the means of the log10 of the probability density that the compared between-source fingerprints are from the same source, for up to 27 minutiae.	115
Figure 59	The function describing the standard deviations of the log10 of the probability density that the compared between-source fingerprints are from the same source, for up to 27 minutiae.	116
Figure 60	The function describing the means of the log10 of the probability density that the compared between-source fingerprints are from the same source, for up to 13 minutiae.	117
Figure 61	The function describing the standard deviations of the log10 of the probability density that the compared between-source fingerprints are from the same source, for up to 13 minutiae.	117
Figure 62	Box plots of values contributing to the mean between-source probability density function.	118

Figure 63	The function describing the means of the log10 of the probability density that the compared within-source fingerprints are from the same source, for up to 55 minutiae.	119
Figure 64	The function describing the standard deviations of the log10 of the probability density that the compared within-source fingerprints are from the same source, for up to 55 minutiae.	119
Figure 65	The function describing the means of the log10 of the probability density that the compared within-source fingerprints are from the same source, for up to 30 minutiae.	120
Figure 66	The function describing the standard deviations of the log10 of the probability density that the compared within-source fingerprints are from the same source, for up to 30 minutiae.	120
Figure 67	Box plots of values contributing to the mean within-source probability density function.	121
Figure 68	Test cases, plotted against, the within- and between-source means.	123
Figure 69	The variation in calculated probability density of one minutia being moved 10 pixels.	125
Figure 70	The variation in calculated probability density of all minutia being moved 10 pixels.	127
Figure 71	The variation in calculated probability density due to manual marking.	128
Figure 72	Marked minutiae on an image.	129
Figure 73	The effect on the probability densities by the swapped minutiae.	131
Figure 74	Diagram showing effect on angle given a change in position and distance.	134
Figure 75	Function of the change of angle with a change in minutiae relative position.	135
Figure 76	Example of a marked unclear latent fingermark.	137
Figure 77	Example of a comparison of marked friction ridge features.	138
Figure 78	Example of a fingerprint with variations of friction ridge endings.	139
Figure 79	Sections of a latent palm mark (Figure 79a) and print (Figure 79b).	140
Figure 80	An image of a mark left by a thumb with subsidiary friction ridges.	141
Figure 81	Regression of within-source cases and the predicted within-source mean function.	144

List of Tables

Table 1	Summary of within-source images and movements inducing distortion.	94
Table 2	Summary of within-source comparisons and minutiae examined.	94
Table 3	Calculated correlations between variables D1diff, D2diff and Adiff.	95
Table 4	Descriptive statistics for D1diff, D2diff and Adiff.	96
Table 5	Calculated correlations between variables D1diff, D2diff and Adiff.	99
Table 6	The covariance matrix for the right index finger.	102
Table 7	The mean vector for the right index finger.	103
Table 8	Mean values for the elements in the covariance matrix and mean vector	103
Table 9	Average values for mu and sigma for all angle and distance differences	104
Table 10	The generic covariance matrix.	105
Table 11	Summary of within-source candidates and minutiae examined	110
Table 12	Summary of between-source candidates and minutiae examined	111
Table 13	Sample of the data produced using the generic mean and covariance matrix.	112
Table 14	Data from between-source comparisons.	114
Table 15	The range and variance of the calculated probability densities in test 1.	126
Table 16	The range and variance of the calculated probability densities in test 2.	127
Table 17	The range and variance of the calculated probability densities in test 3.	128
Table 18	Data generated from compared images with two minutiae in a reversed order.	130

1. Introduction

By visual inspection, fingerprint examiners compare a fingermark left at a crime scene with an officially recorded fingerprint in order to try to decide whether the two impressions were made by the same finger. Because the fingermark may be distorted or indistinct, the process requires great skill and considerable training and experience. Nevertheless it is in part subjective, and has often been severely criticized because of publicly announced mistakes (Stacey, 2005)(The Scottish Parliament).

This research aimed to use data extracted from fingermark features to define bounds for variance due to friction ridged skin distortion, however, it evolved to further explore a potential objective test allowing practitioners to arrive at a positive identification by subjecting it to a metric, thereby providing an objective analysis of the comparison which will give an indication that the examiner's conclusion is correct or not. The metric gives an indication of deviation from an expected result. That is, how far from does the examiners result fall from where a correct identification would lie?

Whist a statistical approach is taken to implement the test, the probability densities calculated are used simply as an indication of the level of support that can be given to the examiners conclusion. There is no intention to calculate actual probabilities or likelihood ratios.

1.1 A brief history of the fingerprint identification science

Fingerprint identification as a methodology has been established over the last hundred years. The identification examines marks made by the anatomical structures of the skin of the palmar and plantar surfaces (hands and feet) known as friction ridged skin.

The fingermark left by a person has historically had significant meaning and was considered as being the “person’s mark”, as if it were a signature. This is apparent in Chinese documents from 220 to 420AD and later used in Indian contracts in the 1850’s (Ashbaugh, 1991). The mark left by a finger contacting a smooth surface is representative of the surface of the skin on the underside of the finger. The skin surface was described by Grew (1684) in terms of the intricate patterns on the surface of the skin. It was later described by Mayer (Ashbaugh, 1991) as having ridges of equal breadth and in patterns displaying similarity between persons whilst each instance was uniquely different. These observations are significant as they are the roots of two underlying principles supporting fingerprint identification. These principles detail classification of friction ridge patterns and the uniqueness of the ridge arrangement.

Purkinje, a professor at the University of Breslau, established nine different patterns of the friction ridges (Berry & Stoney, 2001), these definitions forming the basis for the classification systems that are still in use today with customised extensions.

Sir William Herschel, an English administrator in India, saw the significance of the personal mark and saw their potential in preventing impersonation (Ashbaugh, 1991). Sir Henry Faulds, a Scottish surgeon in Japan, suggested the use of fingerprints for identification in an article published in *Nature* (Tredoux, 2003). Faulds also suggested that the friction ridged skin arrangement was permanent, although at the time this premise was questioned by Herschel.

The fundamental principles of fingerprint identification are essentially as follows (Ashbaugh, 1994):

1. friction ridge patterns that develop before birth do not change during life and even after death until decomposition destroys ridged skin;
2. friction ridge patterns differ from individual to individual;
3. overall friction ridge pattern appearances have similarities that can be systematically classified, even though patterns are distinct in ridge characteristics.

Fingerprint identification was eventually used in the identification of persons associated with criminal activity. In 1892, the Rojas murder case in Argentina was solved by the identification of a fingermark in blood (Berry & Stoney, 2001).

Sir Edward Henry, with assistance from Haque and Bose, developed the Henry fingerprint classification system which was implemented in prisons in India (Berry & Stoney, 2001), and later (Scotland Yard, London) in 1901. This saw the introduction of fingerprints as a forensic science discipline to the world. The Henry system is still in use today.

1.2 Friction ridge skin growth and development

The skin on the underside of the hands and feet is different to the skin on the remainder of the body in that it is covered by corrugated skin known as “friction ridge skin”. The skin is comprised of two layers, the dermis (inner) and epidermis (outer), the epidermis being divided into five further layers. This skin is hairless and, of the variety of glands associated with skin, has only eccrine glands.

The friction ridges develop during the growth of the hands and feet and are complete before birth. The following discussion summarises information provided by Babler (1991).

About 5 to 6 weeks after fertilisation, the hands appear like plates. By 8.5 weeks, the fingers have formed and the joints of the hands are appearing. The development of epidermal ridges (friction ridges) is preceded by the development of the volar pads on the hands.

These pads occur on the finger tips, and the thena, hypothena and interdigital regions of the palm. The importance of the volar pads is that their structure probably affects the configuration of the ridges. The volar pads first appear around the 6th week and grow rapidly until the 10th week. The pads have different shapes depending on whether they are on the palm or the finger. After 10.5 weeks, the pads begin to regress as the hand grows. This regression occurs with the development and differentiation of the friction ridges. At this time, the creases of the hand begin to develop. It's speculated that the movement of the hand or the volar pads influence the resulting creases. The skin is tethered to the underlying structures in the location of the major creases and does not correspond to the underlying bony structures but anchors the skin during grasping (Flatt, 2000).

Before friction ridges begin to develop, the epidermis starts thin and smooth on the surface and at the junction to the dermis. At about 10 weeks, ridges first appear as cell proliferations in the basal layer, forming shallow primary ridges that project into the dermis. As the hand grows, further primary ridges develop between existing ridges. This proliferation produces the branching and islands, and determines the final configuration of the friction ridges. With growth, the primary ridges grow in breadth and penetrate further into the dermis.

At about 14 weeks, the sweat glands begin to develop along the ridges and penetrate into the dermis. By 15 weeks, the stratum corneum (outer layer of the epidermis) appears and the secondary ridges begin to develop. The secondary ridges at the epidermis / dermis junction appear, corresponding in position to the furrow between the primary ridges on the skin surface. The development of the primary ridges now ceases. Between 17 and 24 weeks, the secondary ridges continue to develop, reflecting the primary ridges.

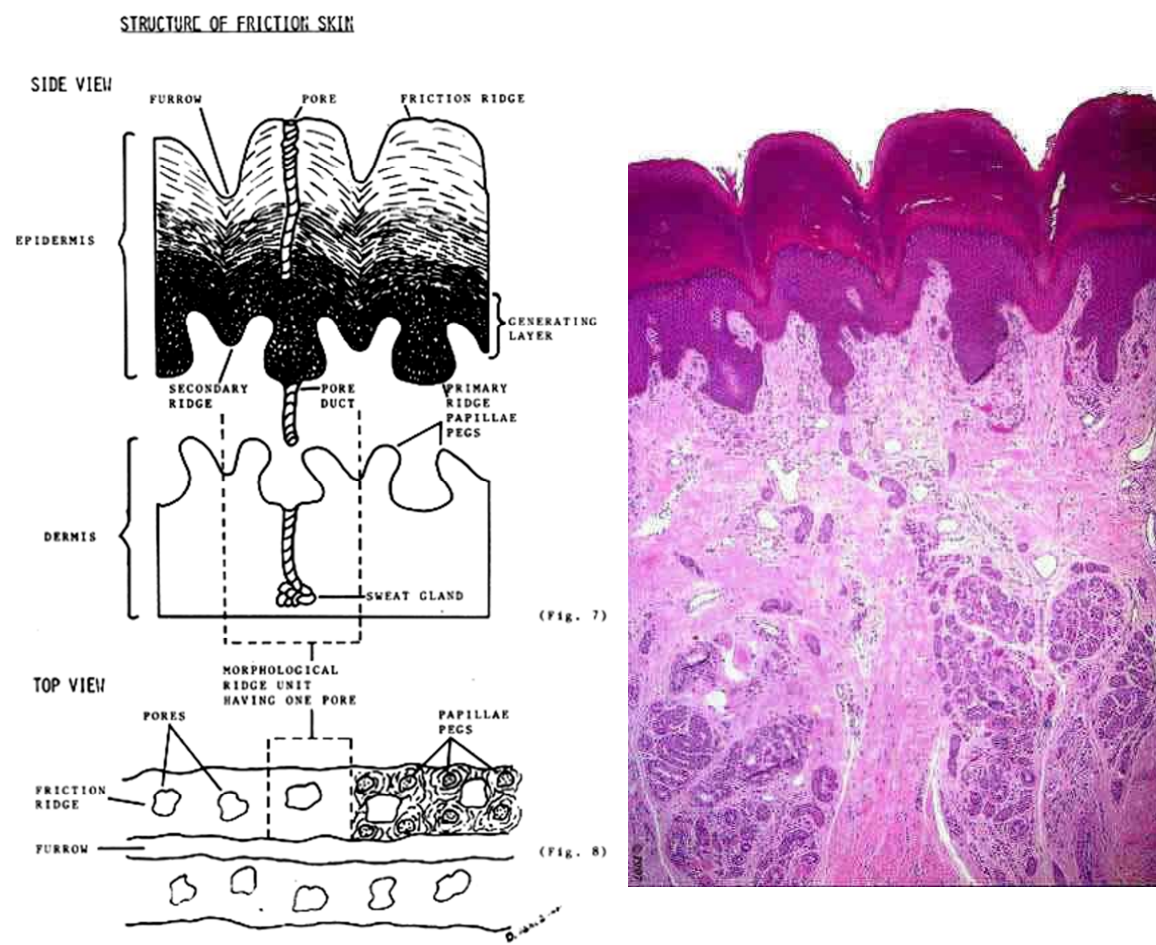


Diagram of the cross section of friction ridged skin (Ashbaugh 1991)

Photograph of the cross section of friction ridged skin (Beeton,2001)

Figure 1 Cross section of friction ridged skin

At this time, the epidermal ridge system has the morphology of an adult. As the secondary ridges develop, peg-like structures called dermal papillae grow in the dermis, protruding into the area between the primary and secondary ridges.

Ashbaugh (1991) describes a “ridge unit” as consisting of a sweat pore surrounded by dermal papillae. During the growth of the skin, these units fuse together to form the individual ridges in the dermis. The development of the friction ridges does not occur as a singular event across the skin. It commences in the fingers at the tip, in the centre of the volar pad, and at the periphery of the digit. The development spreads from the areas of initiation and these growing areas meet to cover the surface.

The final configuration of the friction ridges is said to be influenced by many factors, including:

- growth stress giving rise to directional pressure from cell proliferation;
- volar shape, height and skin thickness;
- neurotrophic factors indicating a relationship between the initial locations of nerves and the development of the primary ridges;
- ridge bundles which lead to an alternative but unsupported theory on friction ridged skin development; and
- skeletal factors indicating relationships between bone size and development and eventual pattern type.

In consideration of the uniqueness of the friction ridge skin, Ashbaugh (1991) states “*All ridge units have been subject to genetic and physical pressures while growing. The plethora of genetic and physical variances during friction ridge formation is the reason why no two*

areas of friction skin will ever be found to be the same, even in a small area. The variables involved are too great”.

Although the uniqueness of skin can be derived from the statement of Ashbaugh, a statistical or empirical proof has not been delivered to date. This further provides impetus behind research such as this.

After the skin has matured and development has ceased, skin cells continue to proliferate from the basal lamina – the junction of the dermis and epidermis – as a part of normal life. The cells migrate to the surface of the dermis over a period of approximately 28 days. During this migration, the cells change shape, acquire keratin, and the nuclei break down resulting in the death of the cell. The cells at the surface of the skin eventually slough off and are lost (Berry & Stoney, 2001). The eventual configuration of the friction ridges remains constant with the person until after death. The only variations will be through dilation (growth) and permanent scarring, should the skin be damaged into the depths of the dermis. Whilst the dermis is not damaged, the constant migration of cells to the surface ensures that the surface configuration of the friction ridges will remain constant (Ashbaugh, 1994) .

1.3 Deposition of latent fingerprints

When a finger contacts a surface, the bulb of the finger and the skin flex to accommodate that contact. The degree of flex will be dependent on factors such as the degree of effort applied, the direction of that effort, and the shape of the surface contacted. The mark that is left behind will be comprised of a variety of constituents of gland secretions and environmental contaminants. The appearance of the mark will be influenced by a number of factors that will result in anything from a clear reproduction of the friction ridge detail through to a mark

bearing indistinct detail and being nothing more than a smudge. These factors are said to include:

- composition of the material deposited;
- amount of material deposited;
- characteristics of the receiving surface; and
- pressure and skin movement or slippage when depositing the mark.

Other factors not discussed will influence the ability to detect a mark.

The function of the hand is associated with grasping and the human ability to manipulate an item. Friction ridges are so named due to their assistance with grasp. Sweat also provides an adhesive quality to assist the grasping process (Flatt, 2000). In handling an item, a person leaves behind marks on that item left as a result of the finger contact. It should be noted that people do not intentionally leave fingermarks; they are left behind as a bi-product of the associated process of grasping. It therefore stands that the following needs to be recognised:

“It is well accepted that wide variations in the amount of detail transferred during any given contact from the three-dimensional world of a finger to the two-dimensional realm of a fingerprint may not permit individualization. Thus, although the ridge pattern arrangement on friction ridge skin is unique, one may not be able to render an identification or an exclusion of a source from the limited amount of detail in certain latent prints” (Budowle, Buscaglia, & Schwartz-Perlman, 2006).

The quality of the fingermark will later be the subject of an examiner’s objective analysis in terms of what information is visible and reliable, taking into account the clarity of the image

and considering the effects of pressure, distortion, media and development techniques (Champod, Lennard, Margot, & Stoilovic, 2007).

1.4 Development of the fingerprint identification methodology

Comparison and evaluation of friction ridge formations takes place in the brain of the examiner (Ashbaugh, 1991). It is a process that requires assessment of the material for comparison and the recognition of features reproduced, based on an understanding of the structure of friction ridge skin, the way it behaves in conjunction with other surfaces, and how a mark is deposited.

The types of features (known as minutiae) that occur in a finger impression are variable but include ridge endings, bifurcations, and dots or islands.

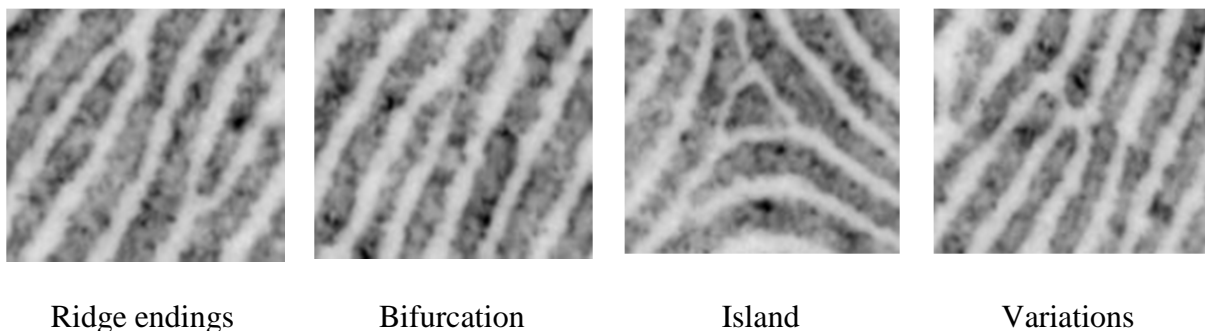


Figure 2 Examples of fingerprint features

Other features that are composites of these basic features occur and the terminology used to describe these varies (Figure 2). Variation in the appearance of a feature may exist due to excess sweat or pressure. For example, the fourth image in Figure 1.2 appears as three ridge endings; however, with pressure and excess sweat, the three endings may be seen to join, producing a feature that would be classified as a bifurcation.

There are other ridge structures that are apparent in marks that can be used for identification purposes. These include sweat pores, ridge edge shapes, creases, scars and subsidiary ridges. All features and the pattern type fall into three categories (Scientific Working Group on Friction Ridge Analysis, 2011):

- Level 1 detail; Friction ridge flow, pattern type, and general morphological information.
- Level 2 detail; Individual friction ridge paths and associated events, including minutiae.
- Level 3 detail; Friction ridge dimensional attributes, such as width, edge shapes, and pores.

Traditionally, fingerprint examiners would look for correspondences between a mark and a print in terms of (Moenssens, 1971):

- General pattern agreement;
- Qualitative concordance (compared ridge details are of the same type and shape);
- Quantitative factor (a predetermined number of matching characteristics has been met), and
- The relationship between ridge characteristics (relative positioning and numbers of intervening ridges between examined).

Note the term “print” or “fingerprint” generally refers to a finger impression from a known source.

The “Quantitative factor” dealt with minutiae quantity, which has influences from Edmund Locard’s tripartite rule that set the basis for fingerprint identification standards (Champod, 1995). In summary, the assertions were:

1. If more than 12 concurring points (features) are present and the fingerprint is sharp, then the certainty of the identity is beyond debate.
2. If 8 to 12 concurring points are involved, then the case is borderline and the certainty of identity is dependent on sharpness, rarity, presence of key class features and clear finer friction ridge details.
3. If a limited number of points are present, then certain identity is not possible, only a probabilistic expression is possible, in proportion to the number of features present.

The first two of these rules were widely accepted and have been representative of practices throughout the world until the 1950's when it was suggested that the type of minutiae should be weighted according to rarity of occurrence, and the detailed consideration of qualitative as well as quantitative aspects was further emphasised. The third rule has never been addressed by fingerprint examiners and has largely been discouraged. The International Association for Identification's (IAI) stance in relation to a statistical approach states that *“Any member, officer or certified latent print examiner who provides oral or written reports, or gives testimony of possible, probable, or likely friction ridge identification shall be deemed to be engaged in conduct unbecoming such member, officer, or certified latent print examiner.”* This ruling has only recently been rescinded (Polinski, Smith, & Garrett, March).

Accordingly, the outcomes resulting from the comparison of a mark and a print will be that:

- The mark and the print have come from the same source; or
- The mark and the print have not come from the same source; or
- The mark cannot be excluded from coming from the same source as the print.

There is no method at present, where an operationally validated expression of probability or likelihood where the examiner cannot give a conclusive inclusion or exclusion, or where there is a requirement for a predetermined number of corresponding features to exist, and that number has not been met.

In 1970, the IAI established a Standardisation Committee whose purpose in part was to review the validity of the requirement for a numerical threshold. Their conclusion was that there existed *no valid basis* for requiring a predetermined minimum number of features to be present to establish a positive identification. Following this, a deviation from the set number requirement began, with a trend toward the current methodology that considers a qualitative and quantitative approach to the identification process. In 1995, in Neurim (Israel), the Standardisation Committee's finding was extended to state that no *scientific basis* existed for a predetermined numerical standard to be used (Champod, Lennard, Margot, & Stoilovic, 2007).

David Ashbaugh of the Royal Canadian Mounted Police, in the early 1980's, introduced the concept of Ridgeology, a holistic approach to fingerprint identification. This required not only the knowledge of the formations and structures of the skin, but an examiner must also have experience based on sound training and exposure to thousands of friction ridge prints. This exposure is required to provide confirmation of the facts scientifically established by pioneers and researchers, through personal observation. It is the examiner's responsibility to be aware, understand and apply that knowledge (Ashbaugh, 1991). The method that Ashbaugh describes involves the processes of Analysis, Comparison, Evaluation and Verification (ACE-V). This method is not specific to the fingerprint discipline as it is also described by (Tuthill, 1994) in a generic criminalistics context. It requires that the examiner makes observations on the mark during an *analysis* of it. This is done before viewing the

reference print to avoid bias from having examined it. Then a *comparison* between the two impressions is followed by an *evaluation* of the information obtained with regard to correspondences and differences. Finally, the conclusion of the examiner must be *verified* by a suitably qualified person as being technically valid.

1.5 Present situation

Most countries in the world utilise the ACE-V methodology; some still require a minimum number of features to be found in both compared impressions. A recent publication from the American National Academy of Sciences (National Research Council, 2009) was highly critical of the fingerprint discipline (and many others) indicating that it was lacking standards and a statistical basis for its outcomes.

In my experience, fingerprint examiners generally do not want or see the need for a statistical approach to fingerprint comparisons. For most cases, the comparison of fingermarks can be done much quicker than the analysis of other methods of identification. The use of automated fingerprint identification systems and digital imaging technologies permits expedient transmission and identification of fingermarks across cities, countries and the world. The position of the Australian Fingerprint Scientific Working Group (Brisbane, May 2011) is that, the introduction of a statistical model is viewed as undermining the operation and effectiveness of the conclusive outcomes of an examiner and is perceived as being ultimately unnecessary. From my experience, there is a clear difference in the views of academics and examiners coming from positions of perceived needs of the fingerprint discipline and judicial system.

This research aims to test a concept that would see probability densities applied to the data that the fingerprint examiner uses to make the identification. Ideally this would occur through the use of computer based comparison software and would require nothing more of the examiner to achieve the measured outcome.

2. Challenges and responses

2.1 Introduction

Whilst the ACE-V process is valid in criminalistics generally, it involves an “Evaluation” process where there is an inherent subjectivity that is due to variations in examiner experience and training, and perhaps knowledge of other aspects of the investigation (Langenburg, Champod, & Wertheim, 2009). Where there is subjectivity and minimal friction ridge detail available, the obvious question arises:

“How much correspondence between two fingerprints is sufficient to conclude that they were both made by the same finger?” David Stoney, a distinguished expert on fingerprints, tells us: An adequate answer to [this question] is not currently available. The best answer at present to the question ‘How much is enough?’ is that this is up to the individual expert fingerprint examiner to determine, based on that examiner’s training, skill, and experience. Thus we have an ill-defined, flexible, and explicitly subjective criterion for establishing fingerprint identification. Any unbiased, intelligent assessment of fingerprint identification practices today reveals that there are, in reality, no standards. That is, the amount of correspondence in friction ridge detail that is necessary for a conclusion of identity has not been established.”(Stoney, 2001).

There is no simple answer to this question. The fingerprint community describes the question as a grey area that is directly affected by the compared materials’ quantity and quality of information (Vanderkolk, 1999). The determination of quantity and quality is influenced by the examiner’s training and experience. But it should also be asked, “Is Stoney’s question reasonable or achievable?”, which it may not be in either case.

There is much dissension in this regard, illustrated by fingerprint comparisons (and other comparative science methodologies) that have brought about challenges in the US in the Federal Court, notably in *US v. Mitchell* 1999 and *US v. Plaza* 2002. *“The confusion and misunderstanding by the legal community stems from a variety of sources, including popular notions about science in general and specifically forensic science, using forensic DNA examinations as a model for interpreting forensic hair examination results, and the difference between calculating probabilities and scientific reliability”* (Houck, Bisbing, Watkins, & Harmon, 2004).

In the absence of any valid comparison between the methods employed for DNA analysis and fingerprint analysis, it is easy to point out perceived deficiencies in the comparative scientific disciplines such as hair or fingerprint examination, with these disciplines, there are no established and accepted models that account for “error” (as defined in terms of measurement and not identity) or Daubert criteria (Berkman Centre for Internet and Society, 1999) as could be applied to analytical disciplines, such as DNA profiling. It should be noted that “error rate” as applied to fingerprint identification has more recently been studied (Ulery, Hicklin, Buscaglia, & Roberts, 2011)(Langenberg, 2009), but not in the context of operational application, that includes verification and other quality control measures.

The tests for admission as evidence in the US Federal Court stem from the Frye and Daubert criteria, each of which have resulted from court matters: *US v Frye* 1923, and *Daubert v Merrell Dow Pharmaceuticals Inc.* 1993. The test criteria applied initially to evidence purporting to be “scientific”. Later as a result of *Kumho Tire Co. v. Carmichael* 1999, this extended to apply to evidence deemed to be “technical”. Whilst there are debates in the US

as to whether fingerprint identification is scientific or more an “art”, there have been numerous Daubert challenges, none of which have been successful.

A significant outcome from a United States Federal court hearing, regarding the “Daubert” challenge in the matter for Plaza (United States District Court, E.D. Pennsylvania, 2002), was that the uniqueness of fingerprints was given judicial notice, meaning that the uniqueness of fingerprints was accepted as fact in that court. This relates loosely to the mark left by a finger, as it is a lesser quality reproduction of the corresponding surface of the skin.

The Daubert criteria for testing scientific or technical evidence in the US federal courts are:

- Is the methodology generally accepted?
- Has the methodology been tested?
- Has the methodology been peer reviewed?
- Is the error rate for the methodology established?
- Are there defined standards for the application of the methodology?

Judges of such courts act as gate keepers for the introduction of evidence (especially novel evidence) and can require that any or all of the criteria are met.

2.2 Knowledge gap

As Donald Kennedy, the editor-in-chief of Science, notes, *“It’s not that fingerprint analysis is unreliable [but] . . . that its reliability is unverified by either statistical models of fingerprint variation or by consistent data on error rates.”*(Zabell, 2005). The world of statistics and the world of comparative sciences appear, at least in the context of fingerprint comparisons, to be worlds apart. The statisticians believe only in statistics and the examiners only in themselves. Accordingly, the current application of statistics to fingerprint

identification is largely conducted in the absence of a fingerprint expert's input or interpretation. There needs to be a circumstance where there is an understanding and acceptance of both manual and statistical approaches to fingerprint analysis. There also needs to be an understanding of what each approach can contribute to the provision of evidence.

2.3 Research contributions

The method of fingerprint comparison can be divided into the two sub-disciplines of identification and verification, which targets applications in the biometrics industry, and mark searching and comparison, whose outcomes may constitute evidence in criminal proceedings. The latter is where this research is targeted.

An approach to fingerprint comparison, besides manual methods such as ACE-V, is to model the measurable aspects of the friction ridge skin. A model (Duda, Hart, & Stork, 2001) is comprised of descriptions of the subject that are typically mathematical in form. The manual method for feature measurement considers relative feature position, angles from one feature to others, classification of the features, and the number of intervening ridges between features. It does not incorporate actual measurement of distances and angles between marked features in a comparison, although this is implicit in the manner in which a person compares fingermarks. The path from one feature to the next has a direction relative to the finger orientation, and the number of intervening friction ridges between two marked features is representative of the distance between those features, due to the relatively consistent frequency described by the number of ridges and valleys per unit length.

There are various publications that detail models for fingerprint comparisons that produce a variety of results, including the production of likelihood ratios supporting, or not, the

hypothesis of individualisation, or expressions of fingerprint individuality based on various measurements and quantities of data. This research seeks to simply analyse the mark left by a finger using features used in the identification process as marked by an examiner. Measurements will be compared with data describing reasonable bounds for friction ridge skin stretch, that is, the bounds of natural distortion, to provide an ability to test the examiner's hypothesis of individualisation.

Various attempts to describe fingerprint individuality can be summarised (Stoney, 2001) as follows:

Galton, in 1892, worked on the ability to predict areas of friction ridge detail for given sized regions and frequency of occurrence of patterns. Balthazard established a set of defined minutiae, which was later extended by Bose. Expressions of the probability of a type of ridge variation (ridge ending, bifurcation, dot, continuous ridge) were established and modified, for given pattern types. Gupta examined the frequency of occurrence of feature types in specific locations. Roxburgh approached minutia selection on the basis of polar coordinates and ridge counts from an origin and, using this model, calculated the total variability that could occur under that model. Amy considered variance of feature type, using Balthazard's classifications, and also variability in the number and position of minutia. Trauring assumed that all minutiae were randomly distributed and that there were only ridge endings and bifurcations

Cappelli (Capelli, Miao, & Maltoni, 2001) modelled distortion in friction ridged skin when a finger is placed on a fingerprint sensor surface. Cappelli was interested largely in fingerprint verification in biometric access-control systems. He nominated three areas of the skin contact area as shown in Figure 3:

- a close contact region where high pressure does not allow any slippage, which is in the middle of the contact area (region a);
- an external area whose boundary delimits the visible fingerprint area and where light pressure allows the skin to be dragged by the finger movement (region c); and
- a transitional area where an elastic distortion is produced to smoothly combine the above two regions (region b).

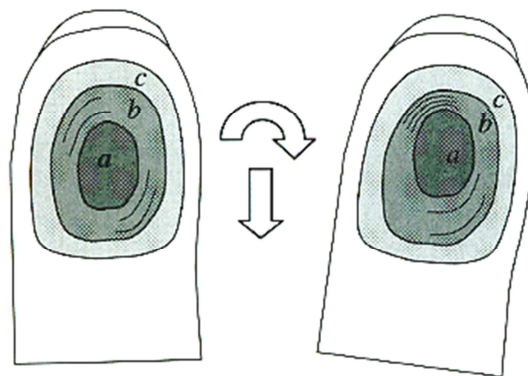


Figure 3 Regions a, b & c of a finger as defined by Cappelli et al.
This shows distortion due to clockwise rotation and downward movement of the finger
(Capelli, Miao, & Maltoni, 2001).

The Cappelli research was undertaken to further knowledge in relation to fingerprint sensing. The context does not entirely coincide with that of crime scene mark analysis, in that the movement of a finger on a surface at a crime scene is not limited to the area of a fingerprint sensor. It does, however, introduce the distinct regions that exist with respect to the onset of distortion due to rotation or translation of the finger. With that in mind, the regions as defined by Cappelli, in the crime mark context, will vary where we see the entire surface of the skin distorted due to gross movement of the finger on the surface resulting in total slippage. It is expected that, with total slippage, regions 'a' and 'b' may be insignificant where the total area of contact is distorted.

Pankanti (Pankanti, Prabhakar, & Jain, 2002) measured minutiae in terms of their Cartesian coordinates and the angle of the ridge on which they reside. The “template” of the mark was therefore defined by a collection (the finger) of data sets (each minutia). An area of overlap was established after reasonable alignment, and the location of corresponding features compared. Features were said to be related if differences in angle and position fell within described tolerances. The tolerance for distance was prescribed by a circle of given radius around each minutia. This model (Pankanti) deals with distance between minutiae on the basis of the Cartesian plane. The plane represents a rigid platform that does not adequately deal with skin distortion. Due to its high flexibility, friction ridge skin distorts readily when there is contact with a surface. The stretch is not uniform across the skin in terms of direction and magnitude (Dinning, 2005). Due to its plasticity, the application of forces, some of which are not orthogonal, produces non-linear distortions in recorded fingerprints (Capelli, Miao, & Maltoni, 2001). There is a gradual change in both minutiae position and angle across the contact area of the skin, and this is affected by the pressure applied and any rotation or translation of the skin on the contacted surface. The variation of the relative positions of the minutiae across the surface of the contact area is therefore also non-linear. The model needs to compare positions of the minutiae with each other (with a degree of tolerance) and not with the plane on which it sits. Others (Neumann et al 2006, 2007) use the feature type in their descriptions; however, the feature classification can vary with variations of pressure and movement, and represents a limitation in such a model.

Egli et al (2006) looked at methods of visualising fingermarks from both samples of latent (fingermark) deposits and “Livescan” devices and used these samples for the purpose of determining within- and between-source variability and a probabilistic approach to fingerprint evidence. “Within-source” refers to marks that have come from the same finger,

whereas “between-source” refers to marks that have come from different fingers. They derived benefit from scores obtained from an AFIS system. Results indicated that within-source variability measurements were affected by the visualisation technique, the number of minutiae, and the configuration of the minutiae. The study was supportive of using Livescan systems in the creation of a data set for modelling within-finger variability.

Where others have attempted to demonstrate the individuality of fingerprints, Neumann et al (2006) sought to assess the evidential contribution of the compared mark and print. Features extracted included pattern type, the zone of the finger, minutia type, distance between subsequent minutiae, and relative angles between minutiae. Neumann has described the features as discrete (classifiable) or continuous (variable), and calculated likelihood ratios based on these. Figure 4 shows the relationships of the continuous variables.

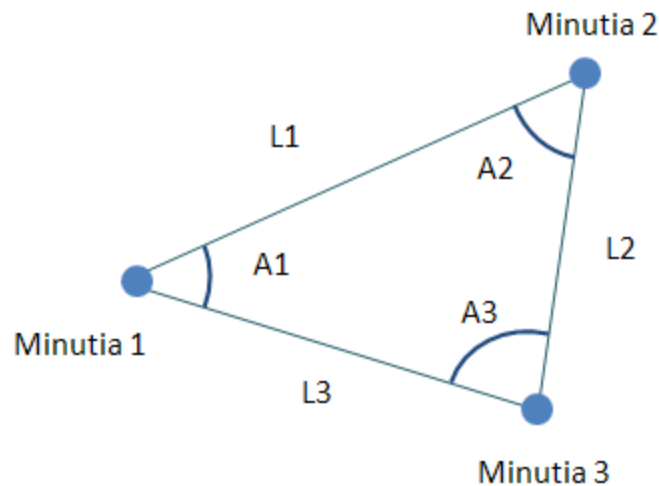


Figure 4 Continuous features as used by Neumann et al (2006).

L refers to the distance to the next minutia and A refers to the angle described by the minutia and the opposite side of the triangle.

Neumann (Neumann, et al., 2006) used established minutiae densities from previous research to calculate probabilities in relation to occurrences of minutiae combinations in pattern types

and frequencies of pattern types. He used Delaunay triangles to describe the relative positions of features. A key aspect of measurements between features is that the degree of change of relative position and angle of path from one feature to the next increases with distance (Dinning, 2005). Delaunay triangles are triangles described by three points in a manner that no triangle boundary contains a fourth point. There is no consideration of how far apart the minutiae are and the effect that increased distance may have on the measurements of the angles.

Neumann (2007) later modified his model to incorporate a centroid location, being the mean values of the minutiae Cartesian coordinates. He then selected the minutiae for the feature vectors by commencing at a position vertically above the centroid (in the image) (see Figure 5), and scanning the image in a rotational manner about the centroid, encountering minutiae as the rotation angle increased. He then extracted features for each minutia, which included the minutia type, angle of the minutia relative to the image, distance from the centroid to the minutia, distance between subsequent minutiae and the area described by the minutia, the next minutia and the centroid. Once the rotation was complete, the print could be described by the resulting set of vectors. The centroid can be used as a relatively consistent reference point for the data set that is rotationally tolerant; but the potential problem with this model is that distortion that could cause stretch or compression of the skin, a change in the positions of the minutia, and a possible re-ordering of the minutiae and vectors.

To address distortion, Neumann et al (2006) designed a model to facilitate a sufficiently large sample from which he could derive distributions. The model assumes that distances between the centroid and the vertices for a given triangle can be varied independently. This

assumption can be questioned as the features are, in fact, physically connected, and the changes of position that proximal minutia experience will be similar (Dinning 2005).

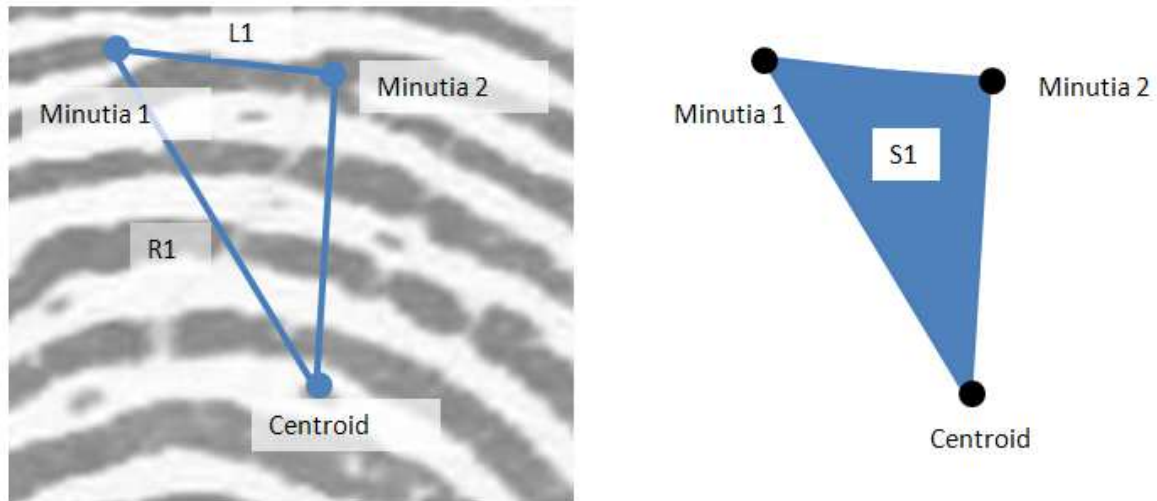


Figure 5 Features extracted by Neumann et al.

R1 refers to the distance from the centroid to the minutia, L1 refers to the distance to the next minutia, and S1 refers to the area described by the minutia, the next minutia and the centroid.

As expected, the variance demonstrated by Neumann with his model is greater where the independence of movement is introduced. Neumann's model is complex and utilises multiple distributions of data. It is also limited at this time to specific fingers and pattern types but appears to be robust and will be further developed.

2.4 This project

The fingerprint discipline is viewed very differently by different persons. Fingerprint examiners generally see no need for statistics. There is much confusion and misunderstanding about both the visual comparison and statistical approaches to fingerprint examination.

However, pressure is being applied from a number of areas to conform to a perceived best practice for forensic evidence, i.e. the application of Bayesian statistics, producing a likelihood ratio representing the degree to which the evidence does, or does not, support the case for the prosecution.

The researcher in this study is a fingerprint examiner of twenty years experience with both academic and fingerprint identification qualifications. The research objective is to establish a simple model that will use probability densities to analyse the data used by an examiner in arriving at a positive identification, and possibly provide supplementary evidence for the conclusion reached by the examiner. It is not proposed that the examiner becomes redundant, leaving the evidence only in the form of a likelihood ratio.

The proposed model aims to describe how much variation in position can occur between proximal minutiae. The amount of variance possible (within-source variation) will be established through experimentation with the fingers of one person. Between-source variation will be established through the comparison of known finger impressions to close non-matched finger impressions obtained through an Automated Fingerprint Identification System (AFIS) data base search, and the corresponding AFIS nominated minutiae compared.

The features extracted in this proposed model relate to what an examiner would state that they use, namely, relative positions of minutiae and numbers of ridges between them. This can be described by the distances between minutiae and the angles between them. Minutiae can include classifiable ridge features, such as endings or bifurcations, and could also include ridge structure such as pores or subsidiary ridges. The proposed model considers feature

location above feature classification. Classification of the features is not included in the model as this may vary between impressions.

2.5 Research objectives

This research aims to:

- Develop a metric that will indicate a degree of support (or not) for the comparative science of fingerprint identification as practised by fingerprint examiners;
- Measure the changes of positions of fingerprint minutiae due to friction ridge skin distortion in terms of the magnitude and direction of change;
- Generate distributions for the amount of change that occurs in positions of fingerprint minutiae both within and between-sources;
- Develop an alternate method for testing prints and marks purported to have come from the same source, to determine a degree of support for the proposition that they have come from the same or another source, based on the degree of apparent match of the locations of minutiae.

2.6 Hypothesis

Friction ridged skin has a stretch limitation; therefore, corresponding minutiae in compared images of fingerprints will vary in their relative positions within limits.

If the hypothesis is supported by this research, the minutiae marked by a fingerprint examiner can be tested in terms of how well the relative positions of all minutiae fit to the corresponding print with reference to that stretch limit.

Data can be extracted from minutiae marked by an examiner on a Cartesian plane in terms of their x and y coordinates. From these coordinates, the minutiae locations and the relative positions of proximal minutiae can be determined. It is assumed that measurements taken from proximal minutiae represent the least variation that should occur, and the further apart the minutiae are, the more skin there is between them and the more the potential for stretch and variation can occur.

The relative positions of minutiae can be determined through triangulation of the minutia in question and its nearest two neighbouring minutiae. From these three minutiae, two distances (the distances from the minutia in question to the other two individually) and an angle determined by the three minutiae can be measured. The variance of such positions is to be established through the examination of within-source data. Once corresponding minutiae in a comparison of two fingermarks are marked, a measure of fit according to established variance limits can be determined.

3. Materials and methodology

3.1 Introduction

The following steps were taken in developing and testing the model:

1. Identify one person for the acquisition of within-source data.
2. Acquire (reference) images with minimal distortion of each finger from that person, to be used as reference images for comparison. Whilst there is distortion in all finger impressions, the reference images must have as little as possible to represent as close as possible the “ground truth” for each finger.
3. Generate a set of (18) images taken from the chosen individual of all of their fingers, with distortion induced by a specified set of movements. This will provide images for the generation of within-source variation.
4. Select ten minutiae (total of 1800) for each within-source finger for measurement.
5. Measure distances and angles between selected minutiae.
6. Establish within-source distributions for the following:
 - a. The variation in distances from a given minutia to the nearest two other features, and
 - b. The variation of angle determined by the three minutiae,
7. Search the reference finger images against the CrimTrac National Automated Fingerprint Identification System (NAFIS) database to find close non-matches which will serve as between-source candidates for comparison.

8. Use minutiae that are nominated by NAFIS as corresponding with the between-source images.
9. Measure distances and angles between selected minutiae.
10. Test each between-source candidate by:
 - a. Measuring each marked minutia and their nearest pair of neighbouring minutiae for the distances and angle, as was done for the within-source data collection;
 - b. Comparing the measurements against the relevant within-source distributions;
 - c. Establish an indication that the examiner's finding is or is not supported.

3.2 Equipment

Nikon Digital Camera D200

The Nikon D200 camera satisfies the needs for this project in that it is a highly configurable camera with interchangeable lenses. The experimental setup for this project involved the use of an AF-s Micro Nikkor 105mm lens set at F36. The camera was used in aperture priority mode with the focus manually set. These and other settings were saved as default. The camera was mounted on a custom built aluminium frame which was placed on the pan of a balance. The Nikon D200 acquires an 24 bit RGB image of dimensions 1936 x 1296 Pixels.

A&D GX-20K Balance

This balance was chosen for a number of reasons. It has a large pan on which the frame supporting the camera and prism can be mounted, giving a very stable platform. The balance has a weight range of 0.1 gram through to 21000 grams at 0.1 gram intervals. The balance

has serial port connectivity that allows it to be queried for weight values or controlled through customised software (such as V++ scripting) should the need arise.

Prism

A perspex triangular prism was used as the finger platen. The finger contact area on one face of the prism could then be seen from a different face and recorded. The prism was mounted in an aluminium casing affixed to the aluminum frame. The prism had been used for previous projects that investigated fingerprint distortion (Dinning 2005 & Richmond 2004), and had therefore been validated as being suitable for such research.

Dell GX520 PC

The PC has a Pentium D processor running at 2.8 GHz with 1 GB of RAM running Windows XP Service Pack 3. An additional 19 inch monitor and an external hard drive were attached. The choice of PC was not vital in this project and needed no specific configuration other than the system requirements of the software used. The camera and external hard drive were connected to the computer via a USB cable.

3.3 Software

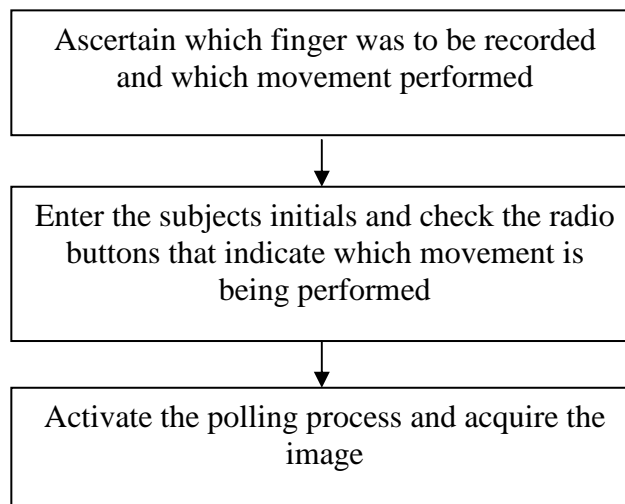
Nikon Camera Control Pro 2.0.0

This software is produced by Nikon for the purpose of remotely controlling Nikon cameras. PC control of the camera was chosen as the entire camera settings can be established through testing, saved and recalled to ensure consistency in the images obtained. A destination folder “test_in” was created, to which the Nikon software was configured to save all acquired images to. Whilst the camera was configured through the software user interface, each image was acquired using an electronic cable release.

Visual Basic 6

Visual Basic 6 is an integrated development environment that allows for the development of user defined programs. A dialog was developed by the author for a specific function. The software polled the test_in folder for incoming images. If an image was found, the software would rename and move the image to a destination folder. This was to ensure that each image acquired was named immediately after the finger movement was performed and the image acquired.

The process was:



The result of the configuration in Figure 6 would be a file name “BC_LI_ac_4”.

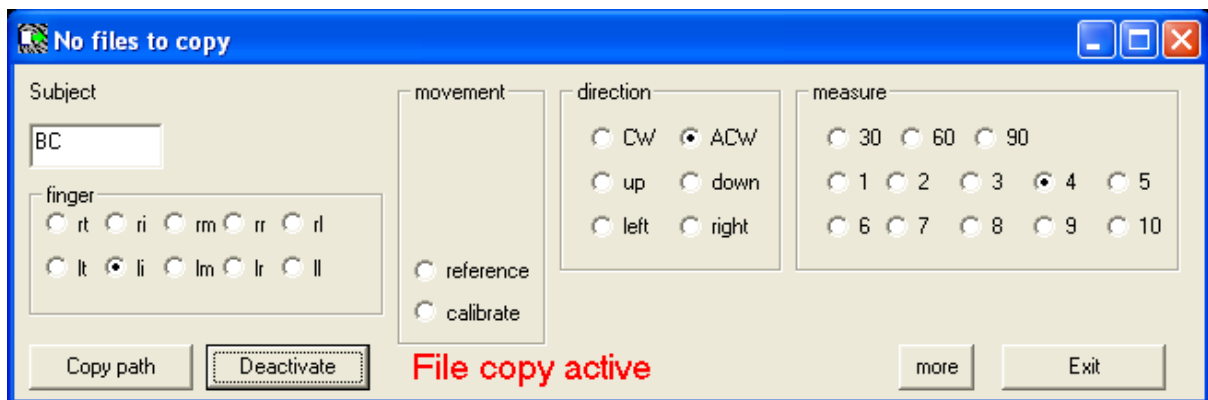


Figure 6 File copier application in Visual Basic. By selecting the various parameters the name applied to an acquired image can be configured to match the movement of the finger.

MetaMorpho 4.2 NAFIS

MetaMorpho is a fingerprint database and searching software provided by Morpho (formerly SAGEM). It is currently the software maintained by the Australian government agency CrimTrac for the maintenance of such records for all Australian police. It provides for the searching, registering and retrieval of fingerprints from people (known source) and from crime scenes (unknown source). A search can be configured with parameters including pattern classification, sex, minutiae placement and search region (state of Australia).

In this project, the software has been used to search fingerprints of known source to find near non-matches of unknown source for between-source comparisons.

There exist other similar programs, however these do not provide access to the Australian Federal Police owned data in the national data base.

Digital Optics V++

V++ 5.0 is a highly flexible imaging application that incorporates an intuitive scripting language similar to Pascal (VPascal). This software was chosen as the author has over ten year's experience developing applications with it and has done similar research with most of the same hardware. The scripting language enables the development of very specific imaging and device controlling solutions to user requirements. The software was used for the geometric correction of acquired images, the manual marking of minutiae on images, and measurement of the angles and distances between minutiae. The correction and measurements were achieved through the writing of customized scripts to achieve specific outputs. The processing of images in this manner allowed for batch processing of images and many calculations to be automated and performed in a short time. Data output from V++ was configured to be in the form of comma separated values (CSV) formatted text file. See Appendix 7.2 for the scripts.

MATLAB

MATLAB 7.4.0.287® is a high-performance language for technical computing. It integrates computation, visualization, and programming in an easy-to-use environment where problems and solutions are expressed in familiar mathematical notation (MATLAB documentation 2007).

This software was used for the processing of data generated in V++ to calculate within-source mean and covariance data. It was also used for the testing of cases using multivariate normal distribution functions, as described by the within-source mean vectors and covariance matrices. Matlab is able to open text files through scripting in CSV format. See Appendix 7.3 for the scripts.

SPSS

SPSS Statistics GradPack 17.0 is a comprehensive, easy-to-use set of data and predictive analytics tools for business users, analysts and statistical programmers (SPSS documentation). SPSS was chosen as it is a simple tool for examining and plotting data for correlations, regression and normal distribution. SPSS accepts data in CSV format as output by V++ and plots data very effectively in a format that is Microsoft Office compatible.

3.4 Choice of finger movements for within-source data collection

The variations in the relative positions of minutiae within a fingerprint are caused by the distorting of the skin when the finger contacts a surface. The bulb of the finger is subject to compression between the bone of the finger and the surface contacting the finger (Maceo 2009). Distortion in the skin can occur due to variations in the normal force applied, the shape of the surface, and the force applied lateral to the surface during the gripping action.

Regardless of the type of surface or the force applied, it is proposed that there is a limit to how much skin can stretch. A number of movements of the finger placed within a range of applied force were selected to introduce high levels of distortion. Neumann (2006) achieved this by placing the donor's finger on the recording device and having the donor move their feet to nine prescribed places. For the study presented here, the donor was only required to move their hand.

The movements were (abbreviations for naming appear in the brackets):

- Lateral movement sideways to the left (lf)
- Lateral movement sideways to the right (rt)
- Lateral movement towards the tip of the finger (up)
- Lateral movement towards the palm (dn)
- Rotation of the finger clockwise (cw)
- Rotation of the finger anti-clockwise (ac)

Each lateral movement involved the placement of a finger without movement, an image acquired, and then the movement performed and another image acquired. Therefore, for each lateral movement, there were two images taken.

Each rotational movement involved the placement of the finger without movement, an image acquired, and then four incremental rotations of the finger (at approximately 11 degrees per interval) with an image acquired on each position, so that in the fourth image the finger has been rotated approximately 45 degrees.

The amount of movement of the lateral and rotational movements was gauged by how much the finger could be moved before it slipped completely on the surface. In the case of rotations, this was approximately 45 degrees and for lateral movements approximately 3 millimetres. A study by Maceo (2009) established that, under high applied force, fingers

slipped completely after a movement of up to 3mm (laterally) or a rotation of up to 30 degrees. The movements chosen for this study were only meant to be approximate but sufficient to cause a range of distortions and ultimately, cases of complete slippage of the finger on the surface within a range of applied force.

Images acquired of fingers subject to these movements were named accordingly. For example, an image named “BC_LI_cw_04” came from Bruce Comber’s left index finger and was the 4th position in a clockwise rotation.

The decision to include a placement of the finger without movement at the beginning of each movement may be argued to lessen the variance in the amount of distortion measured overall. However, based on experience, the author argues that the majority of finger marks located at crime scenes do not show gross distortion.

3.5 Application and chosen range of force

The application of force by the finger to a touched surface is necessary to facilitate grip. As the force applied increases, the width of the friction ridges also increases, thus establishing a relationship between pressure and the amount of effort applied to the finger (Maceo 2009).

3.5.1 Finger, surface and movement relationships

One of the functions of friction ridged skin is that of grip. The structure of the ridges, combined with perspiration, provides the skin with a resistance to slippage. Furthermore, the volar pads (on the finger tips and palms) are pliable and able to mould to an object being handled. Given sufficient rotational or tangential force, the skin will have insufficient resistance to that force and will slip. That is, it loses its grip.

Kinoshita et al (1997) sought to determine, among other objectives, how the minimum required grip force preventing frictional slip, was influenced by tangential torque with tangential force loads.

One aspect of their study concerned the manner in which the slip force (normal force at the point of incipient frictional slip) depends on levels of tangential force and tangential torque in the digit-object contact area. They observed the relationships between:

- Normal force (the force applied by the finger perpendicular to the surface);
- Slip force (the force required to make a finger lose its grip);
- Rotational torque (force applied to make the finger rotate on the surface); and
- Tangential force (force applied to make the finger translate on the surface).

They found that:

- Slip force is linearly proportional to normal force regardless of the digit or surface type;
- There is a linear relationship between normal force and tangential torque required to cause slip;
- There is a linear relationship between normal force and tangential force required to cause slip;
- The friction coefficient, that is the factor that represents a material's propensity to grip, can be considered to be constant across all digits; and
- There is variation in friction coefficients between individuals, particularly with more slippery surfaces.

The significant points to note from these findings for the purposes of this project are:

- That there should be no variation between fingers for when the fingers will slip with similarly applied normal force; and
- There should be no significant differences in the behavior of the fingers, for similarly applied normal force, for different movements (rotation or translation) when the surface type is constant.

It is proposed that the skin will have a limited degree of stretch. The skin applied to a surface with a given normal force, with a tangential force applied (rotation or translation), will stretch to a limit after which the skin will begin to slip. The progression of the slip will commence at the extremity of the contact area and progress towards the centre of effort and towards the middle of the contact area, as demonstrated by Capelli et al (2001). Complete loss of grip will occur when all friction ridges slip.

3.5.2 Rationale for the choice of range of applied finger force in sample collection

Pressure is a factor that is said to affect the amount of distortion that could occur during the finger's contact with a surface. The term pressure is used by fingerprint examiners but is used in a manner that is not in keeping with the term's actual meaning. It is used to describe the force applied by the finger in an attempt to affect the persons' purpose of that grip. One such effect is a distortion of the skin and it is this distortion that will be apparent in the impression of that finger left on the surface.

A short experiment was conducted to view the behaviour of the friction ridges in terms of expansion with force with view to establishing a reasonable range of force to be applied when acquiring friction ridge skin images for use in this research.

Pressure (P) is calculated using Eq. (3.1):

$$P = \frac{F}{A} \quad (3.1)$$

where the force (F) is applied over the area (A).

In this project, the applied force was indicated by the weight measure on a balance on which the camera and prism were placed. For example, if the balance reads 1 kg, then the force applied by the skin is 1kp.

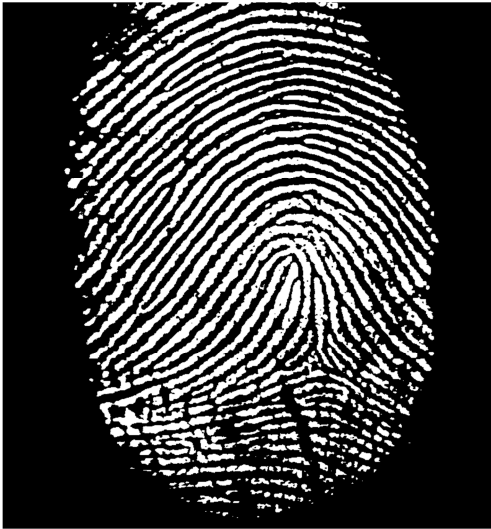


Figure 7a Contact area of a finger at 0.3kp



Figure 7b Contact area of a finger at 1.2kp

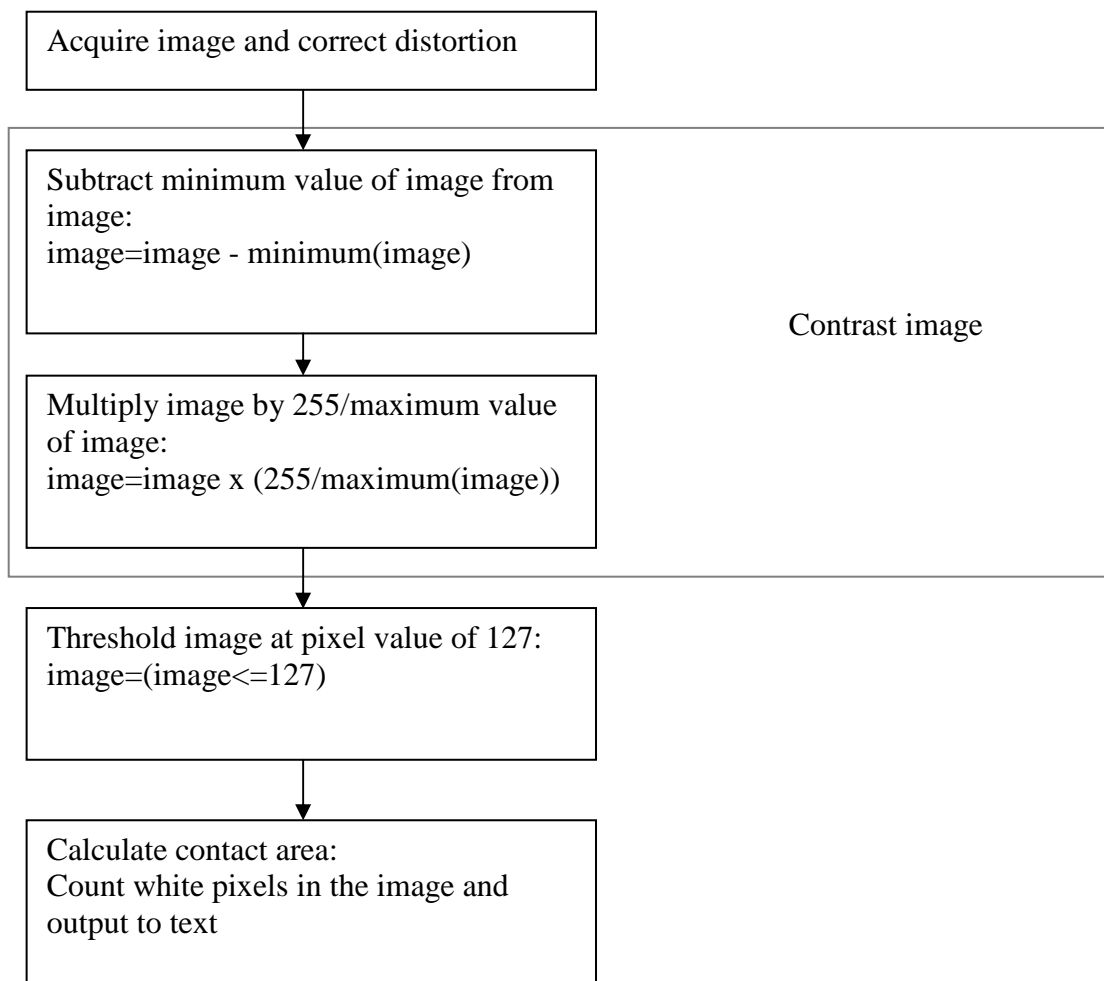
Figure 7 Images of friction ridged skin contact at forces of 0.3kp and 1.2kp.

It can be observed that the ridges are broader and the space between them is narrower, particularly towards the middle of the fingermark, as the applied force increases.

A property of friction ridged skin is that, as the force applied to a surface by the finger increases, the friction ridges expand, thereby increasing the actual contact area of the skin.

Figure 7 shows images of the contact area of two placements of a finger with forces of 0.3kp

and 1.2kp, respectively. Given that the contact area changes with applied force, the change of actual pressure experienced by the skin is not necessarily proportional to the applied force. However, there is a limit to which the friction ridges can expand and if the force is extreme the friction ridges can only expand within physical limits. At a particular point, it can be expected that the ridges cease to expand and the resultant actual pressure then changes in proportion with applied force. An initial experiment was conducted during which a series of images were acquired under increasing force. This series ranged from 0.1kp to 5.6kp with an increment of 0.5kp. The actual applied pressure is difficult to adjust accurately as this is done manually; however, the results indicated a pressure trend as expected, increasing after a limit of expansion was reached. Images were acquired for each approximate application of force. These images were processed as indicated in the following flow chart:



See Appendices 7.2.8 and 7.2.9 for related VPascal scripts.

The graph in Figure 8 shows that the relationship between force applied and the resultant contact area.

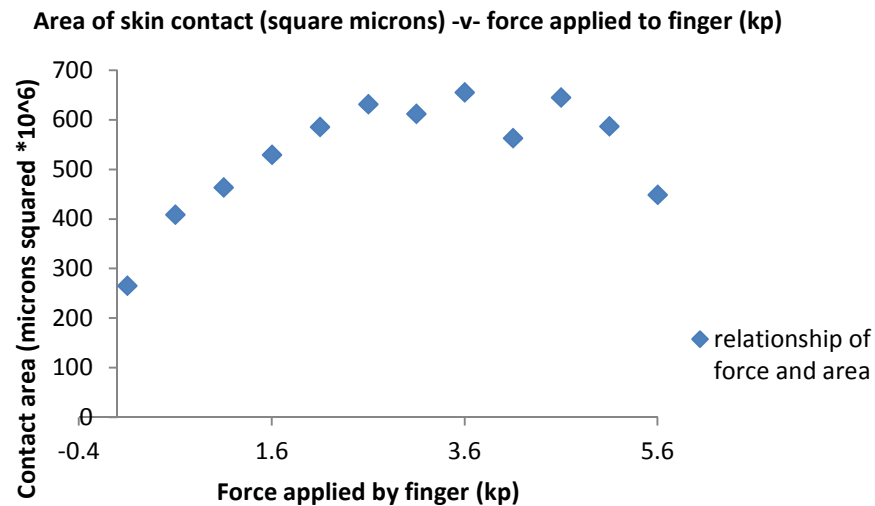


Figure 8 Measurement of pressure on skin with an increase of force applied

Initially as observed in Figure 8, the force changes with contact area, as the friction ridges expand; however as the force increases towards 3kp and beyond, the contact area ceases to change.

Outliers (as in the values for 4.1 and 5.6kp) are caused by the difficulty in applying an accurate and consistent amount of force to the finger. Measurement of the area is also affected, particularly with the higher values of force, with joining of the ridges along the edges as seen in Figure 7b. This is caused by excess perspiration between the ridges at the time of image capture. The image is thresholded before the area measurement is done. Where there is joining or blurring of the friction ridges, the affected area becomes generalised

and the calculated value for the contact increased. These findings are supported by those of Kinoshita et al (1997).

A second experiment was conducted during which another series of images was acquired under increasing force. This series ranged from 0.1kp to 1.5kp, with an increment of 0.1kp.

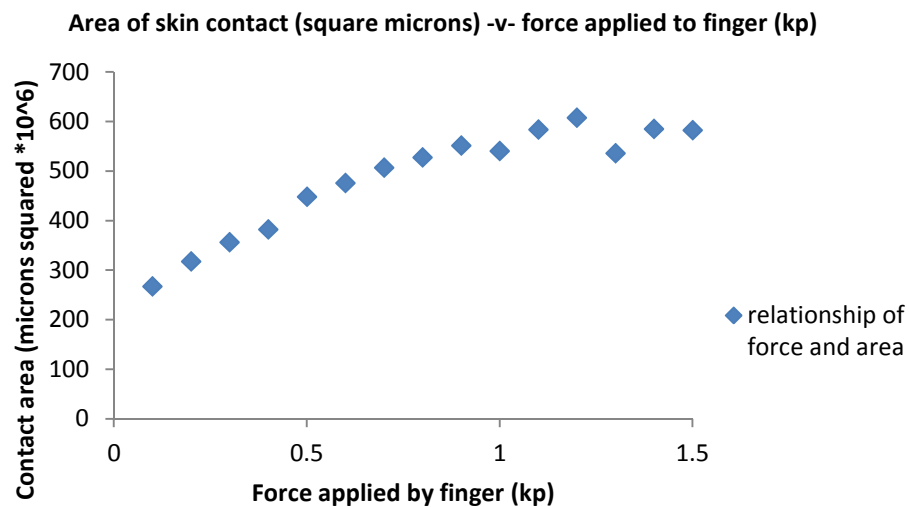


Figure 9 Measurement of pressure on skin with an increase of force applied.

As it can be seen in Figure 9 that, in the range of values from 0.5kp to 1kp, the relationship between applied force and contact area is approximately linear, and therefore provides a stable region for data collection.

In the context of these findings, images for this project were acquired of the contact area of the friction ridge skin under a limited range of normal force up to approximately 1kp. A series of images were acquired in conjunction with incremental movements until complete slippage occurred.

3.3 Acquisition and processing of images; within-source images

To perform this research, measurements needed to be taken that represented the relative positions of proximal minutiae. To do this, minutiae from a finger was recorded and marked so that measurements could be taken. In this instance, the source of the minutiae were images of fingerprint areas in contact with a surface.

Images were acquired by using a perspex prism on which a finger was placed. A Nikon D200 digital camera recorded the contact area of the finger through the prism where illumination supplied to the prism was from high intensity red LED's. See Figure 10.

The camera was connected to a laptop computer via a USB cable and operated through Nikon Camera Control Pro, version 2.0.0 software. The configuration of the camera was determined through trials and the optimal configuration saved as a settings file. The camera was triggered with an electronic cable release and the images transferred automatically to a folder on a USB hard drive. The images acquired were RGB format but appeared red due to the red LED illumination.

The acquired images required processing before any data could be extracted from them. This was due to distortion caused by the camera / prism arrangement and the need to standardise the images for comparison purposes. The processing was done using image processing software V++ in two stages:

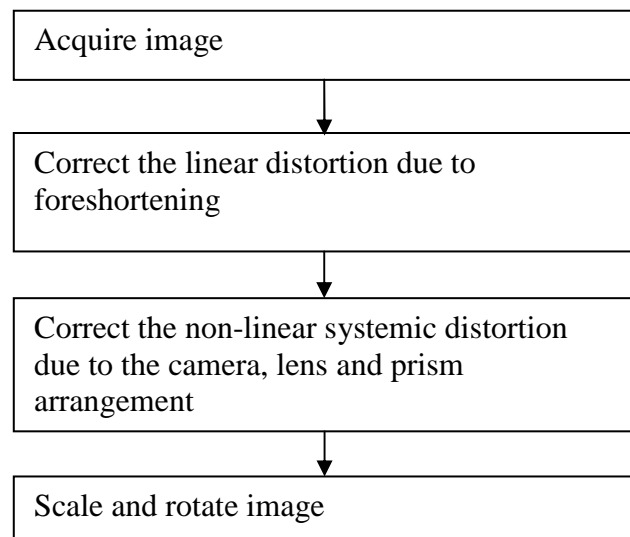




Figure 10 Camera and prism arrangement

3.3.1 Recording of images

The finger placed on the prism created two refractive index interfaces, these being perspex to air and perspex to perspiration. The camera viewing angle positioned the face of the prism bearing the finger at an angle that is greater than the critical angle producing total internal reflection, thus only the friction ridges bearing perspiration was recorded. The perspiration exists on the friction ridges that comprise the underside of the fingers. Where there is an air to perspex relationship (which is the case between the friction ridges), total internal reflection occurs and no light is recorded (See Figure 11). In most instances, it was necessary to load the friction ridged skin with skin secretions from the forehead before recording the image. The prism behaved in a similar manner to live scan devices; if the skin was dry, there would be little friction ridge detail visible.

Where there is a perspiration to perspex interface, refraction occurs allowing the skin contact area to be recorded as brighter than between the ridges, resulting in the friction ridges being visible as bright red lines against a black background.

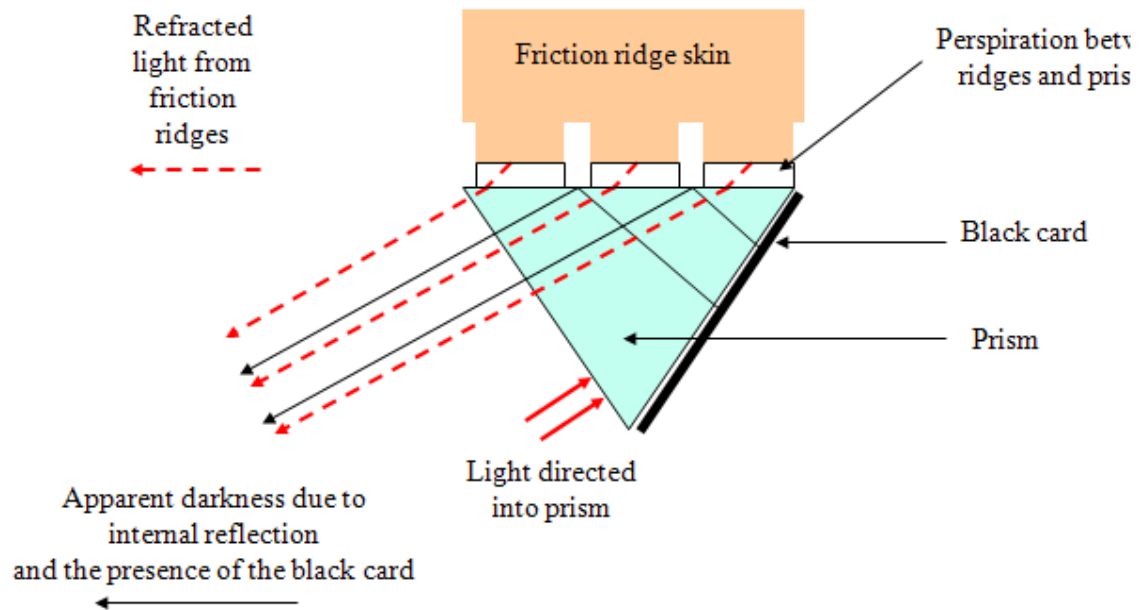


Figure 11 Schematic diagram of the friction ridged skin contacting the prism

The image in Figure 12 is an example of a recorded image.

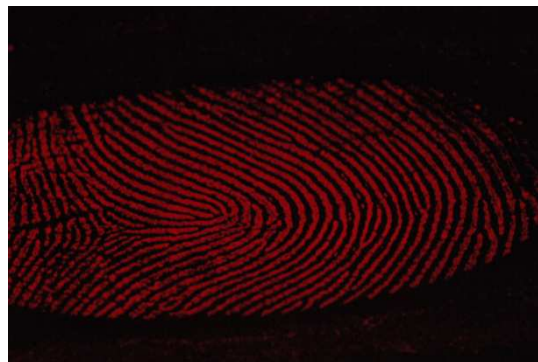


Figure 12 Example of an acquired image of the friction ridge skin contact area

As each image was saved by the Nikon software to a designated folder, the image was moved to a final destination folder and renamed according to the parameters of the image (subject,

movement, etc.). Figure 6 shows a Visual Basic interface to facilitate the renaming consistently and automatically.

3.3.2 Correction of foreshortening

To achieve total internal reflection between the friction ridges, the prism needs to be viewed from an angle no less than the critical angle for the air/perspex interface. This causes foreshortening of the resultant image in one direction as shown in Figure 13. Correction is therefore needed to overcome that foreshortening.

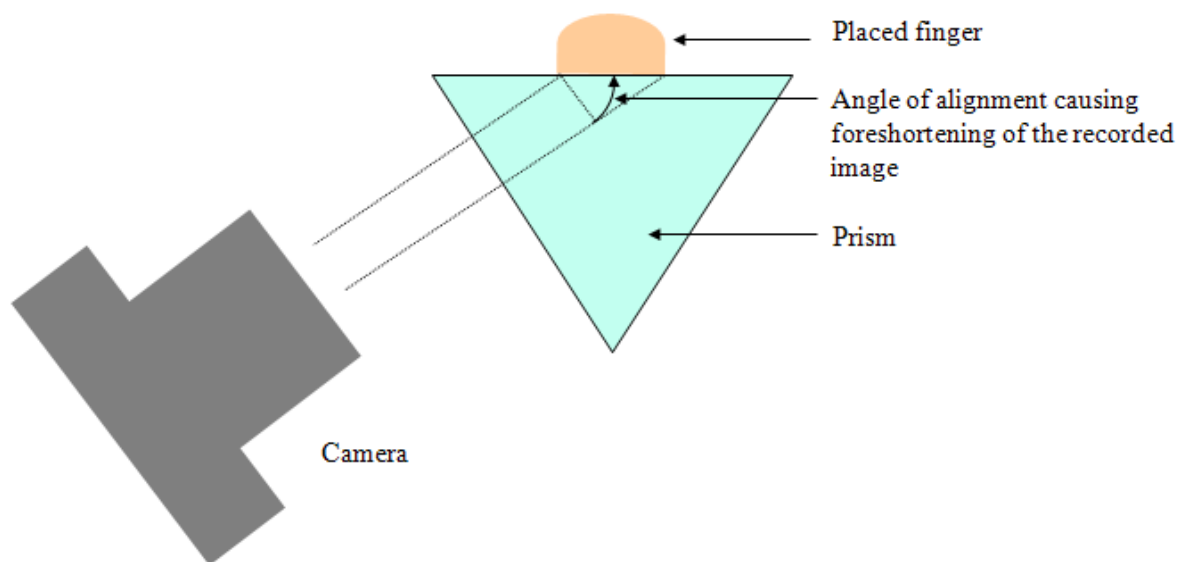


Figure 13 Schematic diagram showing the cause of foreshortening in an acquired image

The degree of foreshortening can be calculated by placing an item of known proportions (in this case a square piece of rubber) on the prism and measuring the resultant image. Measurements taken for X and Y dimensions as per Figure 14, give a relationship between the x and Y values for the recorded image. In reality, the X and Y values for a square are equal; however, given the foreshortening, the Y value will be less than the X. Once

measured, the foreshortening can be overcome simply by enlarging the image in the Y direction by a factor of X/Y . This correction was achieved using a script in V++. This, however, does not overcome all of the systemic distortions in the optical configuration employed.

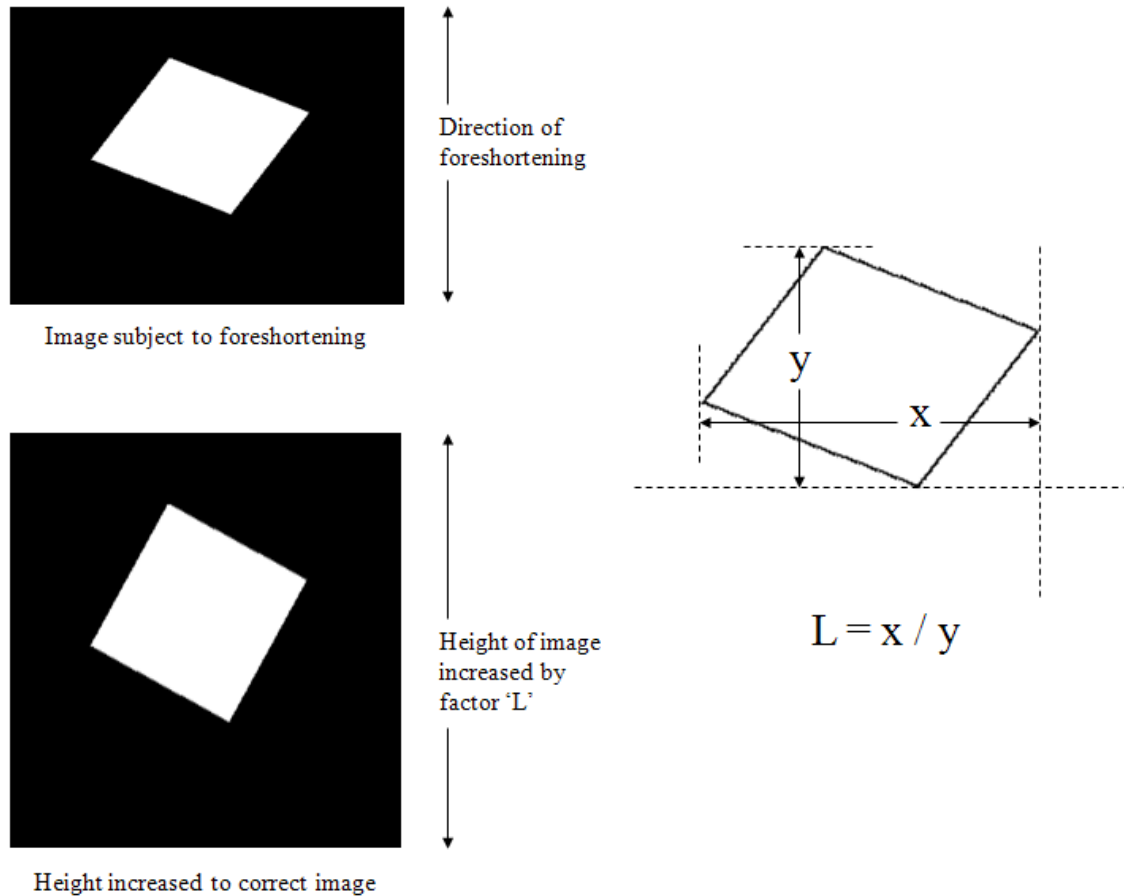


Figure 14 Method of foreshortening correction

3.3.3 Correction of non-linear systemic distortion

Systemic non-linear distortion was overcome by geometrically adjusting the images to a target image. To ascertain the degree of systemic distortion present, an image was acquired of a laminated section of 1mm-scale graph paper. To allow the refraction process to take place to record the image, a thin layer of hair gel was placed on the prism to simulate

perspiration. The graph paper was pressed firmly onto the prism to expel excessive gel and keep the graph paper flat on the prism.

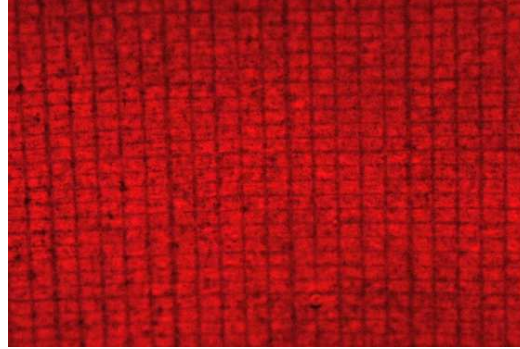


Figure 15 Image acquired of the 1mm-scale graph paper

The acquired image (see Figure 15) was processed to overcome the foreshortening in the Y dimension. A target image was then created with a grid of the same frequency as the graph paper in the acquired image. The V++ software contains a warping function that allows an image to be geometrically mapped to another image. This requires the placement of corresponding “control points” on each image in the same order and marking corresponding features. The graph paper image and the target images then had control points added as per Figure 16.

The graph paper image was then geometrically corrected using the V++ “warp” function resulting in the images shown in Figure 17. In essence, the function forces an alignment of the control points and, in doing so, distorts the selected image. This distortion process corrects the systemic non-linear distortion present in the acquired images.

The uncorrected images of the graph paper and of the generated target were saved as reference images for the batch processing of fingerprint images.

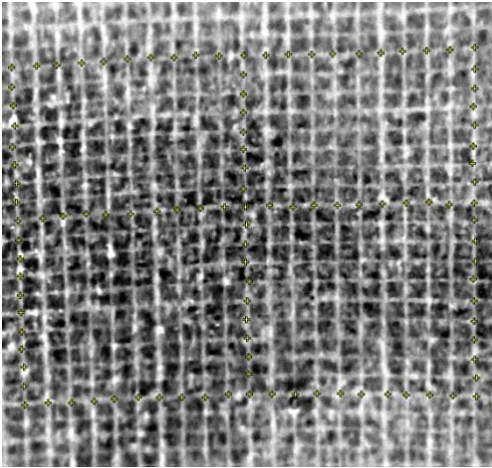


Figure 16a Graph paper image with foreshortening corrected, with control points

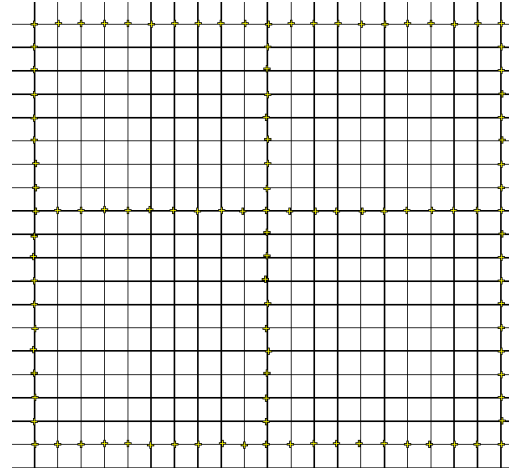


Figure 16 b Target image with corresponding control points

Figure 16 Graph paper image and the target image

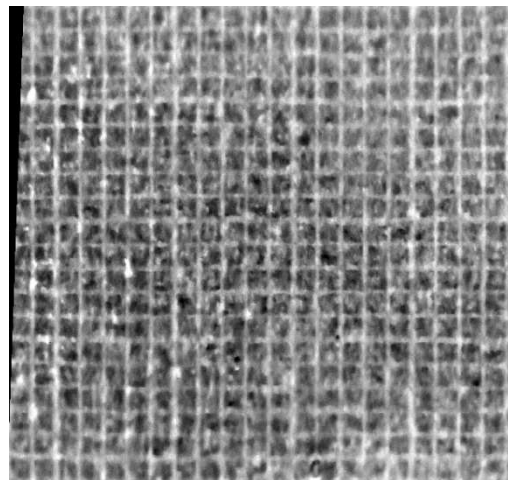


Figure 17 Graph paper image corrected for systemic non-linear distortion

The images were opened using a VPascal script and the locations of the control points used for systemic distortion correction.

3.3.4 Image processing summary

The images acquired on the prism were processed using VPascal to:

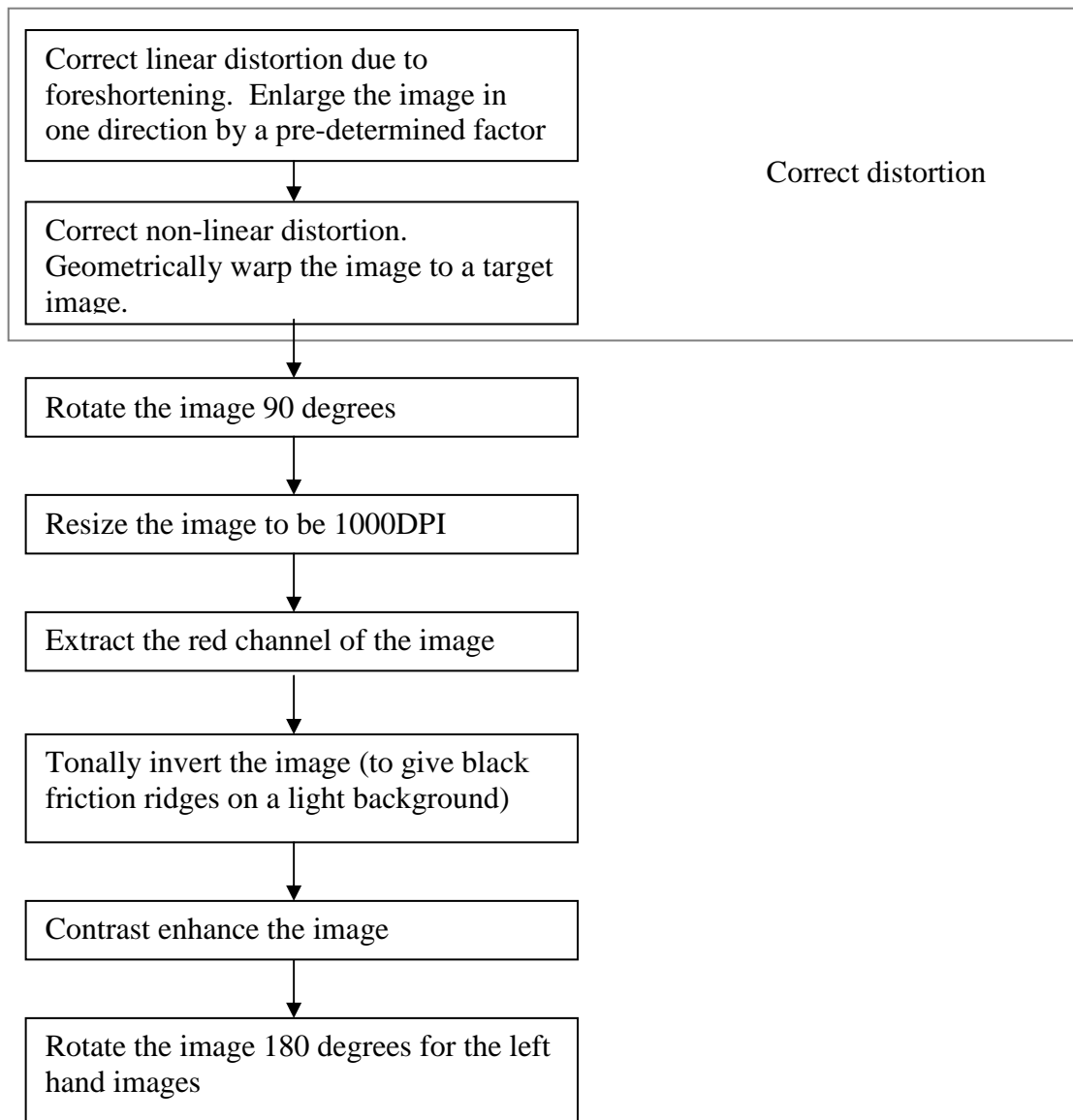


Figure 18 shows an example of the originally acquired image and the product of the processing. See Appendix 2.1 for the VPascal script.



Figure 18a Original acquired image



Figure 18b Corrected and processed image

Figure 18 Acquired and processed images

The images of the skin contact areas acquired through the prism were viewed as if the finger was viewed and not the mark. The implication of this is that the prism-acquired images and those obtained from inked impressions or AFIS systems will be mirror images. It therefore required that one of the sets of images needed to be mirror (reflected) images of their originals.

3.4 Acquisition and processing of images– between-source images

The images acquired through the NAFIS were processed using VPascal to:

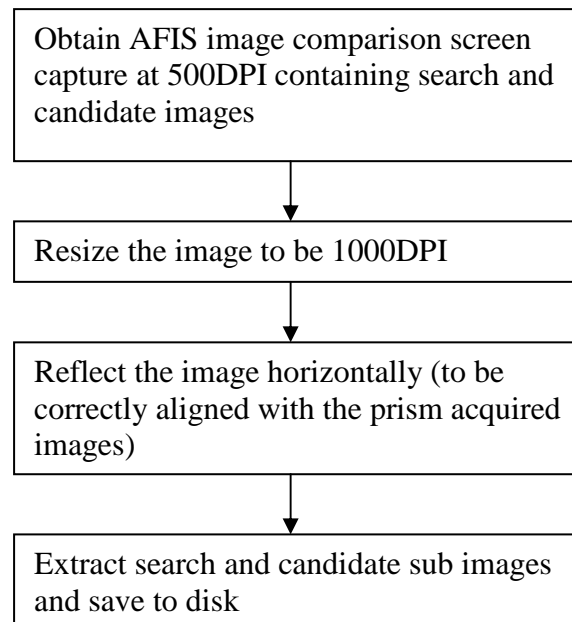


Figure19 shows the screen capture from NAFIS and Figure 20 shows the extracted and processed images. See Appendix 2.2 for the VPascal script. The NAFIS images include green minutiae markers that indicate the location and direction of the NAFIS nominated corresponding minutiae.



Figure 19 Screen capture of a NAFIS comparison

These NAFIS marked minutiae are the basis for the between-source data. Note that the images in Figure 19 and Figure 20 are from the same source and, in this instance, do actually correspond.



Figure 20 Extracted images of search image (left) and candidate image (right).

Note the corresponding minutiae marked with the green markers.

3.5 Comparison of images and generation of data

A “normal” reference image was used as a control to compare against the within-source distorted images and the between-source images. The normal images were a straight impression of the finger as normally placed on the prism without any introduced distortion. An example of this is shown in Figure 21.



Figure 21a Reference image



Figure 21b Distorted image due to rotational movement of the same finger

Figure 21 Sample images: reference (normal) and distorted

Distorted images were compared with the reference image obtained from the same finger. The sets of images had coinciding areas of skin recorded and the related minutiae marked in the same order.

3.5.1 Method for marking of minutiae

The generic file format for V++ is Tagged image File Format (TIF) for which the authoring company Digital Optics have registered proprietary tags for “flags”. Flags in V++ are small crosses that can be superimposed on an image at the location selected by a mouse click. They do not change the image data but appear superimposed on the image where the mouse is clicked. Flags that are placed on images and saved as TIFF through V++ retain the flags in the saved image.

Note that not all minutiae that exist in an image will be used as they may not appear in all other images of the same fingerprint, due to the movement of the finger possibly causing an area of the finger to no longer be in contact with the prism as shown in Figure 22

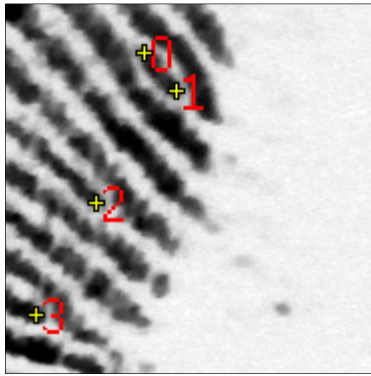


Figure 22a Segment of a left index finger image with four marked minutiae

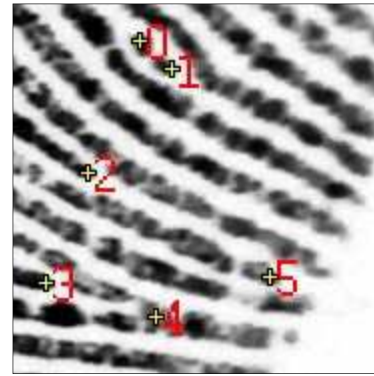


Figure 22b Segment of another left index finger image from the same finger with more minutiae visible.

Figure 22 Two images of the same finger showing a difference in available minutiae.

showing a section of two images of the same left index finger. Figure 22a shows four marked minutiae whereas Figure 22b shows the same finger rolled slightly further to one side resulting in two more minutiae contacting the prism. In this instance, not all minutiae can be compared. Areas where minutiae may not appear will be at the edges of the finger contact area.

Flags were manually placed on the images, on ridge endings, bifurcations and dots, in accordance with basic rules. The flags were placed manually as opposed to an automated process, as the practical application of the model under development would require an examiner to mark minutiae as they normally do according to current protocols. Where automated feature recognition is employed by systems such as AFIS, manual correction of the automated process should always take place as minutiae are often falsely placed where there is background noise or the impression is weak.

The regime for marking minutiae in this research is consistent with established regimes in that it borrows rules, but not all. It does not adhere to no one method alone. In reality, it does not matter what the regime is, as long as it is applied consistently by the examiner for both the mark and the reference images. Note also, that there is no concern about consistency of marking the regime between examiners, because we are not comparing images marked by different examiners, we are comparing images marked by one, and that examiner should be consistent.

Ridge endings: Based on an assumption that all friction ridges end in a similar manner and that the ending is round in shape, the flags were placed at the centre of an imaginary circle that approximately fitted the end of the ridge as shown in Figure 23.

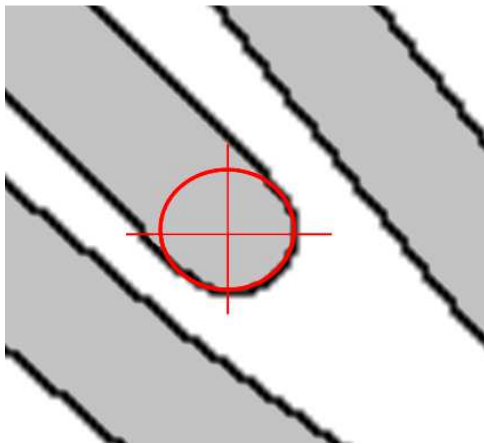


Figure 23a A circle that fits the end of the friction ridge has been superimposed on the ridge and the centre of the circle marked by crosshairs.

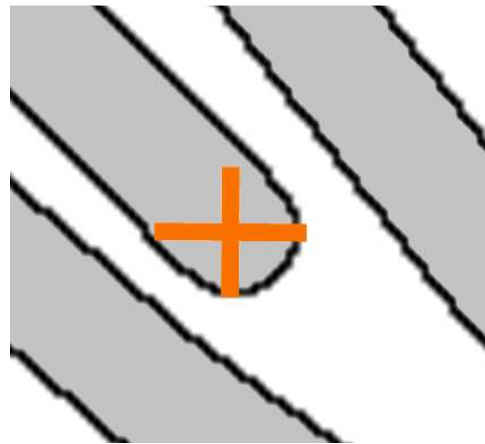


Figure 28b A flag has been placed on the intersection of the crosshairs at the centre of the circle.

Figure 23 Diagram showing the method for placing flags on ridge endings

Bifurcations: The flag is placed at the intersection of imaginary lines that run along the centre of the joining friction ridges as shown in Figure 24.

Dots: The flag was placed at the centre of the dot. The centre is defined as the intersection of the lines of the two axes, (length and breadth) as shown in Figure 25. It should be noted that not all friction ridges are the same in shape and that approximations were needed in some instances. It is also expected that the placement of markers or flags in any comparison process, as carried out by a fingerprint examiner, will be influenced by previous training with various AFIS systems and training with manual classification systems, which can both influence the interpretation of a fingerprint and the location marking of minutiae.

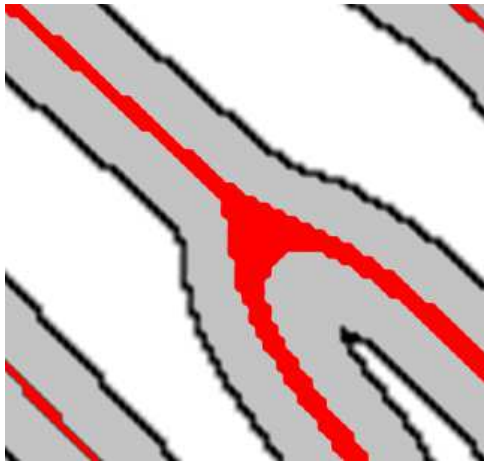


Figure 24a Bifurcating friction ridges with lines along the centre of the ridges. The lines intersect in the middle of the joining area of the bifurcation. The flag is placed at that intersection.

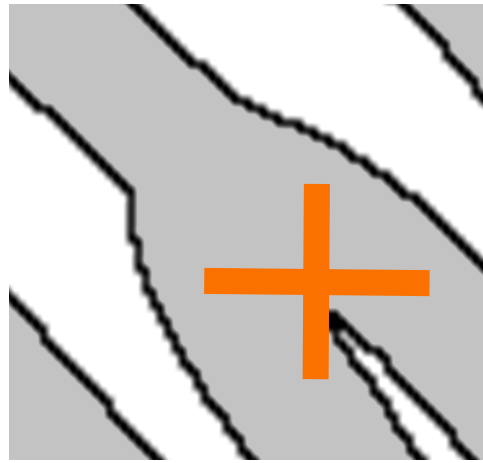


Figure 24b A flag placed on the bifurcation

Figure 24 Diagram showing the method for placing flags on bifurcations

What is most important is that the method for the marking of features is consistent for the one examiner. If compared fingerprints are marked consistently, then the model as described here will give reproducible results.

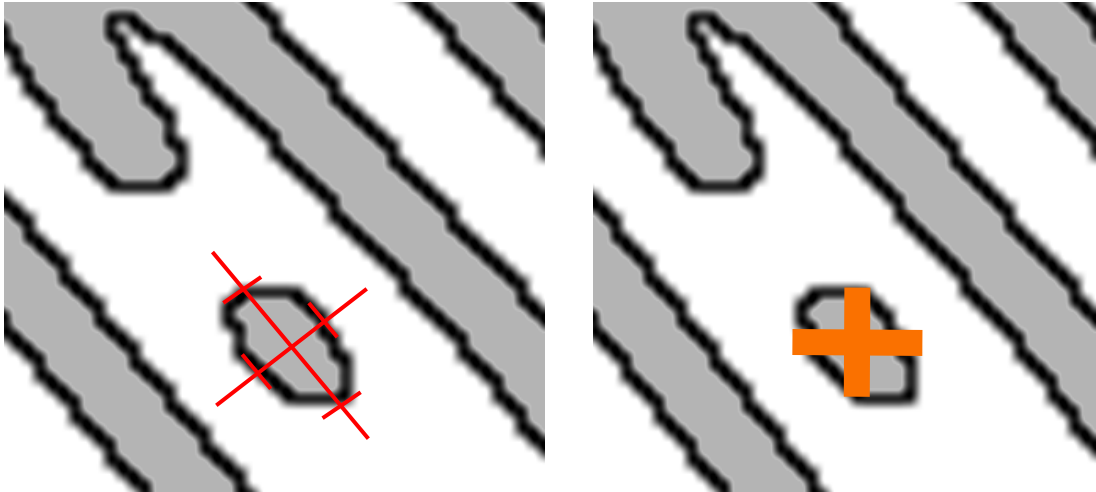


Figure 25a Two lines placed on the dot represent the longest and shortest axes of the dot. The flag is placed at that intersection. Figure 25b A flag placed on the dot.

Figure 25 Diagram showing the method for placing flags on dots

At times there are differences in appearances for the same minutiae as reproduced in different impressions. An example of this is where it appears that, in one impression, a ridge ending occurs and in another impression a bifurcation appears. This can legitimately occur where there is a variation in pressure or perspiration on the surface of the finger (Maltoni, Maio, Jain, & Prabhakar, 2005). With greater force, friction ridges expand and can be seen to join to adjacent ridges. Where this occurs, the compared images need to be marked in a manner that is consistent, being cognisant of the difference in appearance.

Figure 26 shows a schematic diagram of friction ridges with three minutiae marked. Minutiae 1 and 2 show a ridge ending and a bifurcation, respectively, in both images.

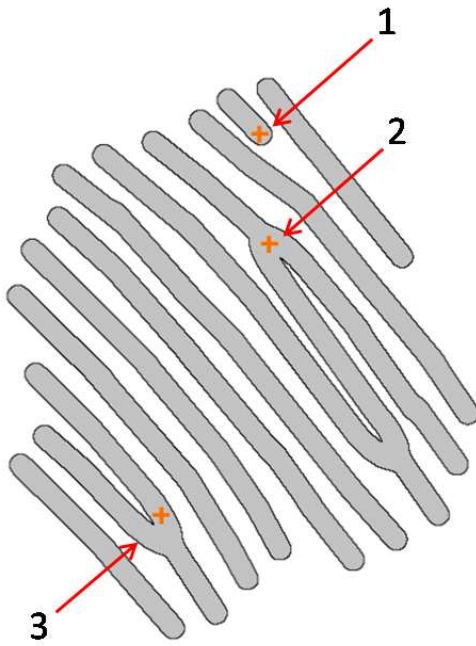


Figure 26a Minutiae flagged as 1: ridge ending, 2: bifurcation and 3: consistent with a ridge ending in the compared impression.

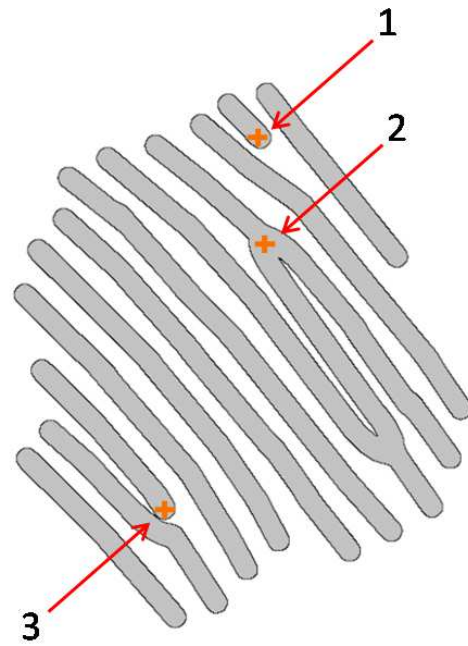


Figure 26b Minutiae flagged as 1: ridge ending, 2: bifurcation and 3: ridge ending

Figure 26 Diagram of showing a difference in the placement of a minutia.

Minutia 3 in both images correspond, that is, they have been made by the same area of skin, but appear differently. In Figure 26a it appears as a bifurcation and in Figure 26b as a ridge ending. The placement of the flags is consistent in both. The decision to mark them both the same (as ridge endings), is based on the examiner's interpretation of the impressions and the examiner must be prepared to explain such a decision. Not to mark them consistently would undermine the proposed model.

To obtain between-source data, the AFIS nominated candidates for comparison and the AFIS nominated "corresponding" minutia were used. The minutiae were manually flagged as shown in Figure 27 by placing the flag in the middle of the AFIS marked minutiae.

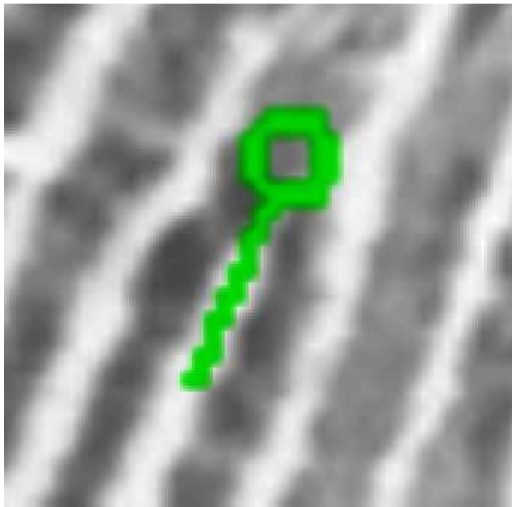


Figure 27a Minutia nominated by AFIS. The circle indicates the minutia position and the “tail” indicates the direction of the minutia.

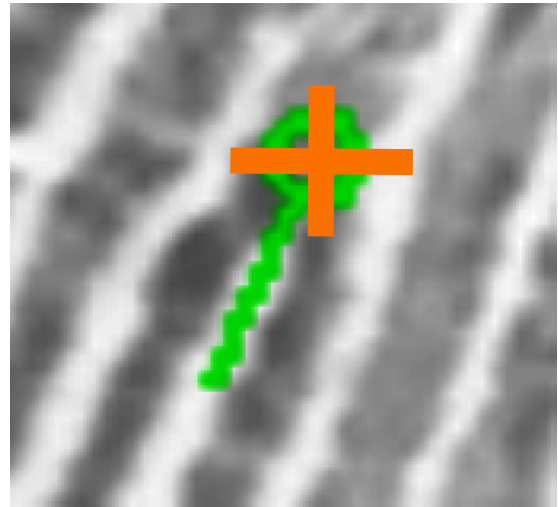


Figure 27b Minutia flagged according to the AFIS with the manual flag placed in the centre of the circle.

Figure 27 Example of an AFIS nominated minutia and manual flagging.

3.5.2 Collection of within-source data

Within-source data was obtained by acquiring images of known fingers, marking the corresponding minutiae, and then taking measurements. For a fingerprint examiner, such as the author, the locating and marking of corresponding minutiae in this study is a simple task as the images of the friction ridges are of high quality and have no interference from factors that affect normal finger marks, such as surface changes or variations in the strength of the latent deposit. As images being examined are from the same source, the comparison and allocation of corresponding minutiae is an easy task as the corresponding minutiae are simple to locate.

3.5.3 Collection of between-source data

Between-source data in this project is representative of what would otherwise be identification errors. This would, in terms of case work, be where an examiner has wrongly linked a fingerprint associated with a crime with the wrong individual. There are few documented examples of such errors and, as such, there is little existing material to establish between-source data. Furthermore, the instances of such errors are usually associated with a poor reproduction of the friction ridged skin on a surface, which in itself makes the minutiae difficult to locate and mark; therefore such cannot reasonably be relied on to generate robust between-source data.

To approximate erroneous comparisons, it was decided that the Australian National Automated Fingerprint Identification System (NAFIS) would be used to compare images of fingers from different sources and associated minutiae that, according to the system software, correspond to each other.

The NAFIS is designed to accept an image of a fingerprint from an unknown source and find in its database the closest matching marks. Whilst the algorithm that is used is proprietary and not public knowledge, the performance of the NAFIS indicates that it returns a list of candidates for potential owners of the fingerprint, ranked according to the location and orientation of minutiae, and the quantity of minutiae in agreement.

With the list of candidates returned from NAFIS are images of the questioned fingerprint and the associated candidate's fingerprint. Superimposed on the images are the minutiae considered to be in agreement. These minutiae can then be used to generate data for between-source finger comparisons.

As a database, the main function of the NAFIS is to store records, retrieve records and enable a search to compare records. A search that is performed has parameters that can be used to reduce the size of the search. These parameters include friction ridge pattern classification, gender of the owner of the fingerprint, nomination of which finger left the mark, and the geographic region from which it is suspected that the owner of the fingerprint resides.

Modification of any of the parameters except the geographic region could have an effect on the data generated. If, for example, it was sought to generate between-source data that is representative of random persons, then gender and pattern classification need to be left unassigned, otherwise the results will be biased in that we may return records that are closer to the submitted fingerprint. For the purposes of this project, no search parameters were set and only records owned by the Australian Federal Police were accessed (for reasons of practicality and legality).

The NAFIS can be used in a number of ways as a searching tool for fingerprints. Two such methods, “open” and “closed” searches can be utilized for between-source image selection depending on the rationale. Open searches are a one-to-many query where the source is not known; Closed searches are a one-to-one query or a verification.

Open searches compare the submitted fingerprint with all records in the selected regions of the NAFIS database. In terms of between- source data collection, this does provide useable data, however, the candidates returned will be a product of the NAFIS’s function, in that it is designed to find records that have similarly placed and oriented minutiae. This candidate selection process is not truly random and will possibly bias the data and show between-source variation that is more similar to within-source than it should be in reality. If random fingers

were selected outside of the NAFIS and compared, then a closed search (a comparison in the NAFIS against that one selected finger) could be conducted. It is expected that there would be greater variance in the between-source results. This, however, has not been tested or otherwise verified.

The results from any NAFIS search can display minutiae that are in agreement (corresponding), minutiae not in agreement, or show all minutiae. It therefore must be acknowledged that not all minutiae in the known finger or in the candidate finger will be used in this study. There is no issue in this in that the between-source comparison is only simulating an error in identification (i.e. looking at similarities, not differences).

3.5.4 Order of minutiae examined

The data collected relied on the images being marked to show the location for each minutia of interest. When the images are compared, the minutiae compared have to be in the same order and, where the nearest two minutiae have to be nominated, the nearest two had to be the same for all images, including the reference image. The marking of the minutia was a manual process where no “pairing” algorithm was used to associate corresponding minutiae in the marked images. To this end, a “distance map” was created for each reference image. This was created through a V++ script (see Appendix 2.3) and produced a $n \times n$ image where n is the number of marked minutiae. The image has pixel values in the first column (0) representing the minutiae numbers 0 to n and columns 1 to n having pixel values representing the nearest, next nearest to the n th nearest minutiae. The distances image as shown in Figure 28 can be referenced simply in a V++ script to find an order of nearest minutiae and apply the same order to other images being compared.

For example, if we use the distance map in Figure 28, the pixel value for Distances [7, 2] equals 24 indicating that the seventh nearest minutia to minutia 2 is minutia 24. Note that the origin of the image is at the top left and has coordinates [0,0]. In this example, the pixel at [7,2] is at the intersection of the 8th column and the 3rd row.

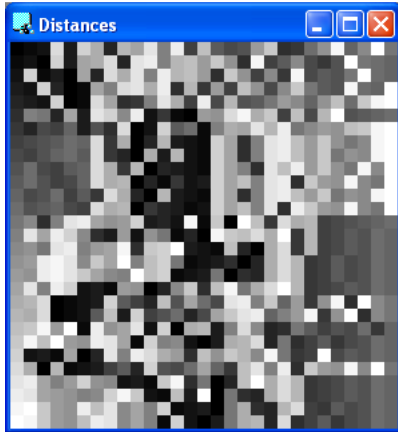


Figure 28a Distance map for the reference image for the left index finger

0	1	2	24	3	23	19	4	20	18
1	2	0	23	3	18	19	24	4	25
2	23	1	3	0	18	4	24	19	25
3	2	23	4	0	1	18	14	24	25
4	3	2	23	0	1	24	18	5	6
5	14	13	4	18	3	25	23	15	26
6	4	8	7	11	3	9	5	24	0
7	8	9	10	12	11	24	6	19	0
8	7	9	11	12	10	24	6	4	0
9	12	8	7	10	11	24	19	6	20
10	12	9	7	8	11	24	19	20	0

Figure 28b A section of the numerical values for the distance map containing the first ten columns and rows only. The first column represents the minutiae numbers in the order marked. The rows from the second column onwards represent the other minutiae in terms of nearest to furthest away.

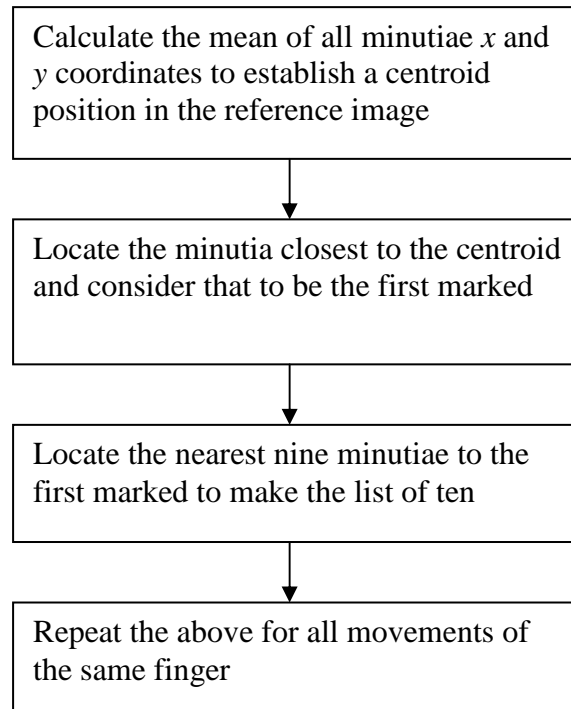
Figure 28 A distance map for the left index finger and corresponding pixel values.

When measurements were taken from a reference image, a distance map was created. When a distance map was created from an image to be compared (within-source or between-source) the distance map was referenced to ensure that the order was the same for compared minutiae.

3.5.5 Selection of minutiae for measurement

The reference image for each finger was opened with images of all movements of that finger. All corresponding minutiae were marked on all images and in the same order.

Whilst all minutiae were marked, data from only 10 minutiae were extracted. The selection of minutiae was done by marking all corresponding minutiae and then selecting the ten nearest minutiae to the centre of all the minutiae. The following flowchart demonstrates this process.



The ordered list of ten marked minutiae was generated for the reference print, and the referenced minutiae and their order used to select minutiae for all other images from the same finger. This ensured that the measurement and comparison of within-source variation was done with respect to the same minutiae in each subsequent image. This therefore indicated what variance occurred within each minutia for all images of each finger.

Figure 29a shows the reference image for a left index fingerprint with 28 minutiae marked. Once marked, the Cartesian coordinates can be extracted from the minutiae thereby allowing measurements to be taken. Figure 29b shows the minutia number and the coordinates for the first ten minutiae closest to the centroid. The numbering of the minutiae was an automated process done in V++ with a script. See Appendix 2.7 for the script.



Figure 29a The reference image of an index finger with numbers indicating the location of the selected minutiae. The number has been superimposed on the image to the immediate right of the marked minutia.

min #	X coord	y coord
0	344	542
1	360	584
2	327	588
24	348	472
3	287	585
23	314	618
19	410	490
4	234	562
20	255	464
18	321	682

Figure 29b Coordinate data taken from the first ten central minutiae in Figure 29a.

Figure 29 Marked minutiae for a left index fingerprint and coordinate data.

Figure 30 shows a section of a left index fingerprint with minutiae marked with flags and the minutia numbers superimposed.



Figure 30 Section of image BC_LI_ref displayed in V++.

Flags are placed marking minutiae and with minutia numbers superimposed.

3.5.6 Measurements from selected minutiae

For each selected minutia, the nearest two minutiae were nominated through measurements of distance from the minutia of interest to all other minutiae. This was based on the positions of the minutiae in the normal image.

Each selected minutia M had the following measurements calculated:

- Distance D1 to its nearest neighbouring minutia N1
- Distance D2 to its second nearest neighbouring minutia N2
- Angle A being the angle subtended by the rays $\overline{MN1}$ and $\overline{MN2}$.

Figure 31 shows a schematic representation of the three minutiae and the measurements extracted.

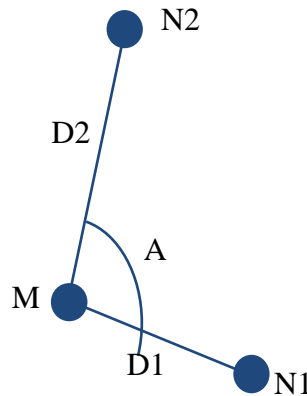


Figure 31 Schematic diagram of a minutia (M) and the two nearest minutiae (N1 and N2).

Measurements extracted are D1, D2 and A.

The rationalisation for these three measurements is that a change in position of minutiae in fingerprints from the same source is a result of the stretch of the skin.



Figure 32a Minutiae plotted on the left index finger

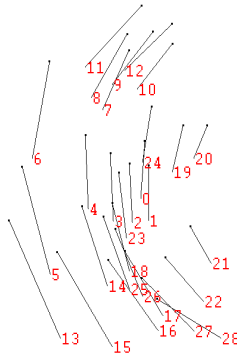


Figure 32b Lines drawn indicating the change of position in the corresponding minutiae



Figure 32c Minutiae plotted on a within-source image rotated clockwise

Figure 32 Plotting of the change in minutiae position; within-source.

The change is from the reference image of the left index finger to an image of a within-source fingerprint under clockwise rotation. The numbers in Figure 32b correspond to the reference image minutiae positions and the lines indicate the change of their position to that in Figure 32c.

The change of position of minutiae across the surface of the skin due to distortion varies incrementally (Dinning 2005) and, on this basis, it is suggested that there is a limit to how much this change can be, and that the change should be gradual and consistent across the skin in terms of the amount of movement (distance) and the angle of that movement. Figure 32b shows an example of the change in position of minutiae in compared images of fingerprints from the same source. It can be observed that the relative change in position between proximal minutiae is gradual. Figure 33b shows an example of the differences in position of minutiae in compared images of fingerprints from different sources. It can be observed that the apparent change in position between proximal minutiae is not gradual and appears to have little consistency.



Figure 33a Minutiae plotted on the left index fingerprint

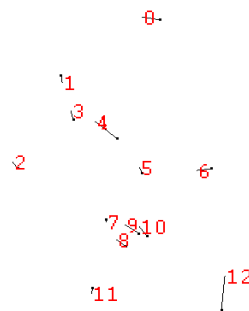


Figure 33b Lines drawn indicating the change of position of the corresponding minutiae

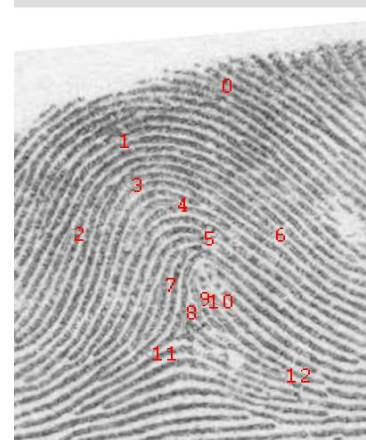


Figure 33c Minutiae plotted on a between-source image with no movement

Figure 33 Plotting of the change in minutiae position; between-source.

The change is from the reference image of the left index finger to an image of a between-source fingerprint. The numbers in Figure 33b correspond to the reference image minutiae positions and the lines indicate the change of their position to that in Figure 33c.

The relative positions of proximal minutiae and, in this case, one minutia and its nearest two neighbours can be ascertained through triangulation. This is adequately described using the two distances (D1 and D2) and the angle (A). It is proposed that differences in positions of minutiae in fingerprints from different sources will be greater than for within-source fingerprints.

The choice of measurements extracted relate directly to some of the information in the images that a fingerprint examiner will state that they use during the comparison of two fingerprint images. The examiner will compare:

- Type of minutia. This is a discrete variable that can change with pressure variation so is not used in this project.
- Relative position. This can be accounted for with the triangulation of minutiae using D1, D2 and A.

- Number of intervening friction ridges between compared minutiae. This is proportional to D1 or D2 as the widths across a friction ridge can reasonably be assumed to be constant when comparing proximal minutiae.
- Direction of minutiae. It could be argued that the direction of corresponding minutiae is similar in the compared fingerprint images as they will be coming from corresponding areas of the fingerprint due to the expected ridge flow, so there is limited value in this variable. Furthermore, there is limited change in angle expected from localised skin stretch. This is not used in this project.

3.6 Errors generated by using digital images for measurement

The term digital image refers to a two dimensional light intensity function $f(x, y)$, where x and y denote spatial coordinates and the value of f at any point (x, y) is proportional to the brightness of the image at that point (Gonzalez & Woods, 1992). The values of f in the image define the tonal values of the images. The rate of change of the values for f allows the definition of edges and shapes in the image.

Based on the visible shapes, minutiae in a fingerprint image are visible and accordingly, their locations can be determined and marked.

Since spatial dimensions in an image are discrete, there is an inherent limited ability to resolve precise locations in an image. Precision of measurements based on pixel locations will be limited by the image's dimensions and be described by a pixel's Cartesian coordinates.

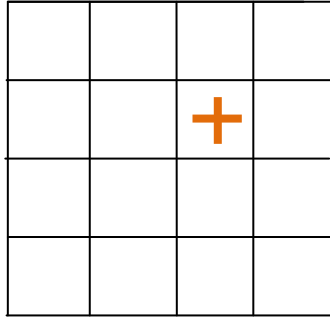


Figure 34a The location of a feature in an image is represented by the centre of one pixel in a Cartesian plane, as indicated by the placement of the cross.

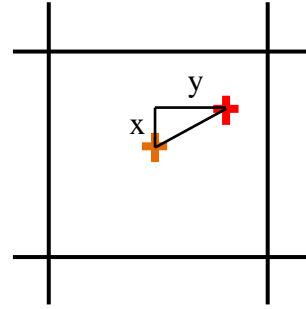


Figure 34b The difference between the centre of the pixel (orange cross) and an actual location (red cross) is represented by x and y . The magnitude of x and y cannot be established based on image measurements alone.

Figure 34 Marking a point inside a pixel's area.

The marking of minutiae on an image is representative of the true location with a degree of error. It is not exactly where the point of interest is.

Each pixel in an image represents not a point, but an area in the field of view of the image. The point that may be nominated as the location of a minutia will fall inside the area of one pixel, which will have coordinates represented by integers. The real location of the point within the pixel cannot be described in more precise terms other than the coordinates of the pixel.

The precision of the location of a marked minutia in an image is therefore limited by the size of the area that the pixel represents. The point in the pixel at which the measurement is taken can be considered to be the centre of the pixel. There is, for each measurement of an angle defined by three minutiae, or, by the distance between two minutiae, a degree of error that can be calculated.

3.6.1 Potential error for distance measurements

The measurement of distance between two marked minutiae is easily calculated using Pythagorean calculations as in Eq. (3.2):

$$distance = \sqrt{(x_2 - x_1)^2 + (y_2 - y_1)^2} \quad (3.2)$$

where the x and y values represent the pixel coordinates for the marked minutiae M1 and M2 as shown in Figure 35. The maximum error that can be included in the location of one minutia is half the distance across the diagonal of the pixel. Assuming that a pixel is square, this diagonal equals half the square root of 2 which is approximately 0.707 times the length of the pixel side. Since the measurement requires the marking of two pixels, the potential error for a measured distance will be plus or minus approximately 1.41 times the length of the pixel side.

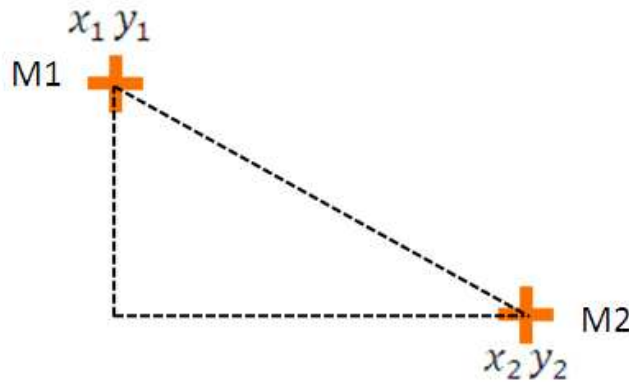


Figure 35 Measurement of distance between two minutiae (M1 and M2).

This requires the marking of the minutiae at given pixel locations; the pixel's position is defined by its x and y coordinates.

The minimum value that the actual distance can be is calculated by Eq. (3.3)

minimum actual distance

$$= \sqrt{((x_2 - 0.5) - (x_1 + 0.5))^2 + ((y_2 - 0.5) - (y_1 + 0.5))^2} \quad (3.3)$$

and the maximum actual distance is calculated by Eq. (3.4).

maximum actual distance

$$= \sqrt{((x_2 + 0.5) - (x_1 - 0.5))^2 + ((y_2 + 0.5) - (y_1 - 0.5))^2} \quad (3.4)$$

Given these two equations, the range of possible actual outcomes and the potential error in any distance measurement can be calculated as the difference between the minimum and maximum distance values. The actual distance will be within this range.

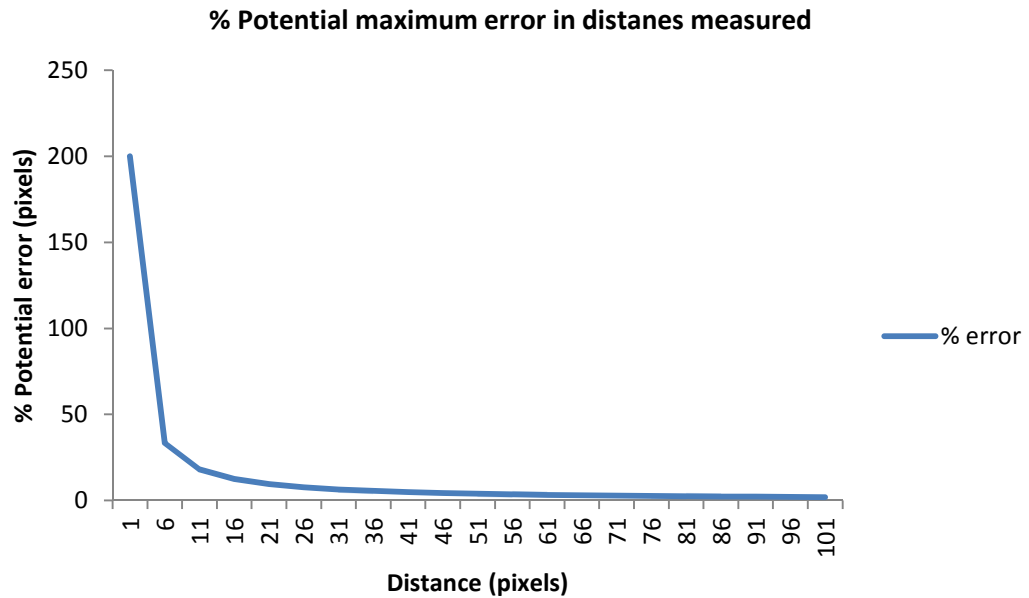


Figure 36 Potential maximum error described as a percentage of the distances measured.

In all cases of measured distance between two minutiae (in pixels), the error will not exceed two times the square root of two, which is approximately equal to 2.83. As the measured distance increases, the significance of the error (i.e. as a percentage of the measurement itself) diminishes as can be seen in Figure 36.

It can be seen that, for distances beyond 40 pixels, there will be less than 5% error occurring. Note that the slope of the percentage error function is low above a distance value of approximately 20 pixels.

3.6.2 Potential error for angle measurement

The measured angle of a ray between two minutiae is limited to a number determined by the distance between the minutiae. This is due to the discrete nature of pixels and their limited precision when being used to measure spatial arrangements. I established a simple method is to determine the number of possible angles that could be described between two minutiae, is to calculate how many pixels exist in the perimeter of pixels at the measured distance between the two minutiae. If the length of the ray is 1, as in Figure 37, it can be seen that there are only 8 possible angles that can be measured.

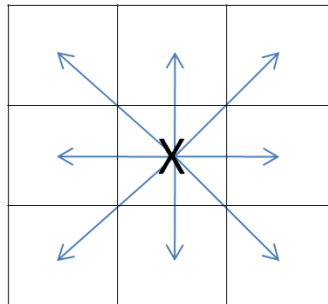


Figure 37 Limitations of angle measurement in the Cartesian plane.
Given a distance of 1 between measured pixels, there can only be 8 possible angles as the outcome of the measurement.

As the distance between pixels increases, so does the number of possible angles. Figure 38 shows the possible angles for distances of 2 (Figure 38a) and 3 (Figure 38b) pixels. Note that the distance is not calculated by Pythagorean calculations, but by the counting of pixels in any direction.

1	2	3	4	5
16				6
15		X		7
14				8
13	12	11	10	9

Figure 38a Given a pixel “X” with a distance to the next pixel of 2, there are 16 possible angles that can result.

1	2	3	4	5	6	7
24						8
23						9
22			X			10
21						11
20						12
19	18	17	16	15	14	13

Figure 38b Given a pixel “X” with a distance to the next pixel of 3, there are 24 possible angles that can result.

Figure 38 The relationship between distance in pixels and number of possible angles.

The number of angles that can be measured from a given pixel to another is defined by the distance between the two pixels and the number of possible angles that can be measured given the number of surrounding pixels in the perimeter at that distance.

The actual angle described by a ray passing through two actual locations cannot be precisely measured using digital images. Such measurement will always have a potential error. The maximum error can be calculated by the following Eq. (3.5):

$$\text{maximum error} = \frac{360/(d * 8)}{2} \quad (3.5)$$

where d is the distance between the two pixel centres. This can be simplified to Eq. (3.6):

$$\text{maximum error} = \frac{22.5}{d} \quad (3.6)$$

The magnitude of the error diminishes as the distance between the pixels increases. This is illustrated in Figure 39.

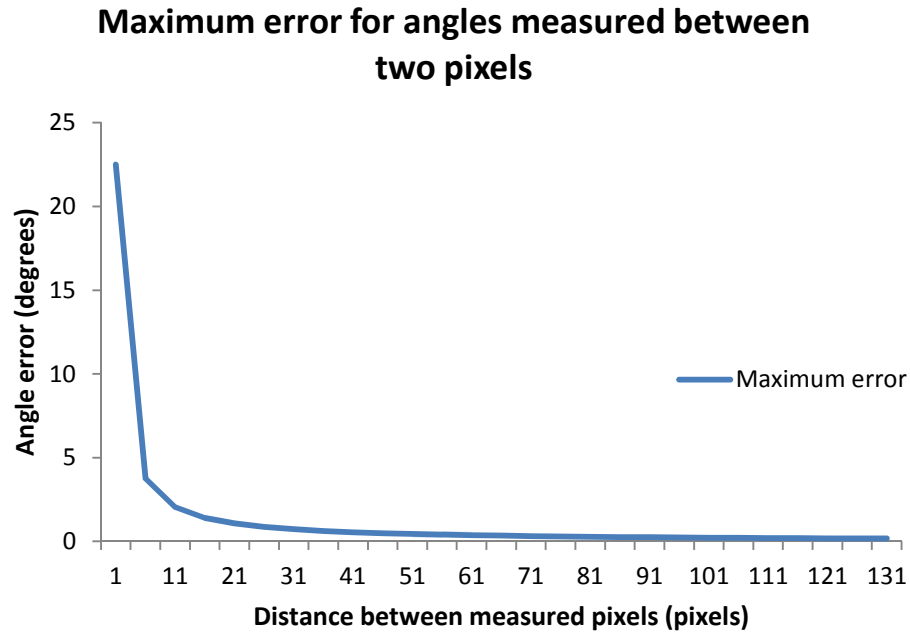


Figure 39 The amount of error in angle measurement using pixels as units.

The amount of error diminishes as the value for the distance between the pixels increases.

Given that, in this project, there are angles described by three minutiae as shown in Figure 31, the calculation of the angle involves two angle calculations. Accordingly, the degree of error is doubled as shown in Figure 40. It also shows that the magnitude of the potential error when the distances between the pixel of interest and the other two pixels exceeds approximately 40 pixels, the error will be less than 1 degree. When one distance falls below 40 pixels, the resultant error will increase. As with distance error, the slope of the function is low above a distance of approximately 20 pixels.

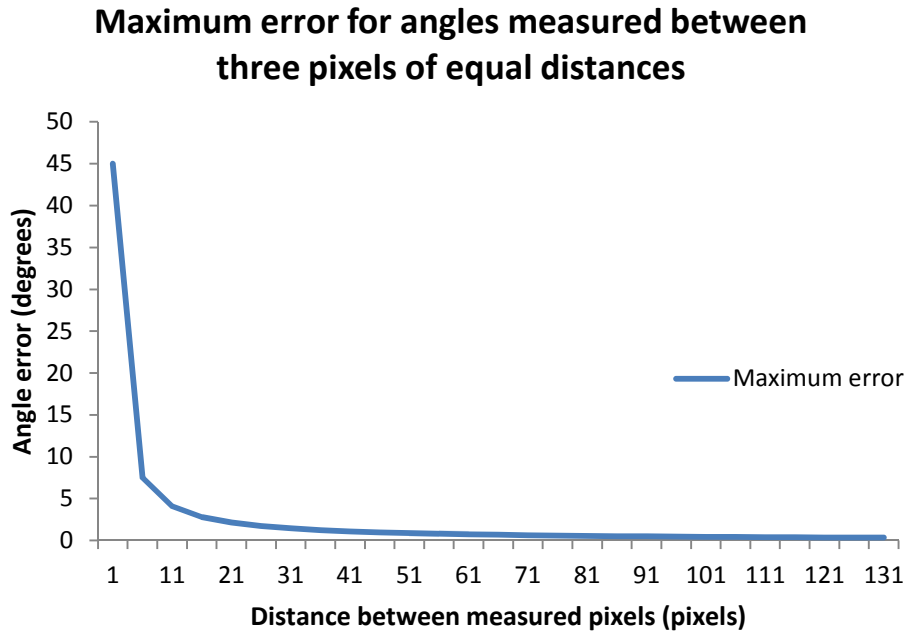


Figure 40 The amount of error due to angle measurement using three pixel locations. It is assumed in this instance that distances D1 and D2 (see Figure 31) are the same.

3.6.3 Error summary

Both distance and angle measurements are affected by errors that decrease as the distances between pixels representing minutiae locations increases. For both distance and angle measurements, the most affected values are those close to 0. Where distances exceed 40 pixels, the effect of the error is minimal. As indicated by Figure 41, the mean values for D1 and D2 extracted in this project is a skewed distribution with the mode at approximately 40. Considering the data graphed in Figures 36, 39 and 40, and their respective slopes being of a low angle from approximately 20 pixels and greater, a decision was made not to incorporate error consideration into this project's data analysis.

The degree of error caused by the digital representation may be insignificant next to the potential error caused by human markup of the compared finger mark and print. Neumann

(2007) showed a degree of variance in the placement of minutiae by different examiners (Figure 42). While this is acknowledged, this research is considers that, the variance will be minimal as any given comparison (in this research or in operational case work) will be done by one examiner and the metric is based on the one examiner's work. The between-examiner variance should not be considered.

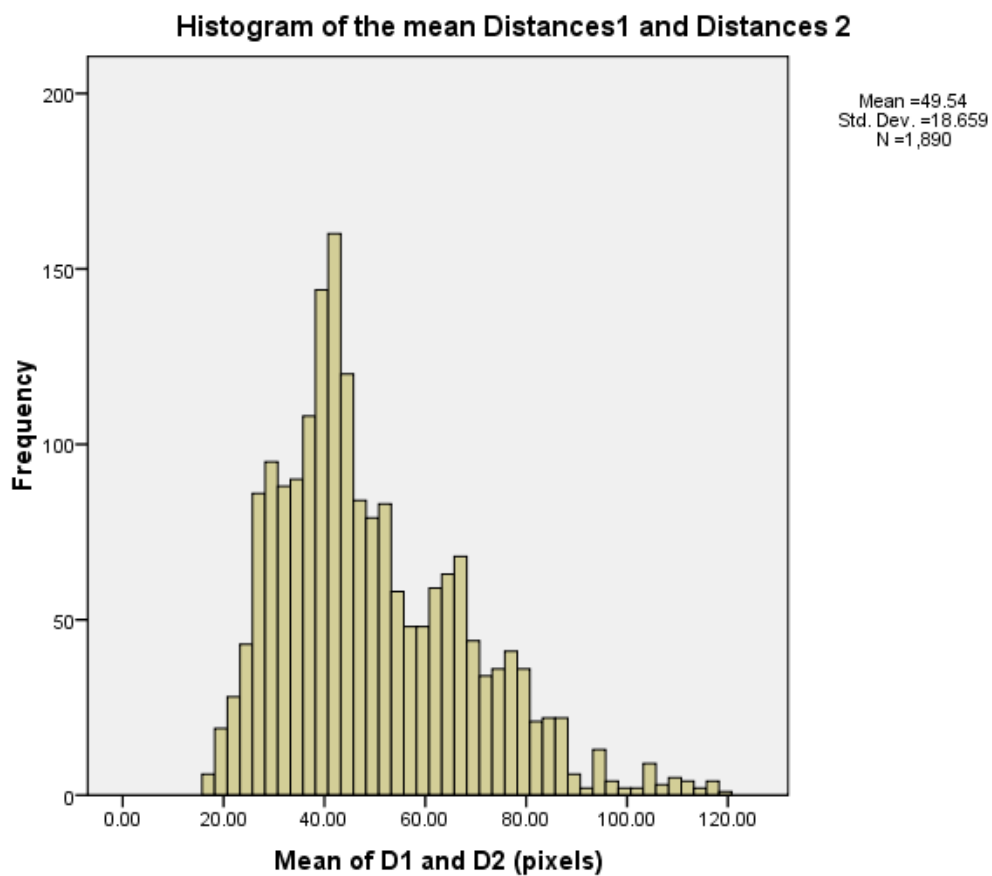


Figure 41 The distribution of means of Distance 1 and Distance 2 values.

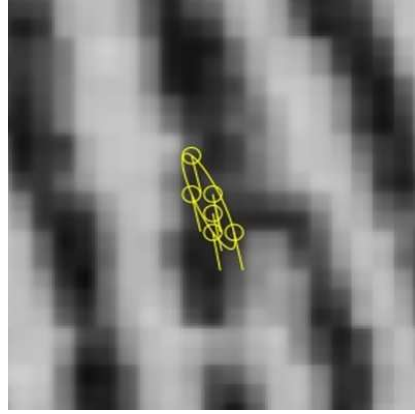


Figure 42 A bifurcation as marked by different fingerprint examiners (Neumann C. , 2007).

3.7 Data extraction

Data was extracted from marked images in the form of measurements of the distance from the minutia of interest to the next nearest minutia (D1), the second nearest minutia (D2) and the angle described by the three minutiae (A) as shown in Figure 31 , and this data was extracted using scripts in V++ (see Appendix 7.2.3).

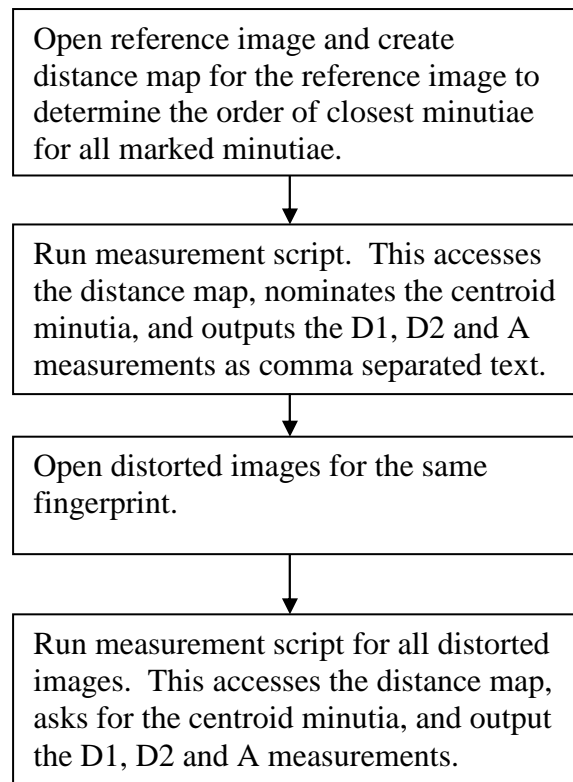
3.7.1 Within-source data

Within-source data is representative of how much variation that can occur in the location of the minutiae for the fingerprint examined. To establish this, data was extracted from a reference image that had no distortion and from a series of other images with induced distortion. The variation in the positions of the minutiae was established by calculating the differences in the extracted values D1, D2 and A, as shown below for D1 Eq. (3.7):

$$D1_{difference} = D1_{reference} - D1_{distorted} \quad (3.7)$$

One script was used to extract data from a reference image and then another to extract data from other images to be compared with the reference image. The running of the script for the reference image also returned the centroid minutiae, which needed to be nominated in the other images.

The following process was used to obtain the within-source data:



Data extracted was in the form of a text file of comma separated values (CSV) for all of the measurements. A header consisted of a row with column titles for each minutia (M1, M2, M3 ... Mn) and for measurements D1, D2 and A. For example, the column header for the measurement of D2 for the second minutia would have the header M2D2.

Since the images compared had all minutiae marked in the same order and the minutiae were compared in the order specified by the reference image distance map, the data extracted

enabled the examination of individual minutiae by comparing each minutia's measurements only with associated measurements from the same minutiae but subject to different distortions.

Figure 43 shows a sample of data from the first two minutiae for the reference image and 18 distorted images for the left index finger. The reference image data is in the first row of measurements.

M1D1	M1D2	M1A	M2D1	M2D2	M2A
32	33	120	32	42	63
29	41	136	29	41	76
29	44	144	29	34	75
30	42	138	30	33	86
36	27	133	36	42	65
37	30	127	37	39	74
33	29	121	33	41	63
31	31	133	31	38	70
29	35	132	29	36	72
31	26	156	31	38	86
36	31	122	36	40	68
39	27	118	39	44	73
39	33	106	39	43	58
38	29	122	38	44	60
36	31	114	36	41	67
40	24	125	40	42	67
38	24	133	38	41	78
25	46	114	25	38	64
25	41	122	25	36	71

Figure 43 The extracted data for within-source variation.

This was saved in the form of comma separated values and contained measurements for D1, D2 and A for minutiae 1 to n. The first row of data was extracted from the reference image and the subsequent rows from the distorted images.

3.7.2 Between-source data

A between-source fingerprint comparison is representative of a comparison of fingerprints that have come from different fingers. As there are few documented cases of comparisons of

this type, there is insufficient data readily available. In this project, AFIS nominated candidates were used and associated data extracted; however, this data could not be used as training data to determine between-source variation, because each candidate nominated does not necessarily have the same minutiae marked as being corresponding. As such, between-source model training data that could indicate between-source variance was not able to be obtained. This data could however be used for testing against the within-source variance.

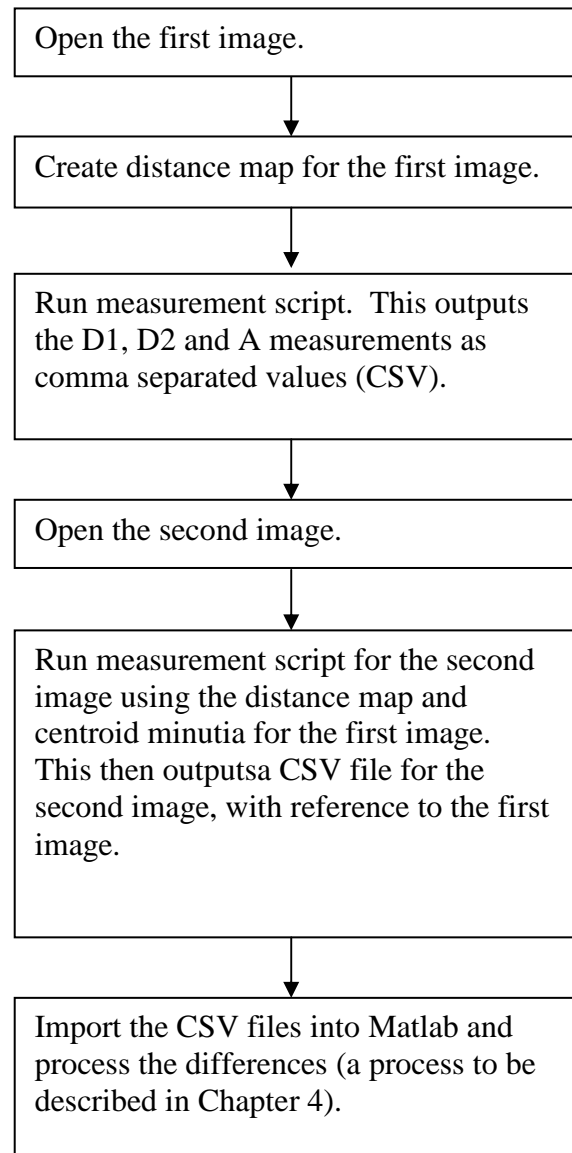
Note that, there was to be a difference in the results obtained here, as the between-source data gathered comes from comparisons of close non-matches. Typically, DNA evidence includes between-source data considering comparisons with random samples.

The results from this research is looking at data that is arguable much closer to within-source and more representative of what may in case work, constitute a potential error of identification.

3.7.3 Test case data

Any two images with corresponding minutiae can have measurement data extracted from them for comparison and testing for a probability that they have come from the same source. This is a repetition of the extraction process as previously described, resulting in two CSV files whose contents can be compared.

The process for test case data extraction was:



4. Data analysis and results

4.1 Introduction

The objective of the data analysis is to examine the differences in positions of associated minutiae in two compared fingerprint images. These differences are simply the actual values of each measured variable in a test image subtracted from the values for the corresponding variable in a reference image. Given distributions of within-source variance for the differences that can occur, any given comparison of two fingerprints where the human examiner is asserting that they have come from the same source, can have data extracted and the differences in the variables tested against the relevant distributions. The contribution of the probability distributions for each minutia will result in an indication that will tend to indicate support or not of the examiner's assertion.

In this research, data was extracted for the purpose of establishing within-source variance. Between-source variance was not able to be established; however, it is possible to test any given case of a compared pair of images against the within-source variance to find the probability density that the compared images are in fact from the same source. This then indicates the degree of support that can be given to the examiner's assertion.

This research has established a proof-of-concept model that allows for the testing of a examiner's conclusion. Data collected has been shown to distribute normally and independently. A generic mean vector and covariance matrix representing the means and variances of the differences of variables D1, D2 and A have been generated, against which test cases can be compared through the application of a multivariate normal probability density function. This chapter describes the data analysis methods used, the supporting evidence justifying the process, and the outcome.

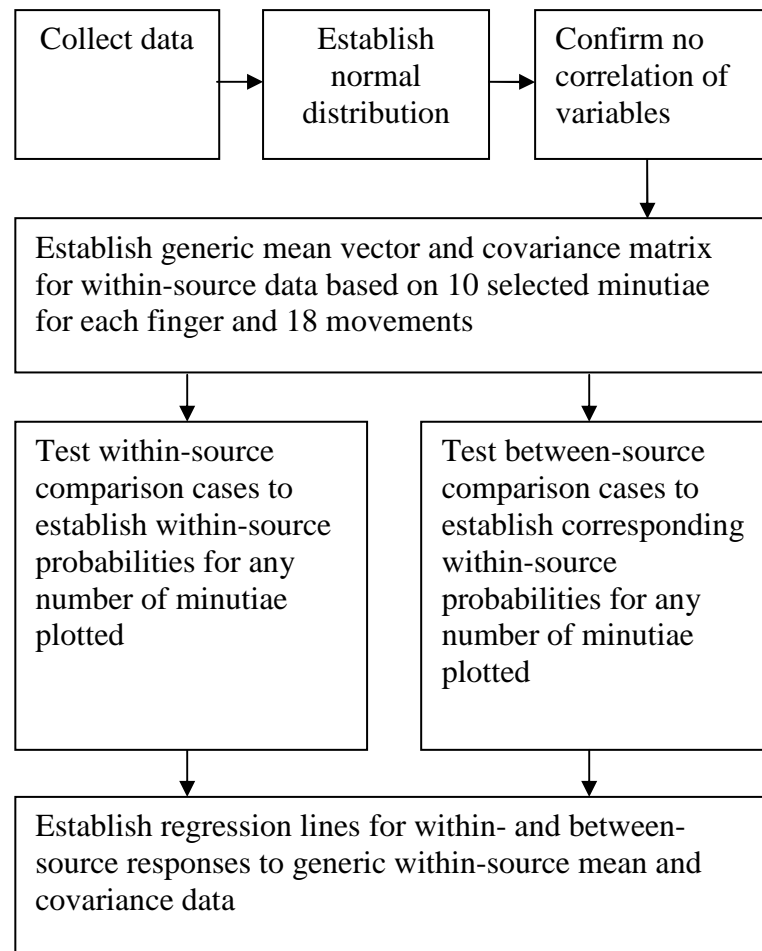


Figure 44 The process to develop the model in this project.

Data were collected from within-source fingerprint comparisons from one donor, and found to distribute normally with no correlation between the measured variables (D1, D2 and A). A generic mean vector and covariance matrix were developed that was representative of the variation that could occur due to within-source skin stretch. Data was collected from within-source and between-source fingerprint comparisons and was tested against the within-source mean and covariance matrix, to produce probabilities that the comparisons tested, were from within-source. Regression analysis was done on the within-source and between-source response probabilities to establish within- and between-source functions, against which test cases could be compared.

The approach in this chapter is to describe the data analysis process theoretically before demonstrating the practical outcomes. The general approach is summarised in Figure 44.

4.2 Use of normal distributions

A “normal” distribution is a function of a variable’s random occurrences that can be approximated by a mean value and a standard deviation. If a sample of a given variable is shown to conform to a normal distribution, then a probability of a specific occurrence of that variable can be obtained by ascertaining where that occurrence exists in relation to the variable’s distribution.

The normal (Gaussian) distribution function is described by Duda (2001) in Eq. (4.1).

$$p(x) = \frac{1}{\sqrt{2\pi}\sigma} \exp \left[-\frac{1}{2} \left(\frac{x - \mu}{\sigma} \right)^2 \right] \quad (4.1)$$

where x is the given variable value, σ is the sample standard deviation, and μ is the sample mean. Figure 45 shows an example of a single variable density distribution for a given variable with a mean value of 0 and a standard deviation of 50.

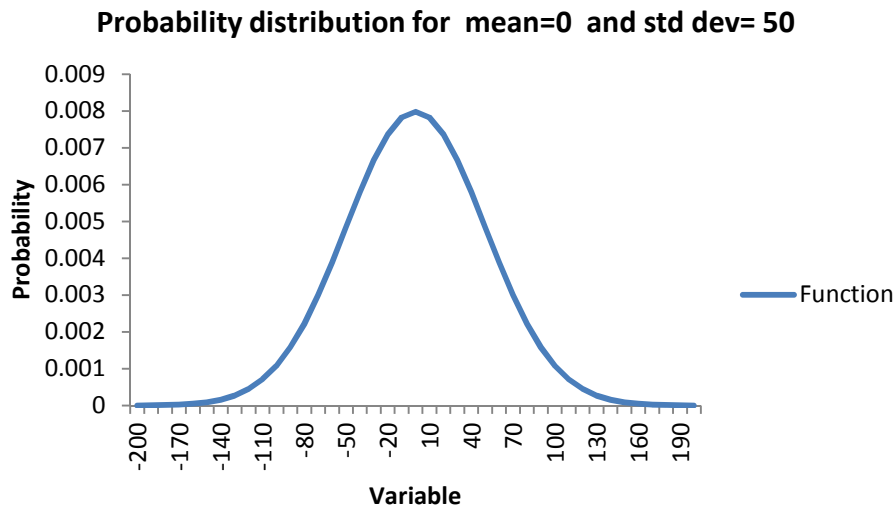


Figure 45 Normal distribution density curve.

Given the function in Figure 45, we can establish the probability density that the occurrence of a variable value will occur, given a random instance of such a variable. For example, the

probability that a value between -80.5 and -79.5 will occur is 0.002218, whereas the probability that a value of between 19.5 and 20.5 is 0.007365. This does not mean that the value near -80 will not occur, but it is more likely that the value near 20 will occur more often. Given a distribution with known mean and standard deviation we can predict the likelihood of occurrence of a specific case.

4.2 Use of multivariate normal distributions

If multiple variables occur "normally" and they are independent of each other, that is, they can vary without having any effect on the other, then the probability of these occurring together is obtained by calculating the probability of each event and multiplying the probabilities together. Probability density for the occurrences of a number of variables coincidentally can be calculated using multivariate probability density functions.

Multivariate normal probability density is calculated according to Duda (2010) in Eq. (4.2),

$$p(\mathbf{x}) = \frac{1}{(2\pi)^{d/2} |\Sigma|^{1/2}} \exp \left[-\frac{1}{2} (\mathbf{x} - \boldsymbol{\mu})^t \Sigma^{-1} (\mathbf{x} - \boldsymbol{\mu}) \right] \quad (4.2)$$

where \mathbf{x} is a d -component vector, $\boldsymbol{\mu}$ is a d -component mean vector, Σ is a d -by- d covariance matrix, and $|\Sigma|$ and Σ^{-1} are its determinant and inverse, respectively. Also note that t denotes a transpose operation. Any number of variables (as denoted by d) can be accommodated in this function. To make use of this function, it needs to be shown that the variables used firstly do not have a significant correlation and secondly distribute normally.

The approach taken in this project involves three measurements taken from each minutia and its nearest two other minutiae. These are taken from the difference in measurements of D1,

D2 and A (as seen in Figure 31) for each minutia examined in two compared images. Thus, each minutia provides us with a three element vector:

$$\{D1_{diff}, D2_{diff}, A_{diff}\}$$

where the subscript refers to the difference in the measured values in the compared images.

The data extracted in any case is a vector of dimension three times the number of minutiae examined. We therefore have a multivariate vector with $3n$ minutiae:

$$[\{D1_{1diff}, D2_{1diff}, A_{1diff}\}, \{D1_{2diff}, D2_{2diff}, A_{2diff}\}, \dots, \{D1_{ndiff}, D2_{ndiff}, A_{ndiff}\}]$$

4.2.1 Use of mean vectors and covariance matrices for calculating multivariate probability densities

The probability density of the occurrence of a given case involving multiple variables can be calculated using the Matlab function “mvnpdf” (multivariate normal probability density function):

$$y = \text{mvnpdf}(X, MU, SIGMA)$$

where y equals the probability density of the multivariate normal distribution with mean MU and covariance $SIGMA$ for a given occurrence of X . MU and X are $1 \times n$ vectors and $SIGMA$ is a $n \times n$ covariance matrix.

The mean vector contains the mean values of each of the variables. The diagonal elements of the covariance matrix contain the variances for each variable, while the off-diagonal elements contain the covariances between variables. If there is no significant correlation between the variables, the off diagonal values can be set to 0. Figure 46 shows the structure of the tested

case vector (X), the mean vector and covariance matrix for one minutia. The structure of the tested case vector (X), the mean vector and covariance matrix for multiple minutiae is shown in Figure 47.

$$\begin{pmatrix} x_{D1diff} \\ x_{D2diff} \\ x_{Adiff} \end{pmatrix}, \begin{pmatrix} \mu_{D1diff} \\ \mu_{D2diff} \\ \mu_{Adiff} \end{pmatrix} \text{ and } \begin{pmatrix} \sigma^2_{D1diff} & cov_{D1diff,D2diff} & cov_{D1diff,Adiff} \\ cov_{D1diff,D2diff} & \sigma^2_{D2diff} & cov_{D2diff,Adiff} \\ cov_{D1diff,Adiff} & cov_{D2diff,Adiff} & \sigma^2_{Adiff} \end{pmatrix}$$

Figure 46 The test case vector, mean vector and covariance matrix for one minutia.

The vectors contain the values for each variable D1diff, D2 diff and A diff. The covariance matrix contains the variances of each variable in the diagonal elements and the off-diagonal elements contain the covariances of the variables. For one minutia there are three variables producing 1x3 element vectors and a 3x3 matrix.

$$\begin{pmatrix} Minutia_1 \\ \vdots \\ Minutia_n \end{pmatrix}, \begin{pmatrix} Minutia_1 \\ \vdots \\ Minutia_n \end{pmatrix} \text{ and } \begin{pmatrix} Minutia_{1,1} & \cdots & Minutia_{1,n} \\ \vdots & \ddots & \vdots \\ Minutia_{n,1} & \cdots & Minutia_{n,n} \end{pmatrix}$$

Figure 47 The test case vector, mean vector and covariance matrix for n minutiae. For multiple minutiae (n,) there are three variables producing 3xn element vectors and a 3nx3n matrix.

In this project, there is a degree of predictability of the value D2 from the value of D1 due to the fact that D2 will always be larger; however, the predictability of the differences is not the same. As it is the variance of the differences that is being examined, the predictability of the raw measurements becomes irrelevant.

A mean vector and covariance matrix for a data set can be calculated in Matlab using the “mean” and “cov” functions. Given this, training data can be analysed to establish the mean and the covariance of that data and then independent cases tested against the data to establish

the probability density of the occurrence of that combination of variable values in the original data set.

To this end, data was extracted from a reference image that had minimal distortion and then from a series of other images with induced distortion. The differences between the reference image data and each of the distorted images' data formed a data set representative of how much each minutia could be expected to vary. From the “differences” data, the mean and covariance values for a given finger's set of minutiae can be established.

4.3 The need for a generic mean vector and covariance matrix

Given that a fingerprint examiner compares a single unknown fingermark with a single fingerprint, there is no scope at that time to determine within or between-source variability for the donors of either impression; we simply have one instance of each. We then need to have a generic process with which the minutiae data can be tested.

The hypothesis in this project, restated, is:

Friction ridge skin has a stretch limitation; therefore, corresponding minutiae in compared images of fingerprints will vary in their relative positions within limits.

Given data representing the degree of stretch that can occur between proximal minutiae, we can test compared finger images, in terms of the variations of the measured variables

$D1_{diff}$, $D2_{diff}$ and A_{diff} . This project will not seek to describe skin stretch for all persons, but will describe this for one person as a proof-of-concept model. The data representing the stretch potential are the elements of the mean vector and the covariance matrix.

The approach to the measurement of relative minutiae position was done with data collected in relation to individual minutiae. The data was collected from each image of the same finger with minutiae being measured in the same order for each image, as described in Chapter 3. This approach was not possible for between-source images for two reasons:

1. An actual between-source comparison constitutes an error in identification, and such examples are not frequently retained or recorded, and
2. Simulated between-source comparisons as nominated by the Australian NAFIS have minutiae nominated that are not common to subsequently nominated candidates, so the individual minutiae cannot be examined for the extraction of between-source data by this method.

Therefore we need an approach that approximates skin stretch for all instances of a finger for the person being examined. Ultimately this would represent *all* fingers; however, this is beyond the scope of this project. Given a generic expression of skin stretch, any two compared finger impressions can have data extracted and be tested against a generic mean and covariance matrix, to produce a probability density that they have come from the same source. This result may support or refute the fingerprint examiner's opinion.

To this end, all fingers of the subject were recorded for a reference image and all movement images, and minutiae common to all images were marked. Data was extracted from marked minutiae in order to calculate the mean and covariance for $D1_{diff}$, $D2_{diff}$ and A_{diff} . This approach ensured that the measurement of positional variance was with reference to common minutiae and not generalised across all minutiae.

4.4 Approach taken for data collection

Data for within-source variance was collected as described in Chapter 3 from images of fingerprint from a known source. Ten minutiae were selected from each image and the measurements taken. Data for between-source variance was not collected due to both the unavailability of true between-source samples and simulated between-source samples available from the AFIS.

It was decided that fingerprints for cases where the compared prints have come from both within- and between-source would be compared with the within-source variance data. The resulting probability densities that the compared data had actually come from within-source should then be high or low, depending on whether the test case was a within or between-source comparison. To this end, the generic mean vector and covariance matrix, representative of within-source variance, was generated to allow cases to be tested.

4.5 Within-source data

To establish within-source variation, an image was acquired of each of the subject's fingers for reference and other images for movements that induced distortion. The reference images were taken from the finger as little induced distortion as possible. For each movement, a finger was placed without movement straight on the prism, and images taken whilst the finger had effort applied in prescribed directions. The movement due to the effort applied caused the desired skin distortion. Table 1 summarises the number of images that were acquired and measured for the within-source analysis. For each finger, ten minutiae were selected based on the reference image minutiae positions. Data was extracted from minutiae from each movement image according to the selected data from the reference images. Table 2 summarises the numbers of minutiae that were measured for data extraction.

Movement	Straight placement images	Moved finger images	Number of fingers	Total images per movement
Left	1	1	10	20
Right	1	1	10	20
Up	1	1	10	20
Down	1	1	10	20
Anti-clockwise	1	4	10	50
Clockwise	1	4	10	50
Total images				180

Table 1 Summary of within-source images and movements inducing distortion.

Finger	Number of images	Minutiae examined	Individual examinations
Right thumb	18	10	180
Right index	18	10	180
Right middle	18	10	180
Right ring	18	10	180
Right little	18	10	180
Left thumb	18	10	180
Left index	18	10	180
Left middle	18	10	180
Left ring	18	10	180
Left little	18	10	180
Total examinations 1800			

Table 2 Summary of within-source comparisons and minutiae examined.

This incorporates 1800 measurements each for D1, D2 (3600 measurements) and A (1800 measurements).

4.5.1 Compliance with the requirements for the use of normal distribution density functions

If we are to use multiple instances of normal probability density calculations, we need to show that the data actually distribute normally and independently before we can use the normal distribution density calculation functions.

It was expected theoretically that the variables $D1_{diff}$, $D2_{diff}$ and A_{diff} would distribute normally. There were no anticipated relationships between these variables. It was however, known that, all measurements of D2 (and not $D2_{diff}$) would be greater than the corresponding measurement for D1 in all cases. However, the measurements of D1, D2 and A are not the variables in the distributions; these variables are the differences $D1_{diff}$, $D2_{diff}$ and A_{diff} which are not subject of the same conditions, and, were expected to be independent.

Data was extracted from all images of finger movements and the differences in minutia positions calculated with respect to the relevant reference images.

		$D1_{diff}$	$D2_{diff}$	A_{diff}
$D1_{diff}$	Pearson Correlation	1	0.102**	-0.186**
	Sig. (2-tailed)		0.000	0.000
	N	1800	1800	1800
$D2_{diff}$	Pearson Correlation	0.102**	1	-0.121**
	Sig. (2-tailed)	0.000		0.000
	N	1800	1800	1800
A_{diff}	Pearson Correlation	-0.186**	-0.121**	1
	Sig. (2-tailed)	0.000	0.000	
	N	1800	1800	1800

** . Correlation is significant at the 0.01 level (2-tailed).

Table 3 Calculated correlations between variables $D1_{diff}$, $D2_{diff}$ and A_{diff} .

Correlation statistics on the extracted differences data was calculated and are displayed in Table 3. The assumptions of independence are supported by the correlation data for the difference variables.

The differences data was plotted in SPSS as shown in Figures 48to 50, which illustrate the distributions of the differences of measurements $D1_{diff}$, $D2_{diff}$ and A_{diff} for all fingers. It can be observed from the histograms that the data distributions approximate a normal distribution, however each of the distributions shows a degree of kurtosis.

Kurtosis (MathWorks, 2008) is a measure of the extent to which observations cluster around a central point. For a normal distribution, the value of the kurtosis statistic is zero. Positive kurtosis indicates that the observations cluster more and have longer tails than those in the normal distribution. The measured degree of kurtosis in each distribution is shown in Table 4.

Descriptive Statistics			
	N	Kurtosis	
	Statistic	Statistic	Std. Error
D1diff	1800	2.068	.115
D2 diff	1800	1.092	.115
A diff	1800	1.246	.115
Valid N (listwise)	1800		

Table 4 SPSS output for the measured degree of kurtosis for the variables $D1_{diff}$, $D2_{diff}$ and A_{diff} .

The implication of kurtosis is that the data is not distributed in the same manner a data would be if distributed “normally”. That is, in the case of a distribution with positive values for the measured kurtosis, there would be less than the expected 68.2% of cases represented in the first standard deviation, thereby causing “fat tails” in the distribution’s histogram. This then follows that the normal probability density calculated for any given case would not be well represented by a normal probability density function.

It is argued that in a large sample, the impact of departure from zero kurtosis diminishes. For example, underestimates of variance associated with positive kurtosis (distributions with short, fat tails) disappear with samples of 100 or more cases (Tabachnick & Fidell, 2001).

There are 1800 samples extracted in each of the variables D1, D2 and A. Given the number of samples (far greater than 100) and the context of the intended product of the research, it is reasonable to suggest that the kurtosis does not dismiss the function that the model performs.

It is acknowledged that the kurtosis exists in the distributions of data for the three variables however there has been no attempt to account for it in this research.

Note that it can be observed in the histograms that the mean values for each distribution is close to zero. This is to be expected because, if there were no differences between compared images, the differences would in fact be zero. The actual values are shown in Table 5, where it can be seen that, considering the range of sampled values, the mean of these values is very close to zero. In each instance of a fingerprint being taken, or a fingermark being left, there will in theory always be some variation in the deposit left. This is due to variance in a number of variables, such as applied force, direction of the applied force, amount of material on the surface of the finger and so on. The differences could be expected mostly to be minimal with more extreme differences being less likely, hence the expected normal distribution.

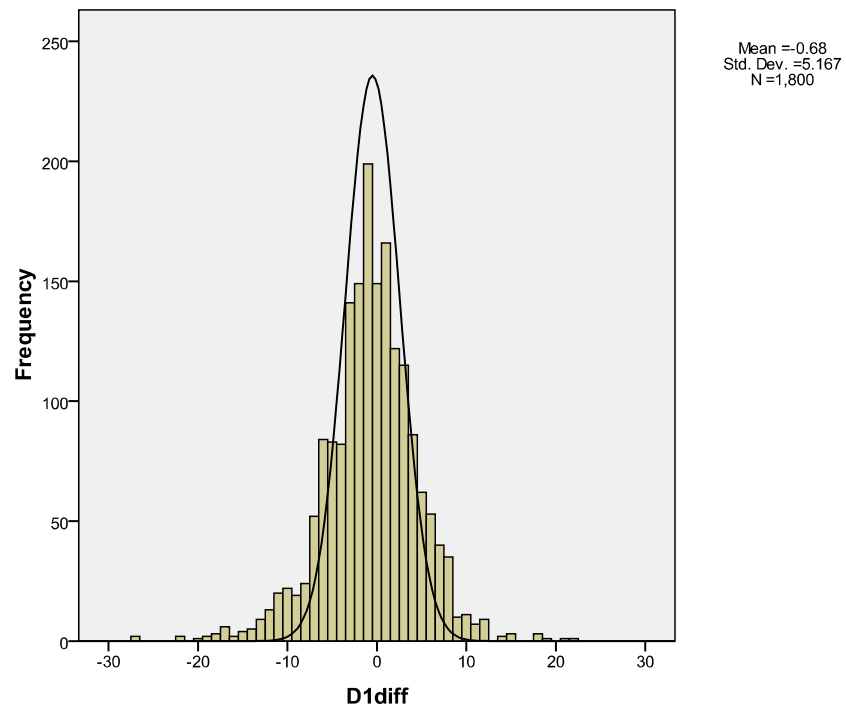


Figure 48 Distribution of D1diff for all finger movements and reference images.

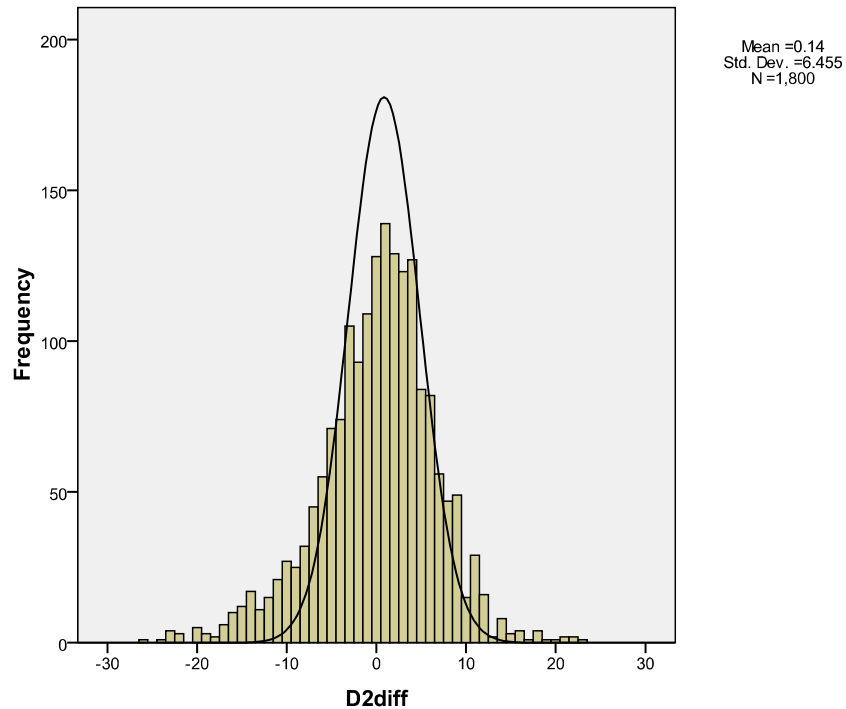


Figure 49 Distribution of D2 diff for all finger movements and reference images.

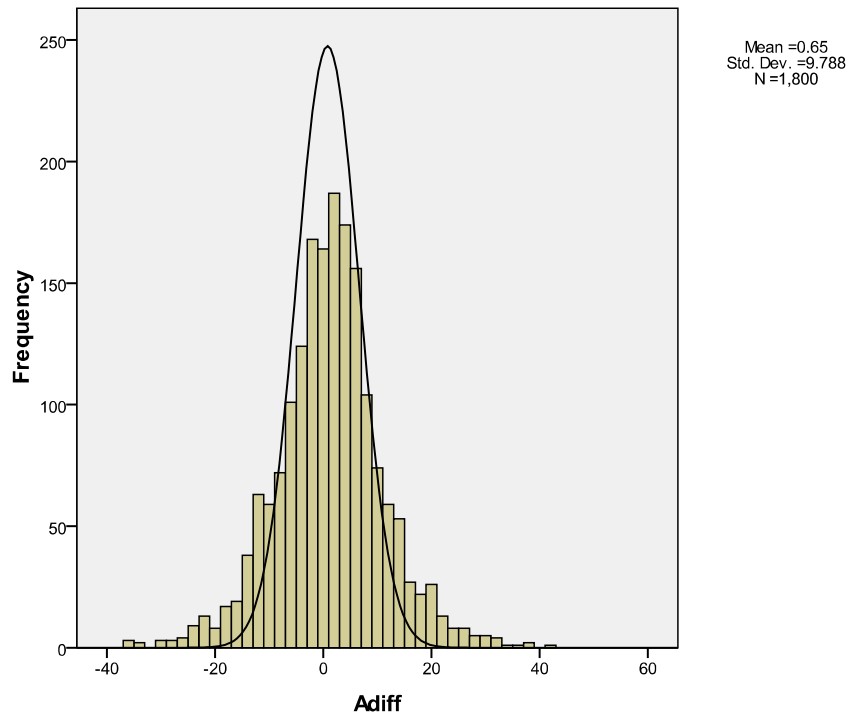


Figure 50 Distribution of Adiff for all finger movements and reference images.

	N	Range	Minimum	Maximum	Mean	Std. Deviation	Variance
D1 _{diff}	1800	49	-27	22	-0.68	5.167	26.699
D2 _{diff}	1800	49	-26	23	0.14	6.455	41.665
A _{diff}	1800	77	-36	41	0.65	9.788	95.798
Valid N (listwise)	1800						

Table 5 Descriptive statistics for D1diff, D2diff and Adiff.

This is for all finger movements and calculated with respect to the reference images

4.5.2 Compliance with the requirements for the use of multivariate normal distributions

The use of multivariate normal probability density functions requires that the variables distribute normally and that they vary independently of each other. The data was analysed using SPSS to show the normality of the variable distributions in the form of a histogram as shown in Figures 48 to 50.

The correlation was demonstrated in scatter plots as shown in Figures 51 to 53 and the actual values calculated and shown in Table 3.

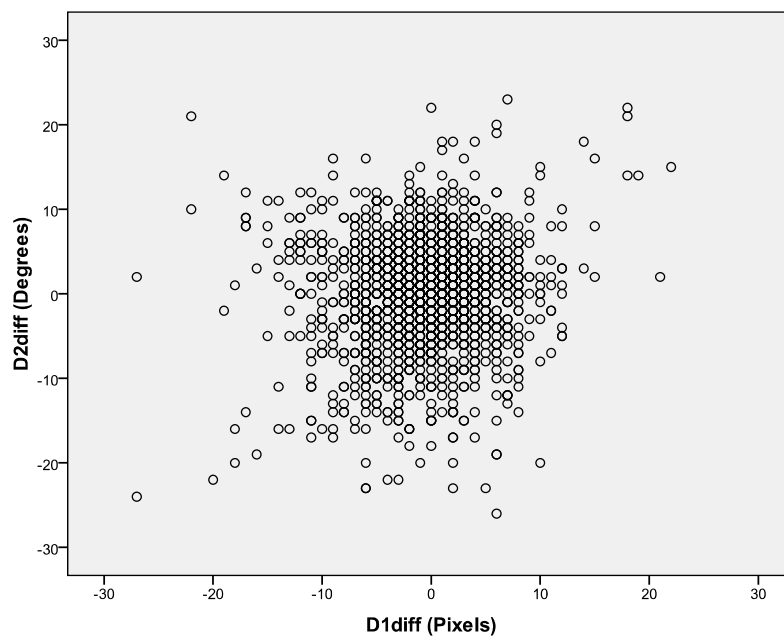


Figure 51 Scatter plot showing the relationship between variables D1diff and D2diff.

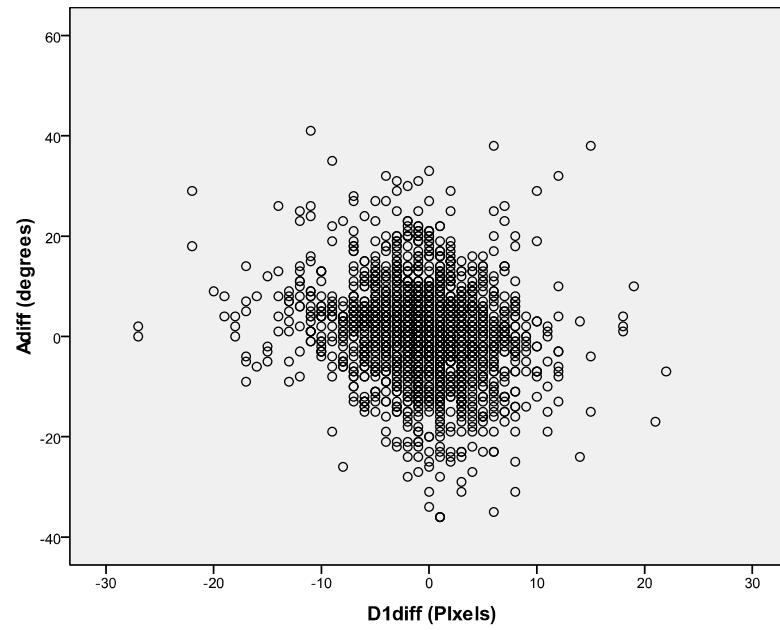


Figure 52 Scatter plot showing the relationship between variables Adiff and D1diff.

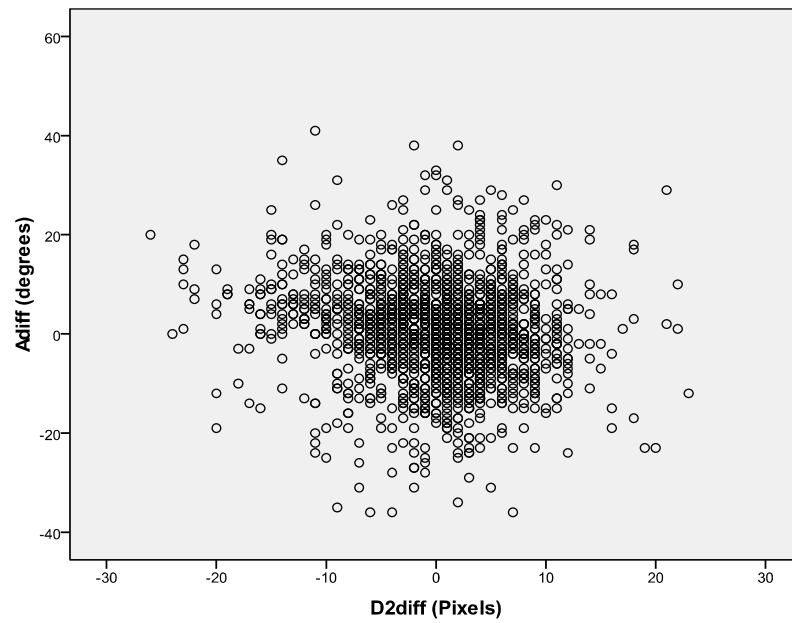


Figure 53 Scatter plot showing the relationship between variables Adiff and D2diff.

4.6 Generation of the generic mean vector and covariance matrix

To generate a generic covariance matrix, covariance values for the three variables ($D1_{diff}$, $D2_{diff}$ and A_{diff}) were obtained for the ten minutiae in each finger, and the variance values averaged. Mean values were also obtained but the generic value set at zero for each variable. This process is explained as follows.

Minutiae difference values for each finger were processed in Matlab using the “cov(x)” function in a script “csv input from V++ 2 no abs_18 values.m” (Appendix 3.4). The “cov(x)” function produces a covariance matrix of $n \times n$ elements where n is the number of variables contained in the data represented by x . The data array x has the variables represented by the columns and the observations for each movement represented by the rows. As each finger for within-source data collection had ten minutiae examined, the covariance matrix produced for each finger had dimensions of 30×30 , which contained data for the three variables for the ten minutiae as shown in Table 6 (left index finger).

	M1D1	M1D2	M1A	M2D1	M2D2	M2A	...	M10D1	M10D2	M10A
M1D1	23.781	0	0	0	0	0	...	0	0	0
M1D2	0	49.323	0	0	0	0	...	0	0	0
M1A	0	0	143.20	0	0	0	...	0	0	0
M2D1	0	0	0	23.781	0	0	...	0	0	0
M2D2	0	0	0	0	10.5	0	...	0	0	0
M2A	0	0	0	0	0	60.800	...	0	0	0
...	0	0	0
M10D1	0	0	0	0	0	0	0	9.3986	0	0
M10D2	0	0	0	0	0	0	0	0	5.0457	0
M10A	0	0	0	0	0	0	0	0	0	27.058

Table 6 The covariance matrix for the left index finger.

The headers for the rows and columns indicate the variables examined. For example, M1D2 refers to the D2 diff for Minutia 1. The elements for the first two minutiae and the tenth minutia are shown. The angle data in this and following tables has been coloured red.

Note that the headings for the columns and rows are labeled without the “_{diff}” suffix for convenience. The values in the diagonal in each fingers covariance matrix represent the variances of the three variables for each minutia examined.

The values of the variances of $D1_{diff}$ and $D2_{diff}$ combined were averaged within each finger’s covariance matrix and then across all fingers to produce the average variance of $D1_{diff}$ and $D2_{diff}$. The means of the variances were established for all fingers. The means of the variables for the left index finger are shown in Table 7.

	distances	angles
mean	20.04477	56.83758

Table 7 Mean values for the elements in the covariance matrix and mean vector for the difference data for the left index finger.

The means of the variance values for $D1_{diff}$, $D2_{diff}$ and A_{diff} from all fingers were averaged to produce the generic covariance matrix values. These are shown in Table 8. These values were inserted into the diagonal cells of the generic covariance matrix as shown in Table 10. Note that the off-diagonal values have been assigned the value of zero, due to the low covariances as established in Section 4.5.2..

	distances	angles
mean	18.53846	54.55538

Table 8 Average values for mu and sigma for all angle and distance differences

The Matlab script also produced a mean vector for differences data for each finger. Table 9 contains the mean values for the difference data for the left index finger.

Variable	mu
M1D1	-1.38889
M1D2	0.166667
M1A	-7.55556
M2D1	-1.38889
M2D2	2.5
M2A	-7.72222
...	...
M10D1	-4.88889
M10D2	2.111111
M10A	9.666667

Table 9 The mean vector for the left index finger.

The elements for the first two minutiae and the tenth minutiae are shown.

Since the mean values for all variables averaged equals approximately zero, and were expected to be so, it was assumed that the mean value should actually be zero. As there was no argument established that would suggest an alternative, the value of zero was assigned as the mean for all variables resulting in a 1x3 mean vector (μ) with all vector elements being zero.

It is expected that the values of a true generic matrix that represents the human population's variance in skin stretch would be different to the values established in this project. However, this does not necessarily invalidate the established values from being included in a testing mechanism. Given that, if the variance values are increased, the resultant distributions will broaden and become less discriminating when testing cases. Equally, if the mean values for the human population happened to be different to the mean established here, then the

functions representing within- and between-source responses to the model will vary accordingly.

	M1D1	M1D2	M1A	M2D1	M2D2	M2A	...	M10D1	M10D2	M10A
M1D1	18.5384	0	0	0	0	0	...	0	0	0
M1D2	0	18.5384	0	0	0	0	...	0	0	0
M1A	0	0	54.5553	0	0	0	...	0	0	0
M2D1	0	0	0	18.5384	0	0	...	0	0	0
M2D2	0	0	0	0	18.5384	0	...	0	0	0
M2A	0	0	0	0	0	54.5553	...	0	0	0
...	0	0	0
M10D1	0	0	0	0	0	0	0	18.5384	0	0
M10D2	0	0	0	0	0	0	0	0	18.5384	0
M10A	0	0	0	0	0	0	0	0	0	54.55

Table 10 The generic covariance matrix.

The elements for the first two minutiae and the tenth minutia are shown.

It is expected that the values of a true generic matrix that represents the human population's variance in skin stretch would be different to the values established in this project. However, this does not necessarily invalidate the established values from being included in a testing mechanism. Given that, if the variance values are increased, the resultant distributions will broaden and become less discriminating when testing cases. Equally, if the mean values for the human population happened to be different to the mean established here, then the functions representing within- and between-source responses to the model will vary accordingly.

Neither of these factors will affect the fact that between-source cases will tend to fall closer to the between-source mean and the within-source cases will tend to fall closer to the within-

source mean. The sensitivity of the test will be affected; however, as a test of the examiner's outcome, the model should be able to give a “supporting” or “not supporting” response.

The performance of the model was tested, which gave an indication of perhaps where the more accurate means exist. This will be discussed later.

4.7 The effect of multiple variables on the resultant probability density

The effect on the resultant probability density, where there are more variables and cases, is that the value of the probability density of the occurrence will diminish. This is because the probability densities are effectively multiplied together. Figure 54 charts the logarithm to base 10 of the probability for multiple events occurring where the event value equals the mean. This is the case where the images compared are the same and the minutiae marked have the same Cartesian coordinates. It can be seen that, even when the event values are the most probable (equaling the mean value), the probability of successive events (compared minutiae) diminishes.

Note that the slope of the function, for what could be described as the best case scenario where there is complete agreement in minutiae positions, is approximately -3.3. In comparison, Figure 55 charts the logarithm of the probability for multiple events occurring where the same image as for Figure 54 has been compared with a copy of itself, with all minutiae moved 10 pixels in a random direction.

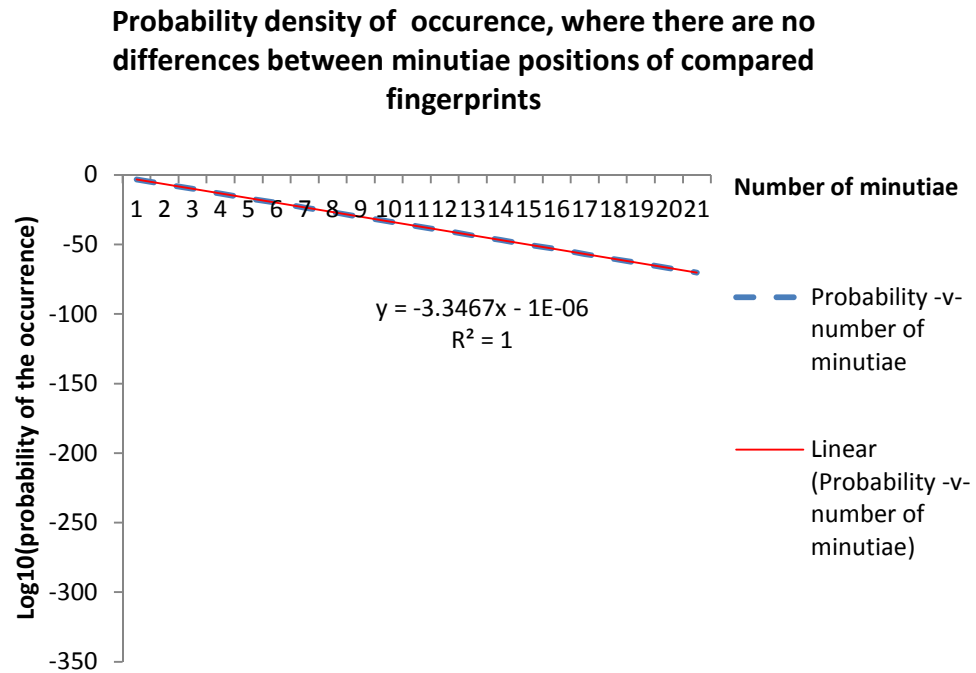


Figure 54 Probability density of multiple events of the same occurrence.

Where there is no difference between the marked minutiae of the compared images the probability diminishes at a steady (same) rate.

The probability density of successive events diminishes at a higher rate as indicated by a slope of approximately -12. This change of slope suggests that, as the $D1_{diff}$, $D2_{diff}$ and A_{diff} values increase, the slope of the function will increase, confirming that the probability density that the compared images are from the same source will be less.

Comparison of the probability densities where there are no differences between compared minutiae positions and where there are random 10-pixel shifts in minutiae positions

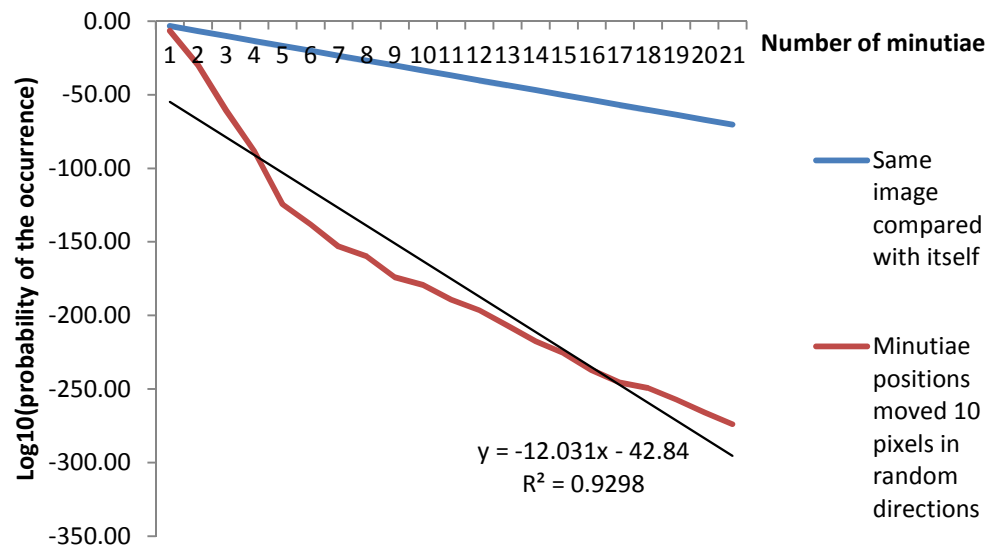


Figure 55 Probability density of multiple events where an occurrence is varied.

Comparison of the probability densities where, there are no differences between compared minutiae positions and where there are random 10-pixel shifts in minutiae positions.

4.8 Establishing regression functions for within- and between-source test response probability densities

The objective behind testing within- and between-source data with the generic mean and covariance matrix was to establish regression functions to allow actual cases to be tested for probable within or between-source origins.

The reference images for the donor in this project were searched against the AFIS in a manner that simulated a developed latent fingermark being searched against all inked fingerprints. Fingerprints of the donor that were nominated by AFIS as a candidate (being a prior record on the AFIS from the donor) were saved for within-source comparisons. These within-source “candidates” were from previous records of the donor on the AFIS database submitted for other reasons previous to this research. Images of fingerprints that were both

incorrect nominations and records owned by the AFP were saved for between-source comparisons. The number of within-source candidates for each finger is listed in Table 11. Figure 56 shows an example of the reference image for the left index finger, a correctly nominated candidate, and the minutiae that AFIS has nominated. Note that there are *very few minutiae that are not included* in the set of minutiae nominated by AFIS as corresponding. There are variations in the positions of minutiae, which is due to the elastic distortion of the skin (Maceo, 2009).

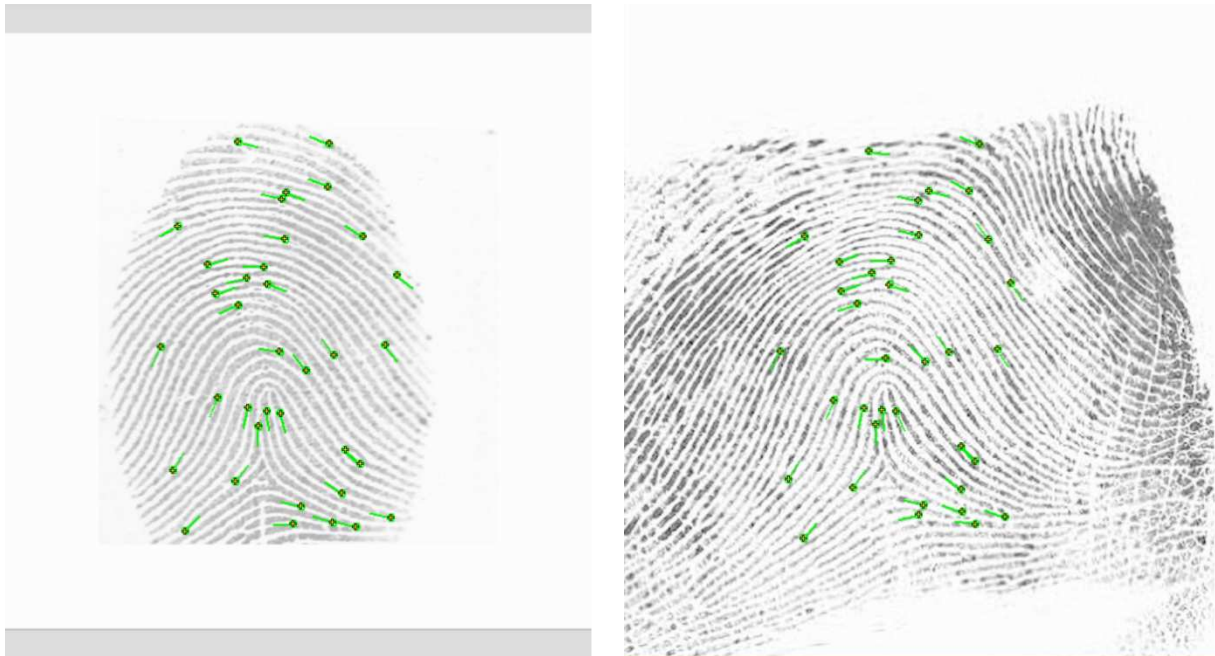


Figure 56 Comparison of a left index finger and the correctly nominated candidate.

There are 36 minutiae nominated as corresponding, as shown by the green markers.

Figure 57 shows an example of the reference image for the left index finger, an incorrectly nominated candidate, and the minutiae that AFIS has nominated. Note that there are *many minutiae not included* in the set of minutiae nominated by AFIS as corresponding. Table 12 shows the number of correct candidates per reference image (for which there are multiple cases) and the number of minutiae nominated by AFIS as corresponding.

Finger	Number of candidates	Minutiae examined
Right thumb	1	57
Right index	1	42
Right middle	1	46
Right ring	1	40
Right little	1	42
Left thumb	1	77
Left index	1	36
Left middle	1	37
Left ring	1	35
Left little	1	30
Total	10	442

Table 11 Summary of within-source candidates and minutiae examined

The mean number of between-source minutiae nominated by AFIS per finger was 25, the minimum number of minutiae was 13 and the maximum 29. The mean number of within-source minutiae nominated by AFIS per finger was 44 and the minimum 30.

The difference in the number of nominated corresponding minutiae for within- and between-source is, in my view as a fingerprint examiner, due to the fact that there is expected to be disagreeing minutiae in a between-source comparison resulting in fewer “corresponding” minutiae being nominated.

The difference in the number of candidates is predictable in that there can only be one correct candidate for within-source comparisons, while there could be a number of candidates whose fingers contain minutiae in similar positions to the reference image. Recall that AFIS is searching for similarities and ignoring all differences.

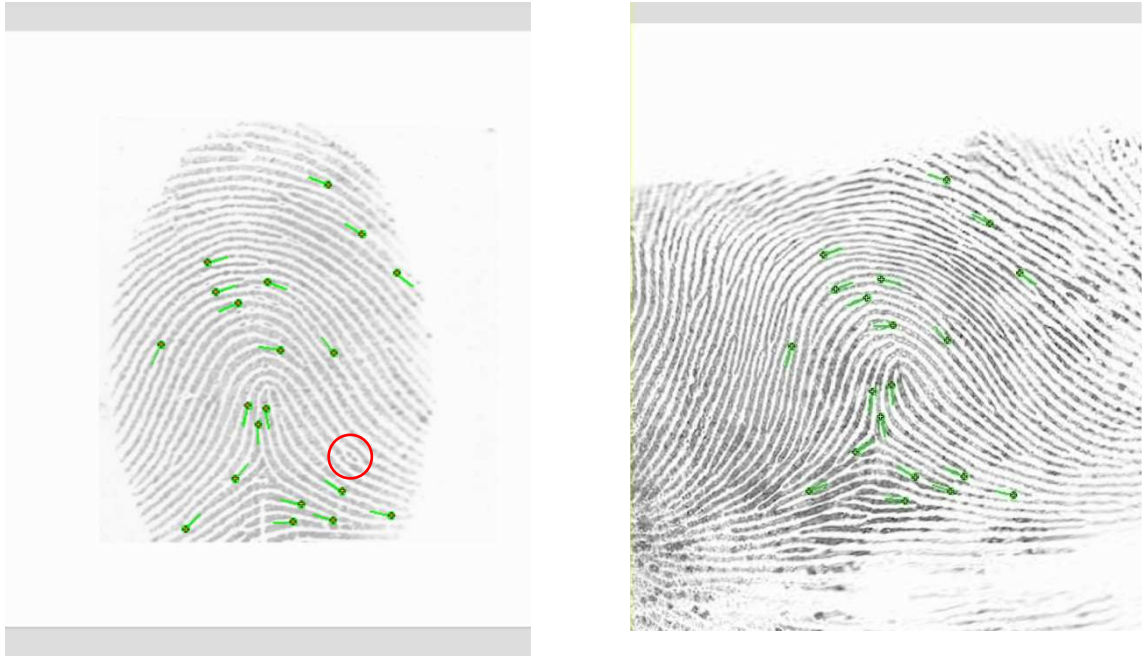


Figure 57 Comparison of a left index finger and an incorrectly nominated candidate.

There were 20 minutiae nominated as corresponding, as shown by the green markers. One of the minutiae not in agreement is indicated by the red circle on the left (reference) image.

Finger	Number of candidates	Minutiae examined
Right thumb	4	103
Right index	1	24
Right middle	4	111
Right ring	4	96
Right little	2	68
Left thumb	8	292
Left index	5	86
Left middle	4	83
Left ring	4	77
Left little	1	15
Total	37	955

Table 12 Summary of between-source candidates and minutiae examined

Data was obtained from all within-source and between-source comparisons. The data for each comparison was tested by the model and probability density data produced. The data produced consisted of probability densities that the comparison was within-source, for one minutia compared, two minutiae compared, and soon, until all minutia had been compared. The data was in the form shown in Table13.

Number of minutiae	Probability density of within-source
1	3.85E-11
2	1.26E-23
3	5.30E-29
4	2.07E-32
5	7.40E-36
6	1.69E-41
.	.
.	.
35	3.46E-215
36	4.28E-219

Table 13 Sample of the data produced using the generic mean and covariance matrix.

A probability density that both fingerprints have come from the same source (i.e. a within-source comparison) is returned for increasing numbers of minutiae. In this example, 36 minutiae in a left index finger have been compared.

The significant part of a probability density returned is the exponent. As such, the log to base 10, of all probability densities calculated, was used when data was plotted or cases compared. Probability density data was collected for all comparisons and input into within-source and between-source spreadsheets.

The means and standard deviations of probability densities, between all fingers, were calculated for one minutia, two minutiae and so on, which produced data that, when plotted, allowed a prediction to be made where a within or between-source comparison would lie, given the number of compared minutiae. Table 14 shows a sample of the between-source comparison probability density data.

Note that, as previously mentioned, not all images contain the same number of compared minutiae. Therefore the mean and standard deviation calculated may not be reliable for cases with fewer fingers compared.

For this reason, data for the means and standard deviations were only taken from data where there were a constant number of minutiae contained in the compared data. This number for between-source data was 13 minutiae and for within-source data was 30 minutiae.

Number of minutiae marked	case1name =Lt 7 w 32 minutiae.csv	Log10(Lt 7 w 32 minutiae)			case1name =Lm 4 w 14 minutiae.csv	Log10(Lm 4 w 14 minutiae)	case1name =Li 4 w 13 minutiae.csv	Log10(Li 4 w 13 minutiae)	number of fingers compared	mean of log(probability)	Standard deviation of the log(probability)
1	2.82E-15	-14.54989	.	.	2.24E-10	-9.649888	3.93E-10	-9.405851	37	-1.18E+01	6.82E+00
2	5.96E-22	-21.22445	.	.	7.68E-20	-19.11467	6.67E-25	-24.17559	37	-2.50E+01	1.31E+01
3	1.81E-37	-36.74347	.	.	9.50E-48	-47.02207	5.77E-30	-29.23871	37	-3.77E+01	2.03E+01
4	5.63E-46	-45.24946	.	.	2.94E-57	-56.53233	7.23E-35	-34.14113	37	-4.75E+01	2.21E+01
5	2.76E-51	-50.55854	.	.	9.52E-64	-63.02158	5.09E-101	-100.2936	37	-6.28E+01	2.94E+01
6	3.84E-62	-61.41531	.	.	1.58E-67	-66.80261	2.37E-122	-121.6257	37	-7.55E+01	3.09E+01
7	3.96E-71	-70.40181	.	.	3.33E-93	-92.47754	1.58E-133	-132.8015	37	-8.64E+01	3.14E+01
8	7.62E-85	-84.11828	.	.	2.87E-103	-102.5415	1.29E-164	-163.8881	37	-9.94E+01	3.36E+01
9	4.73E-92	-91.32549	.	.	1.43E-109	-108.845	1.73E-224	-223.762	37	-1.14E+02	3.88E+01
10	9.98E-102	-101.001	.	.	1.92E-113	-112.7158	2.81E-232	-231.552	37	-1.25E+02	3.87E+01
11	5.38E-108	-107.2696	.	.	3.97E-119	-118.401	5.89E-239	-238.2298	37	-1.36E+02	3.85E+01
12	1.35E-123	-122.8691	.	.	2.39E-123	-122.6224	6.19E-246	-245.2083	37	-1.50E+02	4.05E+01
13	4.25E-133	-132.3716	.	.	1.04E-130	-129.9839	2.90E-261	-260.5374	37	-1.64E+02	4.51E+01
14	1.54E-150	-149.8127	.	.	1.41E-138	-137.8493			36	-1.75E+02	4.50E+01
15	6.66E-158	-157.1766	.	.					34	-1.88E+02	4.07E+01
16	2.46E-181	-180.6096	.	.					33	-2.02E+02	4.30E+01
17	7.50E-190	-189.1252	.	.					31	-2.11E+02	4.21E+01
18	2.16E-199	-198.6651	.						29	-2.22E+02	4.19E+01
19	3.85E-206	-205.4142	.						26	-2.29E+02	4.02E+01
20	7.47E-211	-210.1266	.						23	-2.33E+02	3.70E+01
21	6.56E-217	-216.1829	.						16	-2.41E+02	3.24E+01
22	2.76E-227	-226.5585	.						14	-2.50E+02	2.98E+01
23	2.22E-239	-238.6535	.						11	-2.55E+02	3.18E+01
24	7.83E-252	-251.1065							8	-2.56E+02	3.01E+01
25	1.25E-256	-255.9044							6	-2.62E+02	2.25E+01
26	6.84E-274	-273.1648							5	-2.79E+02	9.08E+00
27	3.31E-281	-280.4796							3	-2.89E+02	7.79E+00

Table 14 Data from between-source comparisons.

The rows represent the number of minutiae marked for each finger compared. The following columns contain the probability data for the compared finger (as indicated by the column header) and the log to base 10 of the probability density. The column titled “number of fingers compared” indicates how many fingers contained that row’s number of minutiae (for example: the highlighted yellow row indicates that 37 images contained 13 minutiae). The last two columns contain the means and standard deviations for the respective rows.

4.8.1 Between-source probability densities for all minutiae

Based on all minutiae data, the probability data for two compared fingerprints from different sources (between-source) can be plotted as shown in Figure 58.

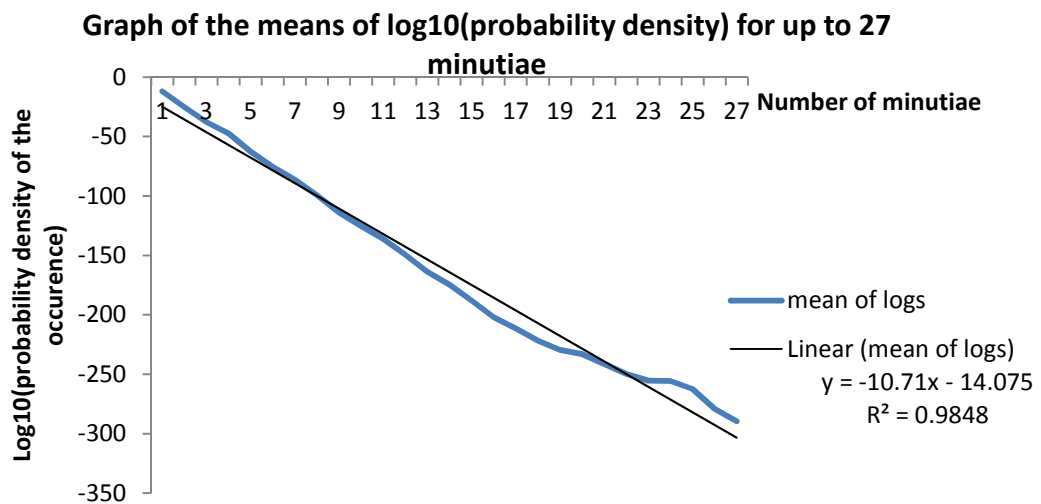


Figure 58 The function describing the means of the log₁₀ of the probability density that the compared between-source fingerprints are from the same source, for up to 27 minutiae.

The regression (trend) line function equation and R^2 , as generated in Microsoft Excel, was also produced through regression analysis in SPSS. This was the case for all of the plotted within- and between-source functions.

Whilst the mean function provides a function that is quite reliable for predicting between-source comparisons for up to 27 minutiae compared, the same cannot be said for standard deviation. Figure 59 shows the function for standard deviation for up to 27 minutiae. Note that this function, for values in the range 1 to 27 minutiae is not linear. It is affected by a diminishing number of compared minutiae due to the lesser number of images with a large number of minutiae to compare; hence, the deviation diminishes with fewer samples.

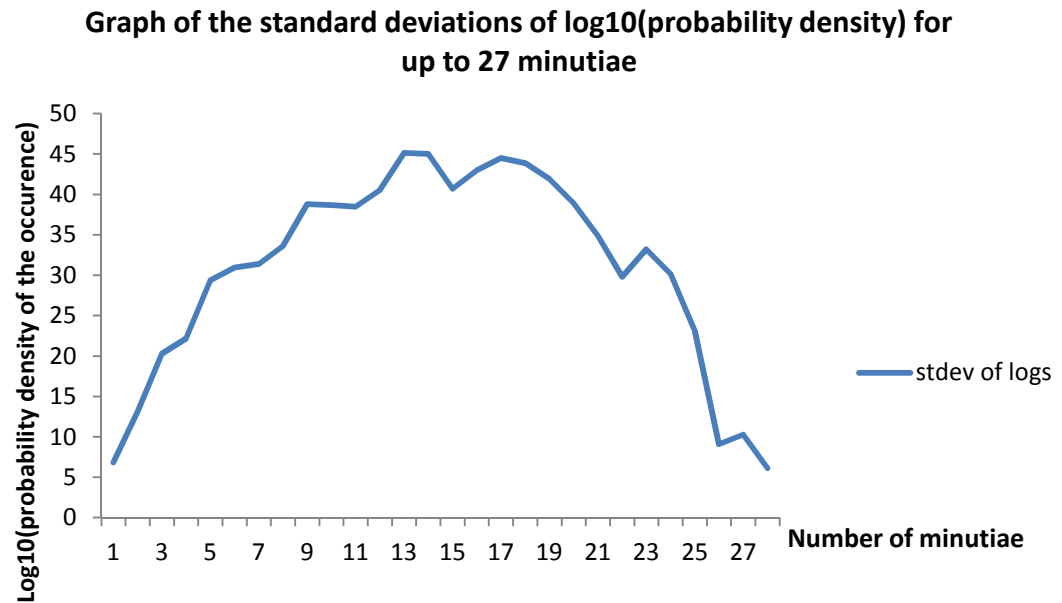


Figure 59 The function describing the standard deviations of the log₁₀ of the probability density that the compared between-source fingerprints are from the same source, for up to 27 minutiae.

As previously mentioned, it is expected that there will be fewer minutiae compared in a between-source comparison and the reliability of the function diminishes as the number of images sampled diminishes.

It was therefore decided to plot the between-source function using only 13 minutiae. Figure 60 shows the mean function and Figure 61 the standard deviation function for up to 13 minutiae in a between-source comparison.

Whilst the R^2 value for the mean function has increased slightly, the R^2 value for the standard deviation function indicates a greater degree of linearity than was previously observed.

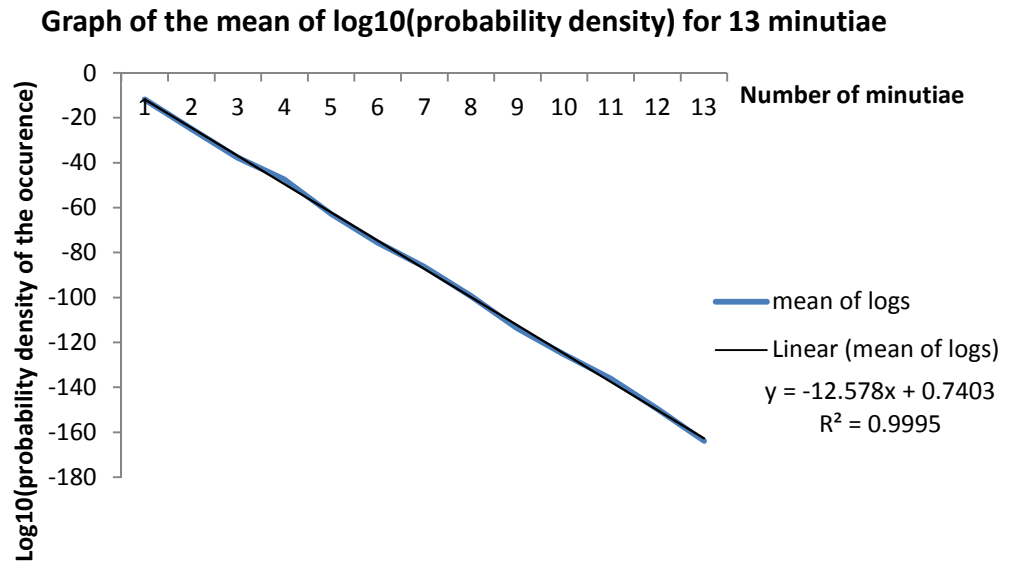


Figure 60 The function describing the means of the log10 of the probability density that the compared between-source fingerprints are from the same source, for up to 13 minutiae.

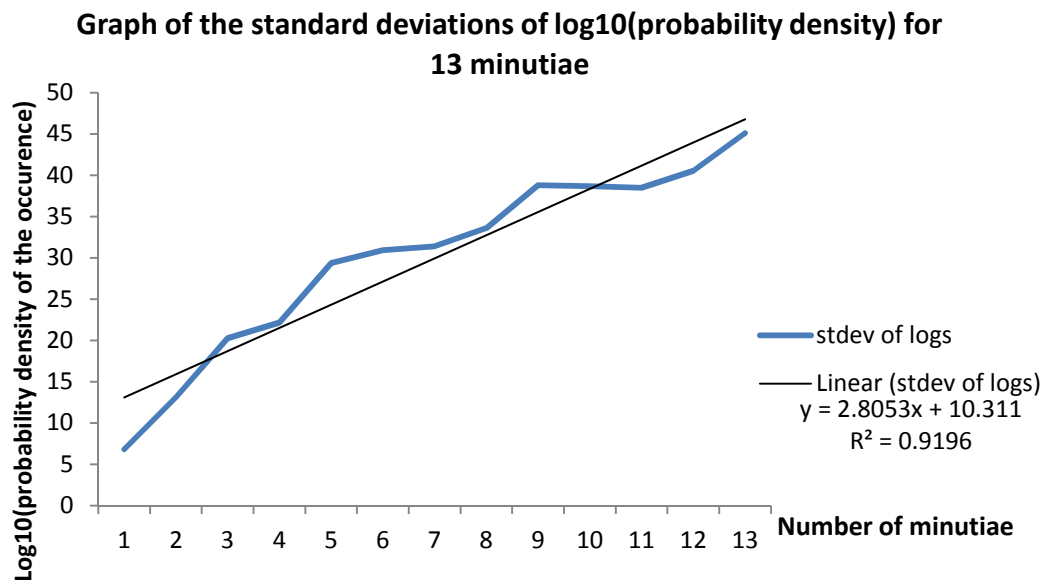


Figure 61 The function describing the standard deviations of the log10 of the probability density that the compared between-source fingerprints are from the same source, for up to 13 minutiae.

The data representing the between-source response for 13 minutiae is illustrated in box plots in Figure 62.

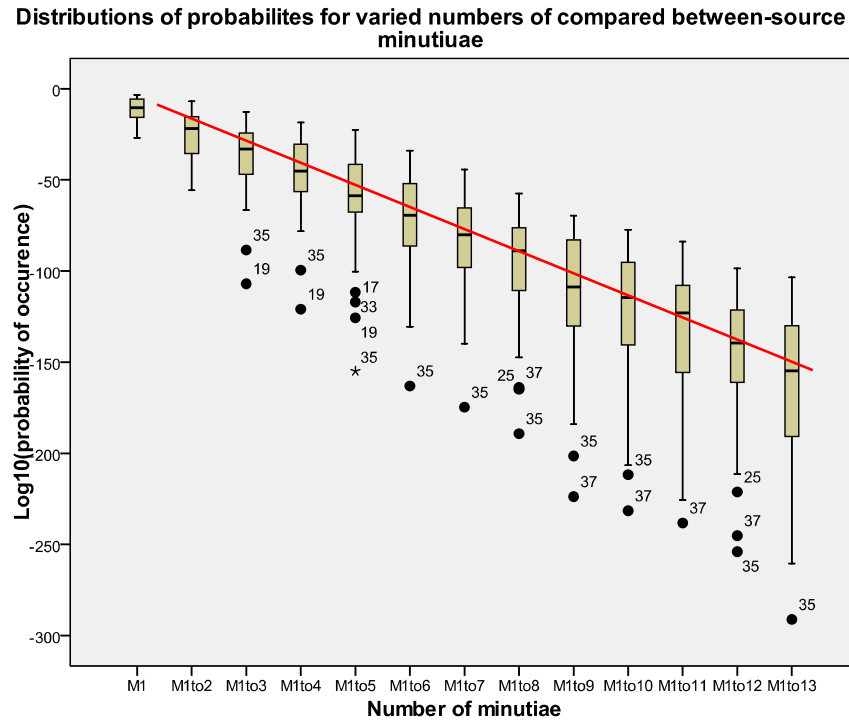


Figure 62 Box plots of values contributing to the mean between-source probability density function.

4.8.2 Within-source probability densities for varied numbers of minutiae

Based on all minutiae data, the probability density data for two compared fingerprints from the same source (within-source) can be plotted as shown in Figure 63. Whilst the mean function is quite reliable for predicting within-source comparisons for up to 55 minutiae, the same cannot be said for standard deviation. Figure 64 shows the function for standard deviation for up to 55 minutiae. Again, the diminishing number of minutiae available for comparison causes the standard deviation values to become unstable.

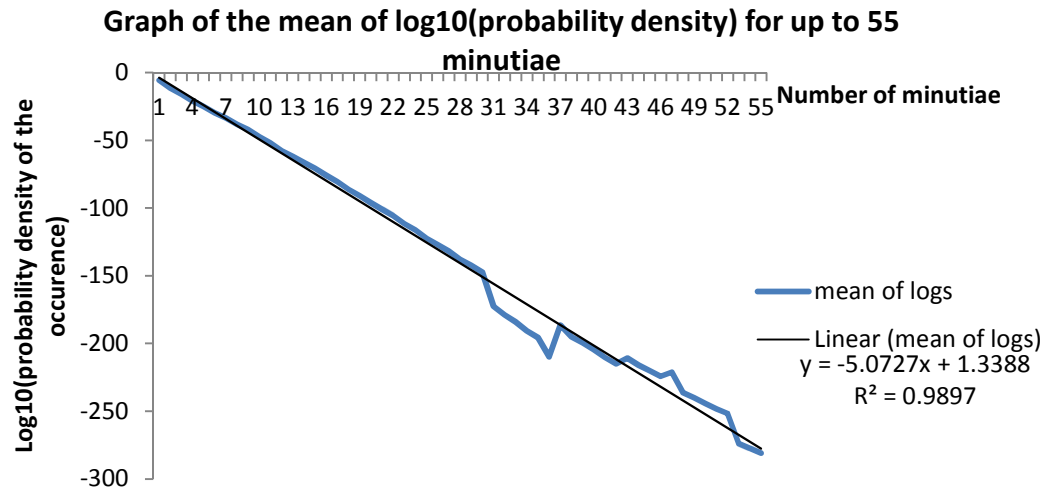


Figure 63 The function describing the means of the log₁₀ of the probability density that the compared within-source fingerprints are from the same source, for up to 55 minutiae.

It was decided to plot the between-source function using only 30 minutiae, as this was the highest number of minutiae that was contained by all compared images.

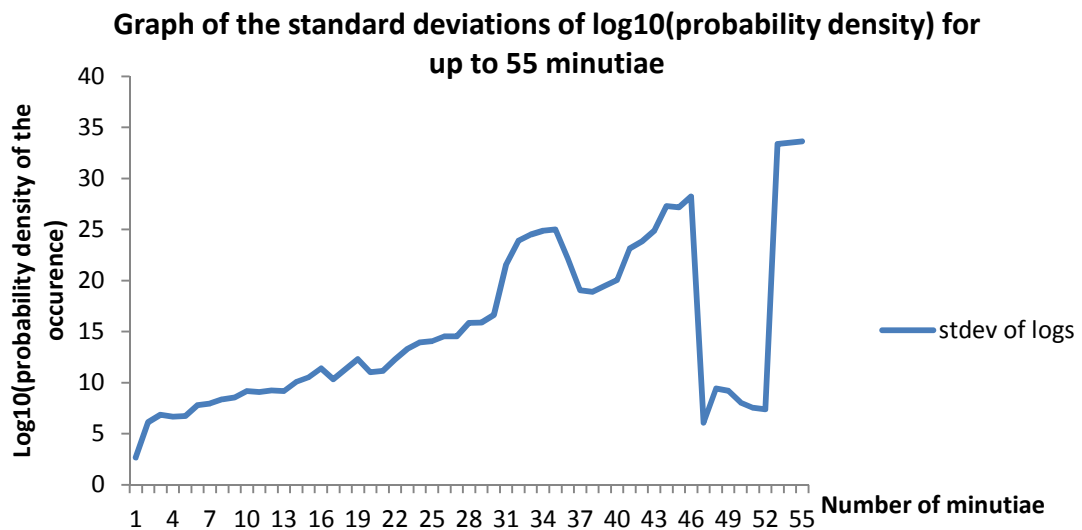


Figure 64 The function describing the standard deviations of the log₁₀ of the probability density that the compared within-source fingerprints are from the same source, for up to 55 minutiae.

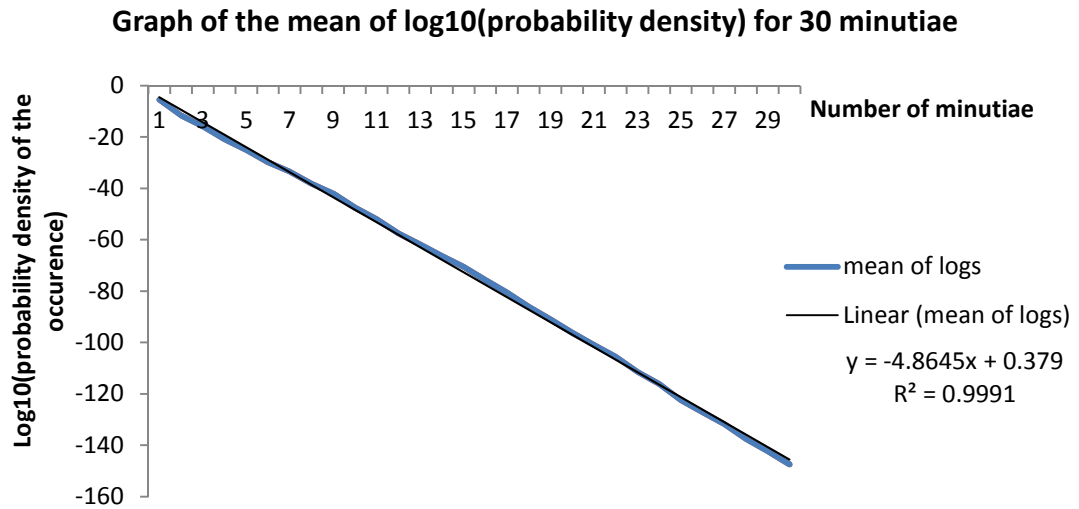


Figure 65 The function describing the means of the log10 of the probability density that the compared within-source fingerprints are from the same source, for up to 30 minutiae.

Figure 65 shows the mean function and Figure 66 the standard deviation function for up to 30 minutiae in a within-source comparison.

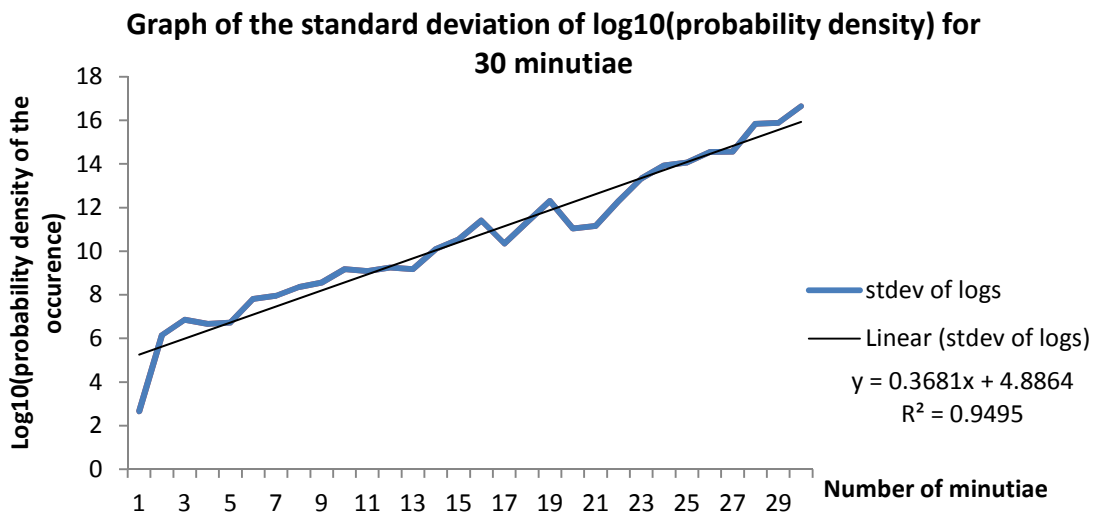


Figure 66 The function describing the standard deviations of the log10 of the probability density that the compared within-source fingerprints are from the same source, for up to 30 minutiae.

The data representing the within-source response for 30 minutiae is illustrated in box plots in Figure 67.

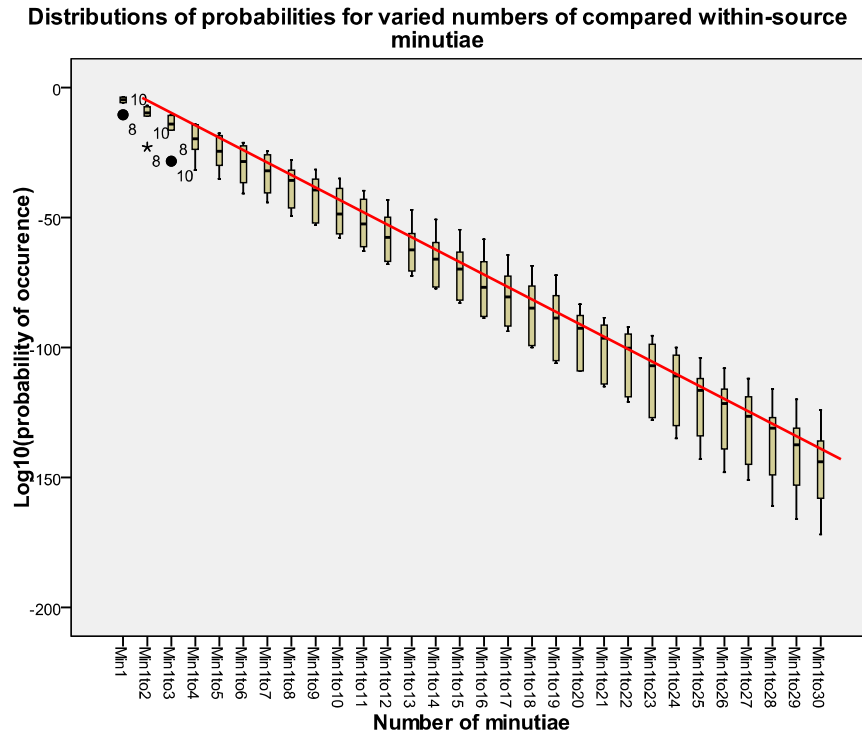


Figure 67 Box plots of values contributing to the mean within-source probability density function.

4.9 Model testing against within- and between-source cases

It could be argued that the establishment of the regression functions in this project will only be representative of the donor and not be applicable to anyone else. In that case, the performance of the model would be in question. It was decided to test the performance of the model with known within-source comparisons from actual criminal investigation cases, and also with simulated erroneous (between-source) comparisons as generated by AFIS searches. This, of course, supposes that the outcomes of the comparisons that are nominated by examiners as being within-source are in fact correct. We will assume that, for the purpose of this research, these outcomes were correct.

To perform these comparisons, two fingerprints were compared for each case, the relevant data extracted, and the model applied to that data. The resultant cases were plotted against the regression functions in terms of the calculated probability density of each case being within-source, and the number of minutiae compared.

4.9.1 Between-source comparisons

Reference images from the donor were searched on the AFIS as latent fingermarks to be searched against all unsolved latent fingermarks from AFP investigations. The searches returned 36 non-matching cases that were owned by the AFP. These had AFIS-nominated corresponding minutiae marked for each case. The images from these cases were compared and data extracted from the marked minutiae. The data was processed using the proposed model and the cases plotted as shown in Figure 68 and is the “Between-source case” series.

4.9.2 Within-source subject comparisons

Latent fingermarks involving a range of distortions were deposited and developed with black fingerprint powder. These were compared with their corresponding reference images, marked and feature vectors extracted. The data was processed using the proposed model and the cases plotted as shown in Figure 68 and is the “Within-source donor” series.

4.9.3 Within-source case comparisons

Fingerprint comparisons from 21 AFP criminal investigation cases were compared and data extracted from the marked minutiae. The data was processed using the proposed model and the cases plotted as shown in Figure 68 and is the “Within-source case” series.

4.9.4 Results of comparisons

It can be observed that the within- and between-source comparisons do not overlap. This is encouraging in that the two categories of comparison are separate; however, given the small number of samples used, it could be argued that there would be an overlap, should greater numbers of cases be tested. Furthermore, given larger numbers of samples, there can be expected to be a greater instance of the reproduction of constellations of minutiae in similar positions.

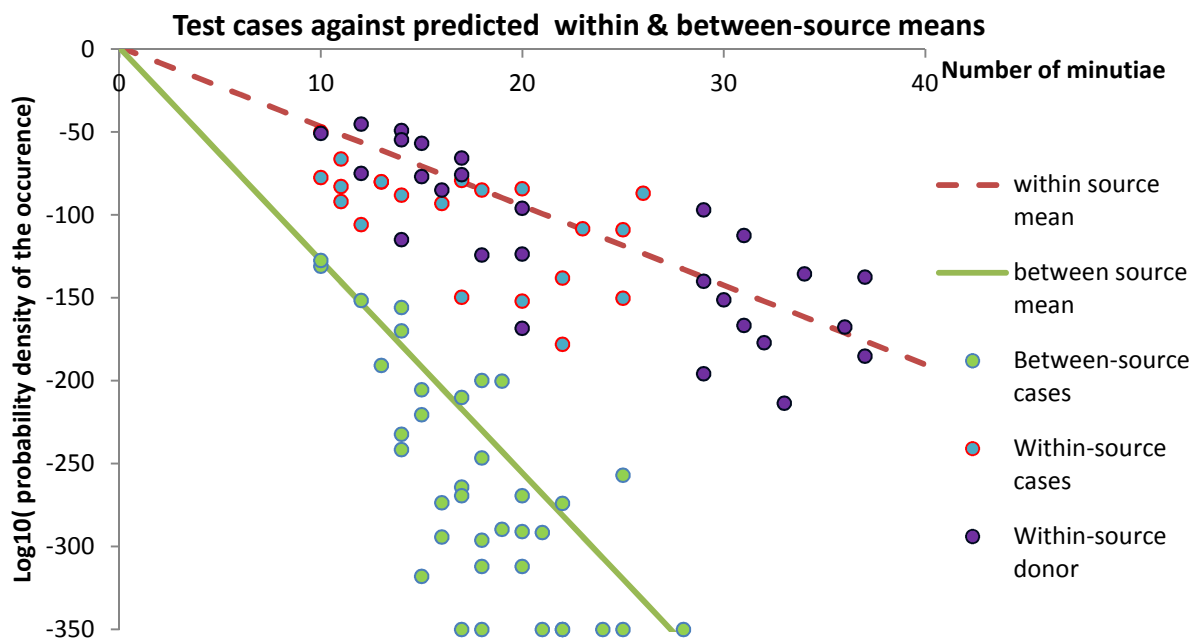


Figure 68 Test cases, plotted against, the within- and between-source means.

In both within- and between-source instances, the bulk of the cases fell below the predicted means. This may be because the generic mean and covariance matrix are based on one person only, and the variance in skin stretch for other donors could reasonably be expected to differ.

4.10 Testing model sensitivity

The reliability of the model will be affected by how it responds to variations in minutiae positions. Such variations of position will be due to different fingerprints being compared or poor marking of minutiae by an examiner.

A number of experiments were carried out on two images. These images were chosen because, when the comparison was initially processed and the probability density of coming from within-source calculated, and when plotted against the within- and between-source functions, it coincided with the within-source mean. Any effect on the probability density outcome due to changes to the minutiae positions would therefore be obvious. The experiments involved the movement of one minutia, the movement of all minutiae, the repeated plotting by an examiner of the same comparison, and the swapping of two minutiae in the marked order. In the first two experiments, the distance that minutiae in the latent fingerprint were moved was set, but the direction was one of 45, 135, 225 or 315 degrees, determined by a script in V++ using random numbers. For these two experiments, the position of the minutiae in the inked fingerprint, was not changed. In the third experiment, positions of minutiae in both the latent fingerprint and the inked fingerprint were randomly moved as a result of the natural variations in the markup process. In the last experiment, the order of the plotted minutiae was the same, except for two minutiae whose orders were swapped.

The image used in tests 1 to 3 involved an image of a fingerprint with 23 minutiae marked. The fourth test used a different fingerprint with 16 minutiae marked. Note that the approximate distance in the period described by parallel friction ridges in this image was

approximately 22 pixels and the difference between predicted mean logs of the probability densities for within-source and between-source is approximately 185 for 23 minutiae.

4.10.1 Test 1: Movement of one minutia by 10 pixels

This experiment involved moving a single marked minutia 10 pixels in a random direction. As there were 23 minutiae marked on the image, there were 23 experiments; one experiment for each moved minutia.

The changes in minutiae positions resulted in a degree of variation in the calculated probability density. These probability densities were plotted as shown in Figure 69. The range of the variation is shown in the data in Table 15. It can be observed that, while there is variation caused by the movement of one minutia by pixels, the effect is not great.

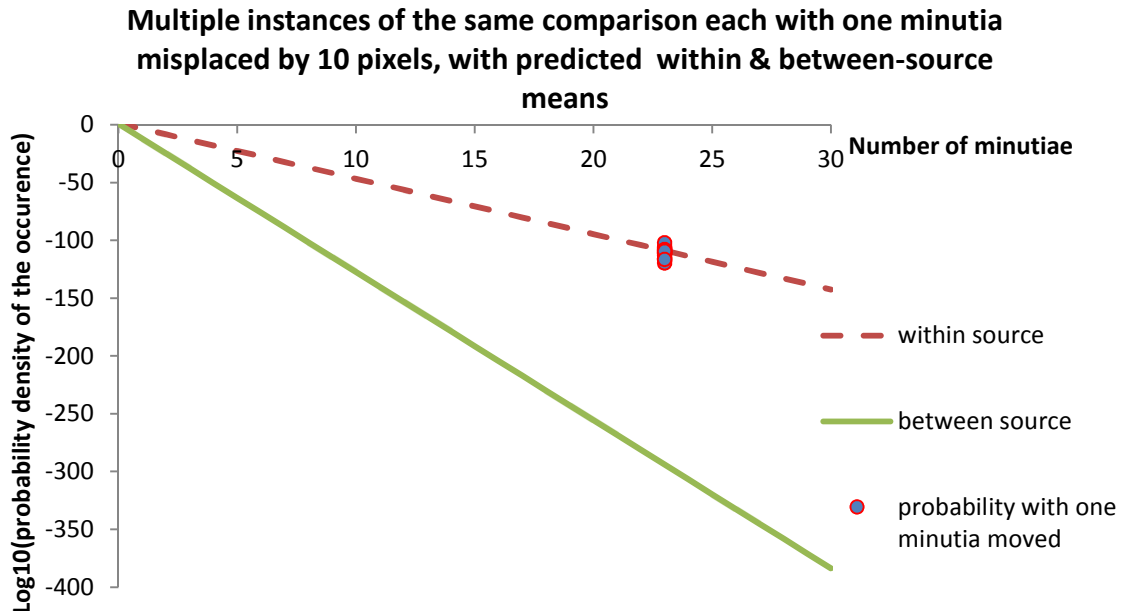


Figure 69 The variation in calculated probability density of one minutia being moved 10 pixels.

There were 23 compared minutiae in the images examined and 23 separate instances of a moved minutia.

The implication for comparisons by an examiner is that one poorly marked minutia may not have a significant effect on the probability density calculated.

Note that, in Table 15, the minimum value represents the lowest probability density of the compared fingerprint and fingermark being within-source, and the maximum value is the highest probability density.

	Probability density of comparison being within-source
Minimum	-1.20E+02
Maximum	-1.02E+02
Mean	-1.11E+02
Standard deviation	4.07E+00

Table 15 The range and variance of the calculated probability densities in test 1.

4.10.2 Test 2: Movement of all minutiae by varied amounts

10 experiments were carried out, where all minutiae were moved in a random direction by an increasing amount. The distance moved was the same as the experiment number in the series; that is, the first experiment the movement was one pixel. In the second experiment the movement was two pixels, and so on up to ten. The results are plotted in Figure 70. The range of the variation is shown in the data in Table 16. It can be observed that, the greater the error of marker positioning by an examiner, the greater the effect on the probability density calculated.

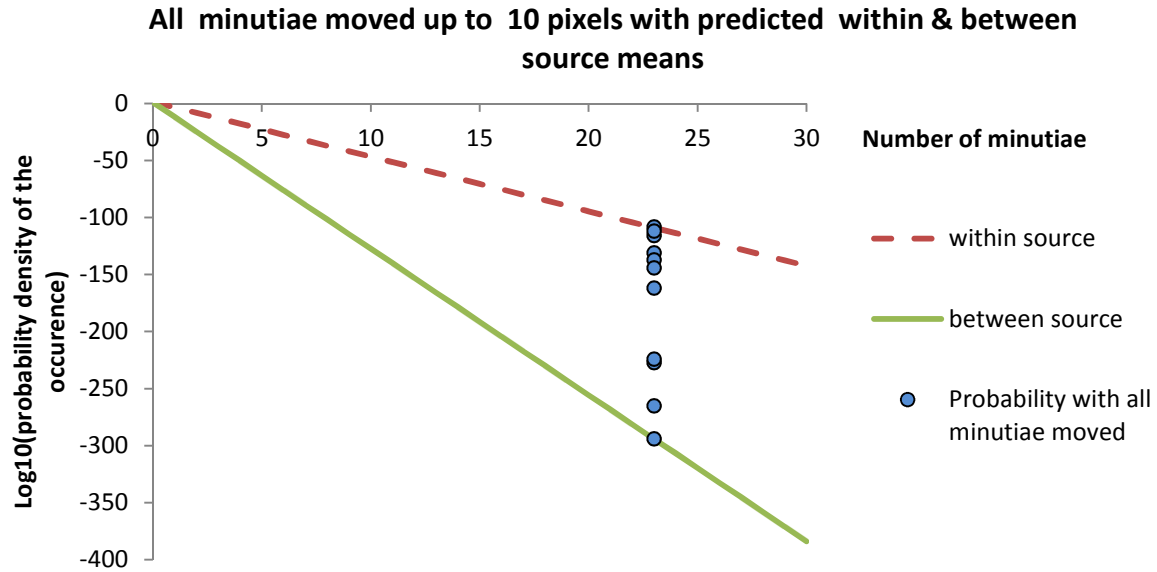


Figure 70 The variation in calculated probability density of all minutiae being moved 10 pixels. In each instance, all minutiae were moved an incrementing amount with the final image having minutiae moved 10 pixels. There were 23 compared minutiae in the images examined.

	Probability density of comparison being within-source
Minimum	-3.00E+02
Maximum	-1.08E+02
Mean	-2.01E+02
Standard deviation	78.89192

Table 16 The range and variance of the calculated probability densities in test 2.

Given that the approximate period of the friction ridges in this instance is 22 pixels and that the greatest distance the marked positions of the minutiae were moved was 10 pixels, it can be expected that if an examiner poorly positions all minutiae, there is the potential that a within-source case could be indicated by the model as between-source.

4.10.3 Test 3: Variation as a result of repeated manual plotting

This experiment involved the comparison of the initial position of the minutiae in the compared images with five more instances of the same compared images, all with new manually (by the same person) marked minutiae in both the latent fingerprint and inked

fingerprint. This experiment was to look briefly at the variance expected to occur through manual positioning of minutiae. The results are shown in Figure 71 and Table 17.

It can be observed that there is, as expected, a degree of variance due to error in minutiae placement. Note that this error does not indicate incorrect minutia nomination, but will nevertheless have an effect on the probability density calculated.

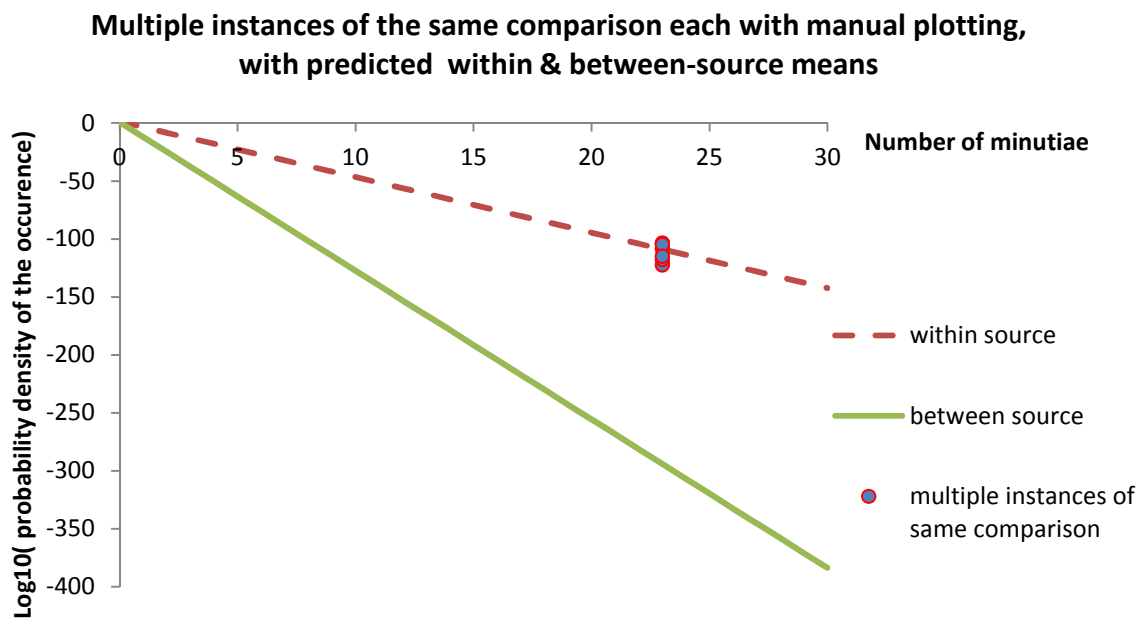


Figure 71 The variation in calculated probability density due to manual marking. In each 6 instances all minutiae were manually marked in the same positions as determined by an examiner. The variation observed is due to human assessment of the actual minutiae positions and a degree of error in the placement. There were 23 compared minutiae in the images examined.

	Probability density of comparison being within-source
Minimum	-1.22E+02
Maximum	-1.04E+02
Mean	-1.12E+02
Standard deviation	7.55E+00

Table 17 The range and variance of the calculated probability densities in test 3.

It should also be noted that all data that resulted in the within- and between-source regression functions was obtained through manual placement of the minutiae. As such, the model was generated with an inherent error due to normal minutiae placement and application of the model must be done with this error in mind.

4.10.4 Test 4: Swapping minutiae placement order

This experiment involved selecting two marked minutiae in the image and changing them in terms of their marked order. Figure 72 shows an image with numbers representing the marked minutiae locations.

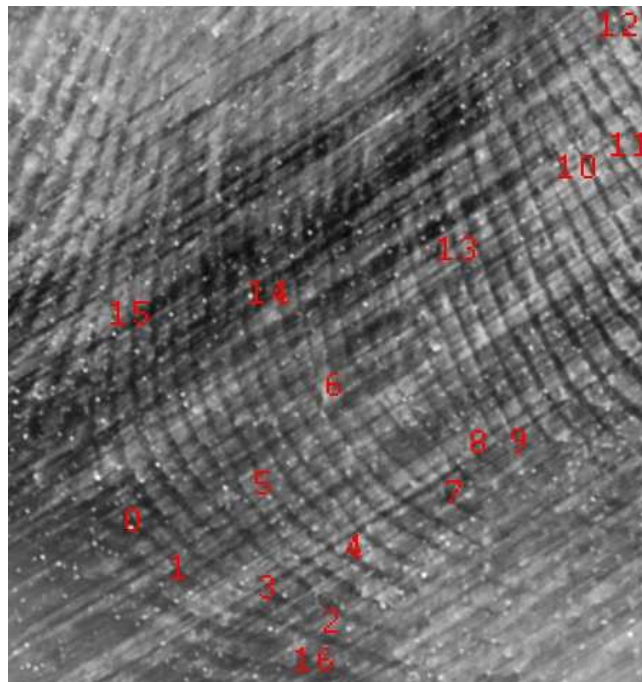


Figure 72 Marked minutiae on an image.
The minutiae are to the immediate left of the number.

In this instance the minutiae marked 2 and 3 were swapped. This simulates an examiner marking all of the minutiae correctly and in the same order, except for the order of minutiae 2

and 3, whose order, in this test case, is reversed. Table 18 shows the data that can be generated from the compared images.

Order	Minutia No.	Nearest 1	Nearest 2	Probabilities		Log10(p)		Incremental Differences		Probability density Differences
				normal	swapped	normal	swapped	normal	swapped	
0	6	14	5	6.0E-06	6.0E-06	-5.22	-5.22			
1	14	6	15	1.0E-10	1.0E-10	-10.00	-10.00	4.78	4.78	0
2	5	3	4	8.9E-15	6.3E-25	-14.05	-24.20	4.05	14.20	10
3	8	9	7	1.6E-19	1.2E-29	-18.78	-28.93	4.73	4.73	0
4	7	8	9	6.8E-25	4.8E-35	-24.17	-34.32	5.38	5.38	1
5	4	2	3	3.1E-29	8.2E-44	-28.51	-43.09	4.35	8.77	4
6	13	10	6	9.5E-38	2.5E-52	-37.02	-51.60	8.51	8.51	1
7	9	8	7	3.2E-43	8.6E-58	-42.49	-57.07	5.47	5.47	0
8	15	14	0	9.8E-51	1.2E-62	-50.01	-61.93	7.52	4.87	3
9	3	2	16	1.5E-54	3.7E-77	-53.83	-76.44	3.82	14.50	10
10	0	1	5	2.3E-58	1.3E-80	-57.63	-79.90	3.80	3.46	1
11	1	0	3	8.0E-62	2.6E-114	-61.10	-113.58	3.46	33.68	30
12	2	16	3	1.6E-65	3.5E-132	-64.79	-131.46	3.70	17.88	14
13	16	2	3	2.7E-69	1.4E-146	-68.56	-145.85	3.77	14.39	10
14	10	11	13	3.0E-74	1.9E-154	-73.52	-153.73	4.96	7.88	2
15	11	10	12	5.5E-79	3.4E-159	-78.26	-158.47	4.74	4.74	1
16	12	11	10	2.5E-85	1.5E-165	-84.60	-164.81	6.35	6.35	1

Table 18 Data generated from compared images with two minutiae in a reversed order.

The rows refer to increasing numbers of minutiae considered as the Order increases. The columns are as follows: Order refers to the order of minutiae examined; Minutia No. refers to the minutia number as shown in Figure 72; Nearest 1 and 2 refer to the 1st two closest minutiae (from which D1, D2 and A are calculated from); Probability densities contain an indication that the image comparison is within-source for both the normal and swapped minutiae arrangements; Log10(p) contains the log10 of the normal and swapped probability density; Incremental Differences contains the difference between subsequent rows; Probability Differences contain the differences in incremental changes; these values indicate, when high, where the effect of poor placement, or, the swapped minutiae, become apparent. The cells highlighted yellow contain reference to either minutia 2 or 3 (swapped minutiae), and the values coloured red indicate an effect of the swap as indicated by the Probability Differences column.

The values in the “Probability Differences” column, show, that when they are when noticeably high, there is a possibility of an error in the marked placement of a minutia. It can be seen in rows indicated by Order 2, 9, 11, 12 and 13. Note that each of these minutiae are either minutia 2 or 3, or, they involve 2 or 3 in the next closest two minutiae. Note also, that for minutia number 4, both minutiae 2 and 3 are the nearest two minutiae. Given their relative positions, the angle will not change, and, the changes in distances measured will not be great. There is therefore, no great change in the Probability Differences.

Where there is an effect of the swapping of the minutiae, the subsequent calculated probability density is also affected. Figure 71 shows the effect of the calculation of subsequently added minutiae, for both the normal marking, and that where the two minutiae have been swapped.

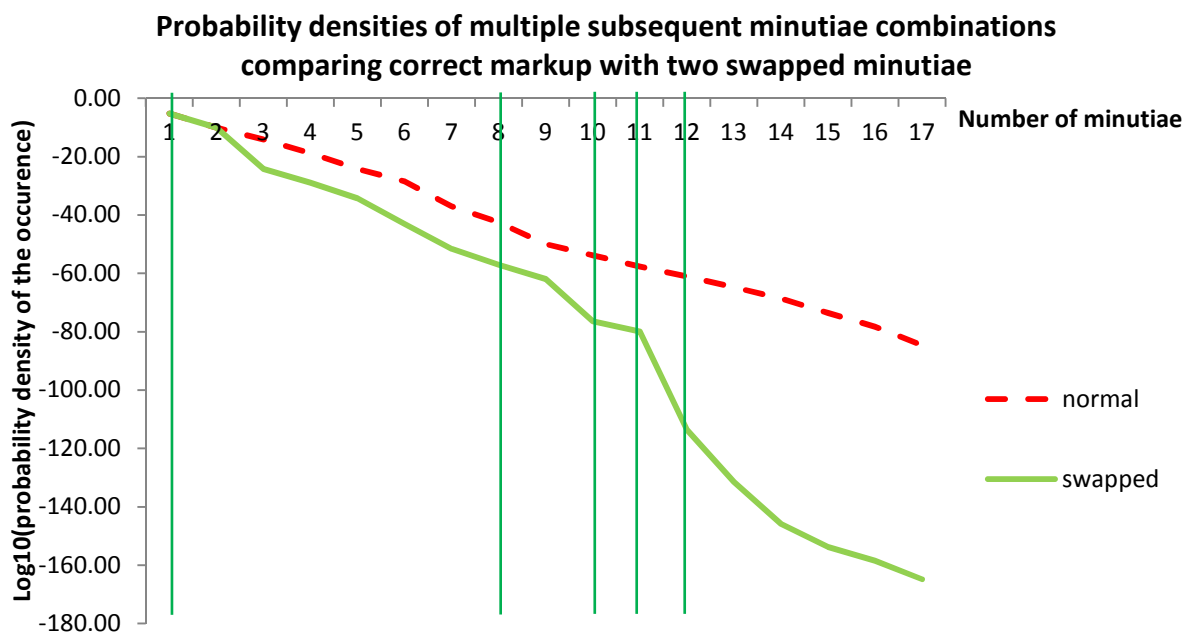


Figure 73 The effect on the probability densities by the swapped minutiae. The green lines are placed over the points on the “swapped” series where the change of the Probability Differences is most noticeable.

Where there has been a large change in the Probability Differences, the calculated probability density will have been affected. This can be seen in Figure 73 where the slope increases as indicated by the green lines. Note that, where there is no large change, the slopes for normal and swapped are relatively parallel.

The effect of swapped minutiae will vary according to the positions of the minutiae (proximal to other minutiae) or when one is the centroid minutia. Given either of these conditions, the effects could be multiple or potentially greater, causing a compounding diminishing effect on the calculated probability density.

Given a low probability density of with-source for a comparison, where it is expected that the comparison is correct (and is within-source), the data in Table 18 can be examined (as a diagnostic tool) to locate any minutiae in question, that may be causing the deviation in probability density.

5. Discussion & conclusion

The objective of this research was to establish a simple model that will incorporate a statistical analysis to test what a fingerprint examiner has used to conclude that a fingerprint and a fingermark have come from the same source.

Whilst there was no actual between-source data gathered, this was not an issue in that the question being asked was, “Is there an indication of support for the proposal that the examiner is correct in their conclusion?” Given this, the model seeks to test data from any instance of a comparison against the distributions for the measured within-source variance. The response from the model is an expression of how well the examiner’s nominated features in the comparison “fit” as if they had come from the same finger. Where there is excessive difference in minutiae positions (i.e. beyond reasonable variance due to natural skin distortion), the response will be less supportive indicating that the comparison is between-source.

This chapter includes model limitations, assumptions, a general discussion, and conclusions from the research.

5.1 Limitations

5.1.1 Training data obtained on a flat surface

This research has used the images of friction ridge contact with a smooth, flat surface, as being representative of all marks and prints left by a finger. In reality, the marks left by a finger will be affected by any variations in the receiving surface. In instances where the surface changes to the extent that the resulting distortion is beyond reasonable variance,

individual areas that are, in themselves, not affected by the surface variation, should be considered individually.

5.1.2 Measurements in the digital environment

Measurements have been made using locations in the image that indicate where variation in minutiae positions has occurred. These locations are represented by Cartesian plane X and Y coordinates.

As discussed in Chapter 3, there is a limited set of angles that can be calculated for any given distance. This will affect all measurements but, more significantly, smaller measurements. Figure 74 illustrates the error function. For distances of less than 40 pixels, there is a potential error of greater than 5% of the distance measured, with that percentage increasing as the distance gets smaller. As the majority of the distances measured were greater than 40 pixels, this error was acknowledged but not otherwise accounted for.

This research used changes in minutiae relative positions to detect potential between-source comparisons. Changes in calculated angles described by three minutiae are easily determined; however, the same degree of change of minutia position measured over different distances produces a different change in angle.

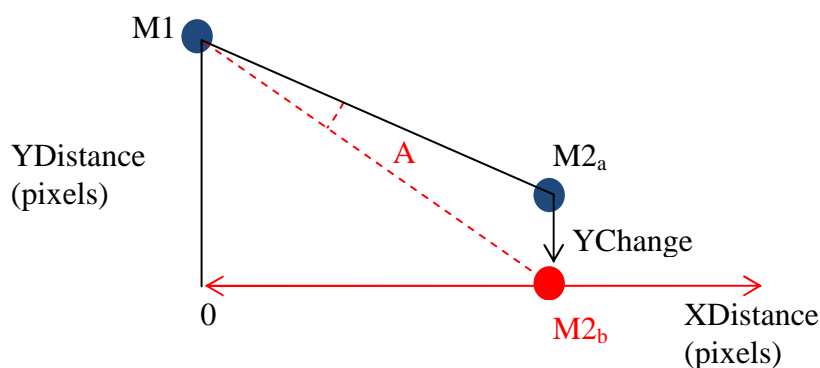


Figure 74 Diagram showing effect on angle given a change in position and distance.

Figure 74 simulates the relationship between two minutiae, M1 and M2_a, where the two minutiae are separated by a distance described by XDistance and YDistance. If M2_a is moved by the distance YChange to the position of M2_b, this will produce a change in the angle to the normal as represented by A. As the x coordinate of M2_a and M2_b varies, the value for A varies also.

The change in A with the XDistance is shown in Figure 75. The distance values in this case for YDistance was 40pixels, YChange was 5pixels, and XDistance varied between 0 and 600 pixels. In this instance, the greatest amount of change of A is where XDistance equals 37 pixels.

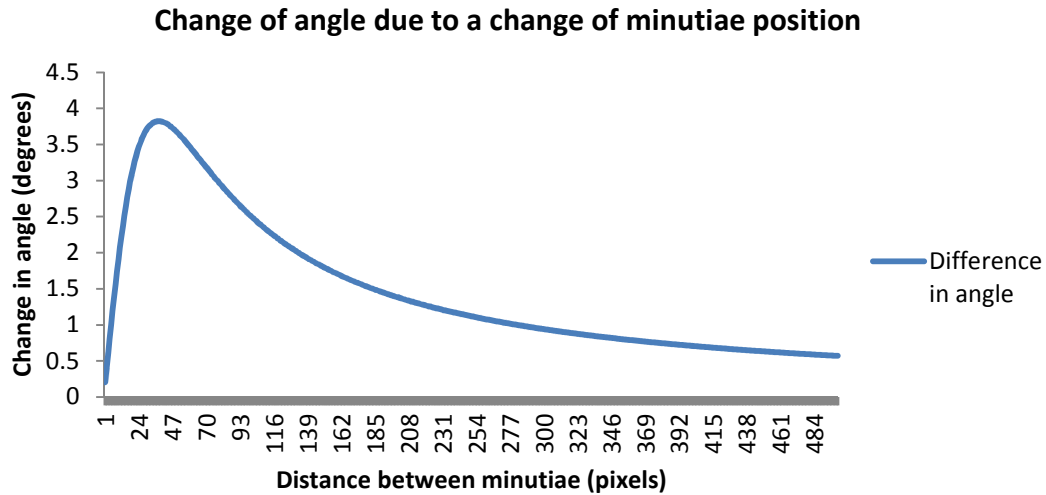


Figure 75 Function of the change of angle with a change in minutiae relative position.

The relationship between the maximum value for A, the YDistance, XDistance and YChange is shown in Eq. (5.1).

$$XDistance = Integer(YDistance - \frac{YChange}{2}) \quad (5.1)$$

It could then be argued that, to optimize the efficiency of a model detecting changes of minutiae positions through angle measurement, the model should select minutiae whose

distances between them maximises the change in the angle. This selection of minutiae should also consider minimising error through measurement of angles over distances that are not too close.

5.1.3 Minimal variables used

This model is very simple in that there are only three variables considered, being the two distances D1 and D2, describing the two distances between a given minutia and its two next closest, and the angle A between those three minutiae. Other models such as that proposed by Neumann (2006 and 2007) are relatively complex and incorporate continuous data through various distributions, classifiable data and distortion models. However, the use of a minimal number of variables is easier to implement into fingerprint comparison software and, as shown by this research, can be used to moderate the examiner's conclusion.

5.1.4 Manual marking of minutiae positions

No feature recognition software was used in this instance for the generation of training data to establish the model. This was done on purpose as it is expected that the application of this model would not see feature recognition done automatically; it would be done through the manual marking of minutiae by an examiner and, as such, we would be testing what the examiner has marked. The effect of this is that the manual marking of minutiae is likely to introduce a greater degree of variance than there is in reality.

A drawback of this (or any other model using feature coordinates) is that inaccurate or poor marking of minutiae may lead to erroneous outcomes from the model. However, the examiner must be held accountable for what they purport to have used.

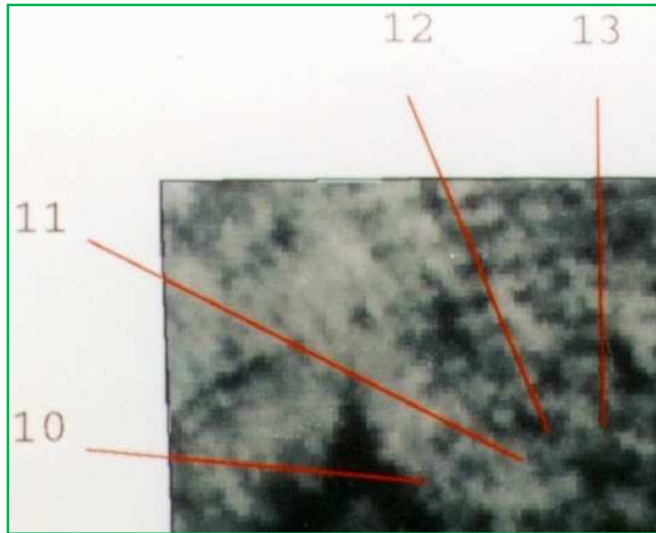


Figure 76a Section of the marked latent fingerprint

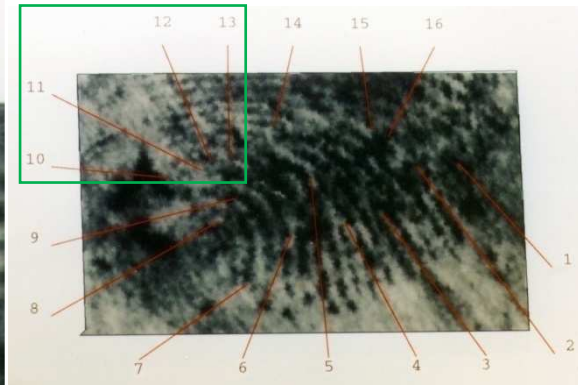


Figure 76b A marked latent fingerprint

Figure 76 Example of a marked unclear latent fingerprint.

(<http://onin.com/fp/fmiru/bumscchartlp.jpg>)

Figure 76b shows a marked latent fingerprint and 76a shows detail of part of the marked image. Features have been nominated at various locations in the latent mark that are not able to be clearly seen. The resolution of the image in this case may have a detrimental effect on its clarity; however, in reality, there is no clear detail to be seen. If the nominated locations of the compared minutiae coincide, it is possible that the model will support a comparison as being within-source even if it is not the case. In any case that includes poor clarity, such as the case dealing with the mark in Figure 76, the examiner must be required to explain what the features are that they have used and indicate in the image where they are.

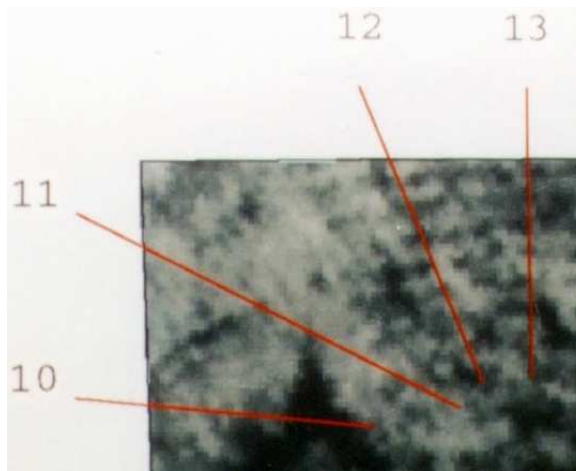


Figure 77a Section of a marked latent
fingerprint

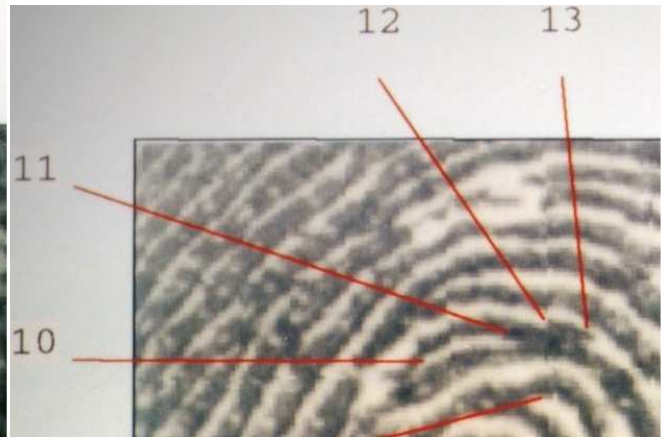


Figure 77b Section of a marked latent
fingerprint

Figure 77 Example of a comparison of marked friction ridge features.

(<http://onin.com/fp/fmiru/bumscchartlp.jpg>, and <http://onin.com/fp/fmiru/bumscchartlp.jpg>)

In Figure 77a, the nominated features are not able to be seen and therefore it will be very difficult for an examiner to satisfy a court of the features' existence. Figure 77b has a high degree of clarity and the features are easy to see, classify and locate. If the examiner is not able to satisfy their peers or a court of the unequivocal existence of their marked features, the model should not be applied.

5.1.5 Variation in ridge structure

Minutiae were marked in accordance with Figures 23 to 25. The variation that occurs naturally within donors is such that classifiable ridge structure will vary, having an effect on the marked minutiae locations. Figure 78 shows the inked print from a donor that has variations in the appearance of friction ridge endings. Figure 78b shows three instances of ridge endings with variable appearance; Figure 78b (top) shows a subsidiary ridge, which is a lesser developed friction ridge. It is a permanent structure that can be used for identification; however, its presence and length will be affected by force of the finger against the surface.

Figure 78b (middle) shows a friction ridge with a tapering end. Again, its length (the termination of the ridge) will be affected by force of the finger against the surface.



Figure 78a Example of a fingerprint

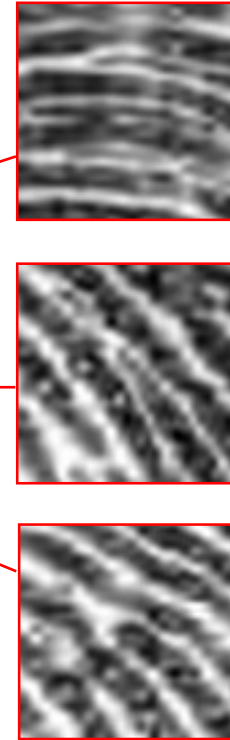


Figure 78b Variations of friction ridge endings

Figure 78 Example of a fingerprint with variations of friction ridge endings.

Figure 78b (bottom) shows a friction ridge with a round end. It is expected that the location of this will be relatively constant with variations of force applied. The problem presented by these variations is that no one rule for minutiae position nomination will adequately deal with the variations that can occur, as the same area of skin can make an impression that varies in a many of ways.

5.1.6 Cases with few features

In a comparison of a fingerprint and print, the fewer the number of features marked the more the functions describing the within- and between-source probabilities (Figure 68) will converge. This means that the fewer the number of features marked, the less discriminating and effective the model will be. Results from such comparisons should be considered with this in mind.

5.1.7 Use of close friction ridge detail

If the fingerprint examiner were to mark many very close minutiae (at distances at less than 40 pixels), it could be expected that this will reduce the probability density calculated that the comparison is within-source due to the errors in angle measurement. If the nearest two minutiae were to be no less than 40 pixels, thereby disregarding the actual closest, then close third level detail locations could be marked and used in the model.

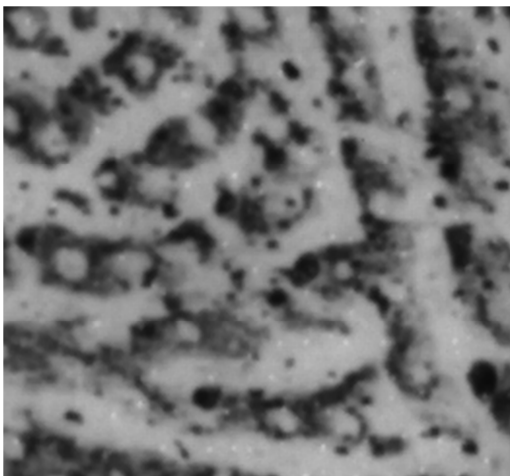


Figure 79a Section of a developed latent mark from a palm

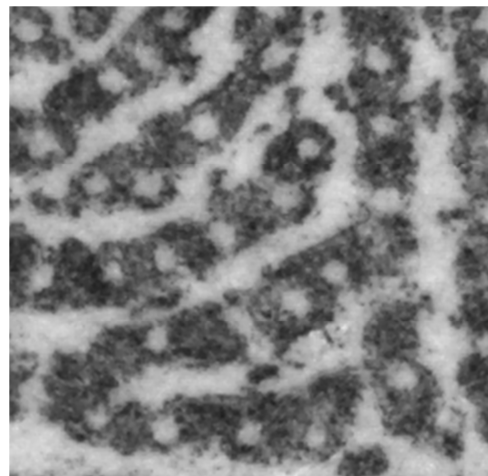


Figure 79b Section of a print from a palm

Figure 79 Sections of a latent palm mark (Figure 79a) and print (Figure 79b).

Note the pore openings (third level detail) seen as white circular shapes within the friction ridges. This is clearer in the print. These structures are likely to be much closer together than will second level detail.

Figure 79 shows a latent mark and the corresponding reference print, both showing clear pore detail. Given that, the approximate distance between friction ridges (at the scale examined in this research) is 22 pixels, if the pores were marked as features, there may be significant error introduced.

These finer details have a better potential for actual feature positioning by an examiner than second level detail, as they are inherently smaller than the actual friction ridge. Figure 80 shows a fingerprint with many subsidiary friction ridges.



Figure 80 An image of a mark left by a thumb with subsidiary friction ridges.

These smaller features have better potential for marking a fingerprint feature with an x and y coordinate, on the basis that the size of the feature is smaller.

These formations are considered as friction ridges that are incomplete in development. They are lower in cross section and are lower and narrower than normal friction ridges. Consequently, they present as a smaller area in a fingerprint and, therefore, the area in which to locate the feature is smaller. The average distance between the marked locations in Figure 80 is 26 pixels, the minimum 14 and the maximum 69 pixels. When the model is applied to

the extracted data, given the 31 marked features, the log10 of the probability density of within-source is -122. Despite any potential error, the returned value in this instance is a clear indication of within-source support. In a clear fingerprint, there may also be more third level detail available than second level detail. Incorporation of a mechanism to measure features beyond a specified distance may reduce angle error to an acceptable error. However, this was not further considered in this research.

5.2 Assumptions

5.2.1 Skin stretch

The hypothesis includes the statement that “*Friction ridged skin has a stretch limitation*” and the model is designed on that basis. It is assumed that there is a limit as to how much skin can stretch and that it will stretch consistently in terms of amount and direction for minutiae that are close. On this basis, when the measured data from compared close minutiae are not similar within reasonable limits, they will be regarded as less likely to have come from the same source.

5.2.2 Proximal minutiae and amount of stretch variation

It is assumed that measurements taken from proximal minutiae represent the least variation that can occur. Based on that assumption, the further apart the minutiae are, the more skin there is between them and therefore more stretch and positional variation can occur. However, as shown in Figure 75, angle variation is less sensitive for minutiae that are further apart, so they should possibly not be considered.

5.2.3 Variations in distortion

It is assumed that the training data generated from the within-source images will be representative of all possible distortions of a finger. If the assumption of limited skin stretch is correct, then it could be argued that the type of distortion occurring is irrelevant; skin can only vary so much.

5.3 Discussion

5.3.1 Generic mean and covariance matrix elements

As mentioned in Chapter 4, the values contained in the generic mean vector and covariance matrix involve two considerations:

1. Are the values reasonably representative of the human population? and
2. Do the values sufficiently discriminate within- and between-source comparisons?

As a result of this research, two distributions are described that are representative of within- and between-source cases. These were generated through case responses tested against the generic within-source data, for varied numbers of minutiae. Clearly if the generic values are “accurate” they will be more discriminating than if they were not. In any case, we can expect that the within-source distribution will have less variance than between, as the between-source, according to the discussed assumptions, will return data that has greater variance than the within-source data. Regardless of accuracy of this model, we will have a within-source distribution that is overlapped by a wider distribution representing between-source. The implication of this is that the use of a likelihood ratio calculated from the probability density that this model calculates, that the mark and print have come from the same source and the probability density that the mark and print have come from different sources, will be limited.

Ultimately, because there are only a small number of variables used, the model will have a limited ability to discriminate between within- and between-source comparisons. However, the usefulness of the model is determined by its intended purpose and, in this research, the intention is to differentiate within- and between-source comparisons as a test of an examiner's outcome.

5.3.2 Straight impressions in training data collection

The series of images that were used for within-source data collection involved the acquisition of the image of fingers placed straight on the prism, prior to any distortion movements being performed. This was done on the basis that not all developed latent fingerprints exhibit gross distortion. The inclusion of these images will have the effect of reducing the variance of minutiae position.

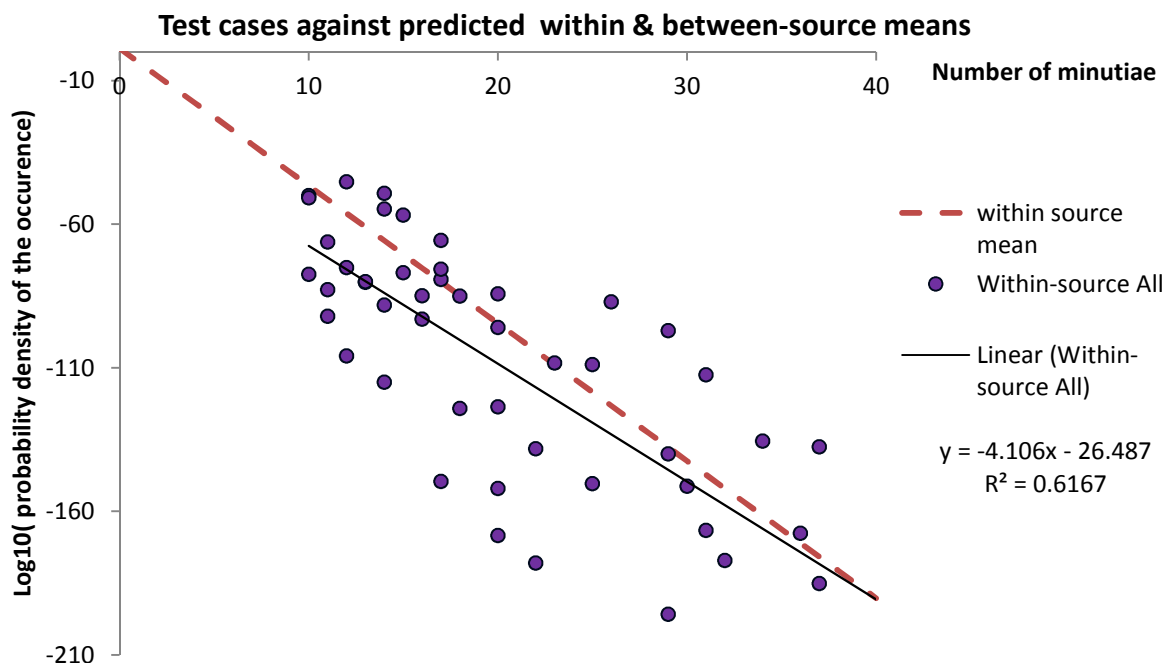


Figure 81 Regression of within-source cases and the predicted within-source mean function.

It could be expected that the slope of the within-source mean function (-4.864), as shown in Figure 65, may actually be different if there were no straight impressions included; however, a regression analysis of the within-source donor sample comparisons and the within-source cases comparisons revealed a slope (-4.106) very similar to that of the within-source mean function. Figure 81 illustrates the two slopes.

5.3.3 Interpretation of results

The model can be used to test a given comparison by obtaining the differences in the angles and distances between corresponding minutiae and testing them against the generic mean and covariance matrix. The probability density of being within-source for the case being examined can be plotted against the within- and between-source functions according to how many minutiae are compared. This will give an indication of a measure of objective support that can be given to the subjective and conclusive outcome of the human examiner.

The area above the slope representing the best case scenario appears on the chart (Figure 54), but it is impossible for an actual case to occur there. This is so because it is not possible to have any better match than an image compared with a duplication of itself.

The log10 of the probability density values that fall below approximately -350 will all appear as -350, as the number formats in Matlab and Microsoft Excel cannot accommodate lesser values.

If a case is plotted in the area between the within- and between-source functions, it is then open to interpretation as to whether or not the conclusion of within-source is supported. Whilst in Chapter 4 the means and standard deviations for the probability densities of within-source were calculated for all cases, it can be demonstrated that these distributions do not necessarily distribute normally. Figure 67 shows the distributions for all within-source

comparisons with numbers of minutiae from 1 to 30. Whilst there is some variance in the degrees of normality, the variance increases only slightly with the increase in numbers of minutiae. The “dots” below some of the box plots show the presence of outlier cases. Figure 62 shows the distributions for all between-source comparisons with numbers of minutiae from 1 to 10. The line in Figures 62 and 67 indicate the approximate slopes described by the mean values. As the numbers of minutiae increase in Figure 62, the variance increases with an increasing skew towards lower values. This is consistent with the plotting of the between-source cases as shown in Figure 68, where most of the cases are occurring below the mean slope.

The distributions of the within- and between-source data suggest a theoretical region between them where the overlap is minimal.

We are able to test cases where there are more samples than those collected in this research, using projections of the slopes for within- and between-source. It should be noted that these are anticipated values. However, it is apparent that, due to the contribution of additional minutiae, the within- and between-source cases tend to disperse further apart as the numbers of minutiae compared increase. Therefore, it is not unreasonable to use such projected slopes in testing cases.

Figure 82 shows an overlay of Figures 62, 67 and 68, each scaled to indicate the range of data used in this research, the variance of the training data, and the distributions of the within- and between-source test cases.

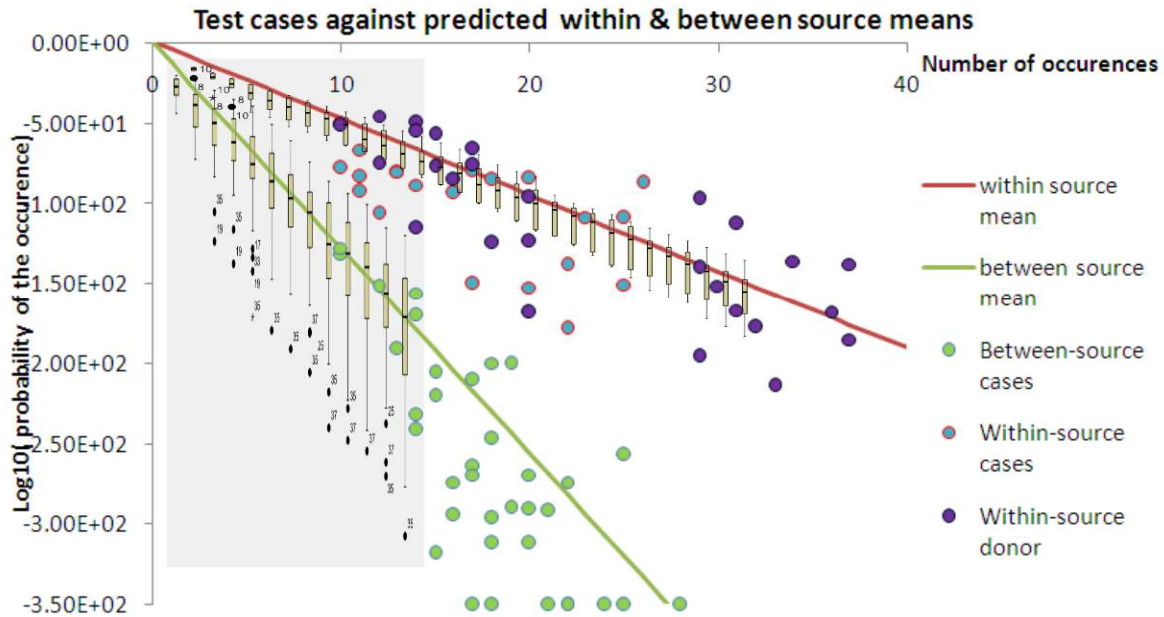


Figure 82 Distributions of within- and between-source box plots and test cases.

The result from a test case should be able to be anticipated. Given that the mean slope for within-source is approximately -5 and that for the between-source is approximately -12, the result should be able to be estimated by multiplying each slope by the number of minutiae. For example, if a case has 10 minutiae, an indication that the comparison is correct should see the \log_{10} of the probability density in the vicinity of -50, and an indication that the comparison is incorrect should see the \log_{10} of the probability density in the vicinity of -120. The result of the test is represented by where the tested case falls in relation to the within and between-source slopes. If the result falls on or above the within-source slope, it is a clear indication of support for the proposition that the mark and print have come from the same person. If it falls on or below the between-source line, it is supporting the proposition that the mark and the print have not come from the same person. Should the case fall between the two slopes, there is room for speculation as to which proposition is supported. Common sense would state that the closer slope is more strongly supported; however, in the absence of

data shown to be more representative of reality and not based on only one person, it may be difficult to justify either way.

It should be noted that, in cases where there is reason for the model to fail, the examiner must be able to explain what these reasons are. Such reasons could include variation in surface contour, excessive perspiration (or contaminant) on the surface of the finger, lack of definition in the developed latent fingerprint, or, another reason that will undermine the measurements involved.

5.4 Conclusion

The purpose of this research was to develop an objective test of a fingerprint examiner's conclusion that a fingerprint and print have come from the same source. This is based on the hypothesis that

“Friction ridged skin has a stretch limitation; therefore, corresponding minutiae in compared images of fingerprints will vary in their relative positions within limits”.

The “limits” have been defined by the generic mean and covariance matrix, and cases tested against these. Considering the performance of the model, in that it is able to differentiate within- and between-source comparisons, it is considered that the hypothesis is supported and the proof-of-concept achieved.

Given that there are, as discussed here, a number of limitations, there is further work needs to be done, and considerations must be borne in mind if the model is used. The model can be

used as a stand-alone test or be integrated into comparison software for the purpose of providing information that will supplement examiners' findings.

There are limitations in the model for various reasons, however, the model is capable of describing a metric summarizing a distance between the within- and between-source responses and therefore can contribute information supplementing that of the human examiner.

There can in nature be, according to theory, no repeats of actual form (no two fingerprints the same); however, it must be considered possible that close repeats of occurrences of fingermark features from different sources, if considered in the absence of all other features and observations, could be incorrectly considered as coming from the same source. Also, the flaw of a model is that, in the absence of human contribution, it can misrepresent fact by not considering all available information. This model uses a very small amount of the information available, but is based on a legitimate argument (e.g.: skin stretch).

This model is not proposed to stand alone, but exist as an independent and purely objective test of an examiner's opinion.

5.5 Further work

1. This research has been done to prove a concept. The data gathered is not assumed to represent the variance that could be expected in the population. Further work to establish regression functions using a ground truth set of comparisons would be advisable.

2. Errors due to small distances may have an impact on the data generated and the final result. Additional research to associate the nearest two minutiae that are not closer than a defined value that minimises error to a determined level. This would allow the inclusion of all third level detail, close or distant, in the mark-up, and the probability density calculation. This would result in a greater number of features to be plotted with, in the case of fine third level detail, greater precision in the locations marked.
3. This research is based on images of the same resolution (1000DPI). There is a need to develop a function that measures the path in pixels, described by all marked minutiae, from the first, through each minutia in order to the last. If this is done in both images and one path length divided by the other, a scale factor will result that will allow for the comparison of images of different resolutions.
4. The values in the generic covariance matrix rely on the images both being at 1000DPI. If the images are at different resolutions, the values for $D1_{diff}$ and $D2_{diff}$ need to change accordingly. If, however, the measurements were taken and represented as a percentage change and not pixels, scale is no longer a concern, so long as the images are of the same relative scale.

6. Bibliography

- Ashbaugh, D. R. (1991, January/February). Introduction to Ridgeology. *Journal of Forensic Identification*, 4(1), 16 - 53.
- Ashbaugh, D. R. (1994). The premise of friction ridge identification, clarity, and the identification process. *Journal of Forensic Identification*, 44(5), 498 - 516.
- Babler, W. (1991). Embryologic Development of Epidermal Ridges. *Birth Defects Original Article Series*, 27(2), 95 - 112.
- Beeton, M. (2001). *Development of Friction Skin*. Retrieved May 15, 2011, from Ridges and Furrows: http://ridgesandfurrows.homestead.com/friction_skin.html
- Berkman Centre for Internet and Society. (1999, April). *The Judge's role as gatekeeper: Responsibilities and power*. Retrieved June 2011, from The Judicialk Gatekeeping Project: http://cyber.law.harvard.edu/daubert/ch5.htm#N_1_
- Berry, J., & Stoney, D. A. (2001). History and Development of Fingerprinting. In H. C. Lee, & R. E. Gaenslen, *Advances in Fingerprint Technology second edition* (pp. 1 - 40). Boca Raton CRC Press.
- Budowle, B., Buscaglia, J., & Schwartz-Perlman, R. (2006, January). *Review of the Scientific Basis for Friction Ridge Comparisons as a Means of Identification: Committee Findings and Recommendations*. Retrieved February 16, 2012, from FBI - Research and Technology - Forensic Science Communications - January 2006 vol (8): http://www.fbi.gov/about-us/lab/forensic-science-communications/fsc/jan2006/research/2006_01_research02.htm
- Capelli, R., Miao, D., & Maltoni. (2001). Modelling plastic deformations in fingerprint images. *Second International Conference in Advances in Pattern Recognition, Vol 2013*, pp. 369 - 376.
- Champod, C. (1995). Edmond Locard - Numerical standards & probable identifications. *Journal of Forensic Identification*, 45(2), 136 - 155.
- Champod, C., Lennard, C., Margot, P., & Stoilovic, M. (2007). *Fingerprints and other ridge skin impressions*. Boca Raton CRC Press.
- Dinning, L. (2005). *Movement of friction ridged skin: a visualisation*. Report pursuant to completion of Diploma Forensic Investigation (Fingerprints), Canberra Institute of Technology.
- Duda, R., Hart, P., & Stork, D. (2001). In *Pattern Classification*. John Wiley & Sons.
- Egli, N., Champod, C., & Margot, P. (2006, August). Evidence evaluation in fingerprint comparison and automated fingerprint identification systems - modelling within finger variability. *Forensic Science International*, 167(2-3), 189 - 95.

- Federal Bureau of Investigation. (2005, January). *Report on the Erroneous Fingerprint Individualization in the Madrid Train Bombing Case*. Retrieved 2011 May, from Forensic Science Communications: http://www.fbi.gov/about-us/lab/forensic-science-communications/fsc/jan2005/special_report/2005_special_report.htm
- Flatt, A. E. (2000). Grasp. *Baylor University Medical Centre Proceedings*, vol 13 (4), pp. 343 - 348. Dallas, Texas.
- Gonzalez, R., & Woods, R. (1992). *Digital Image Processing* (2nd ed.). Addison-Wesley.
- Grew, N. (1684). *The Description and Use of the Pores in the Skin of the Hands and Feet*. Retrieved May 2011, from SAO/NASA ADS General Science Abstract Service: <http://adsabs.harvard.edu/abs/1684RSPT...14..566G>
- Houck, M., Bisbing, R., Watkins, T., & Harmon, R. (2004, March 2). *The science of forensic hair comparisons and the admissibility of hair comparison evidence: Frye and Daubert considered*. Retrieved February 16, 2012, from MMJ - The Science of Forensic Hair Comparisons and the Admissibility of Hair Comparison Evidence: <http://www.modernmicroscopy.com/main.asp?article=36&page=9>
- Kennedy, D. (2003). Forensic Science: Oxymoron? *Vol 302(5651)*, 1625.
- Kinoshita, H., Backstrom, L., Flanagan, J., & Johansson, R. (1997). Tangential torque effects on the control of grip forces when holding objects with a precision grip. *Journal of Neurophysiology*, 78 (3), 1619 - 1630.
- Langenberg, G. (2009). Performance Study of the ACE-V Process: A Pilot Study to Measure the Accuracy, Precision, Reproducibility, Repeatability, and Biasability of Conclusions Resulting from the ACE-V Process. *Journal of Forensic Identification*, 59(2), 219 - 257.
- Langenburg, G., Champod, C., & Wertheim, P. (2009, May). Testing of potential contextual bias effects during the verification stage of the ACE-V methodology when conducting fingerprint comparisons. *Journal of Forensic Science*, 54(3), 571 - 582.
- Lee, H. C., & Gaensslen, R. (2001). In Lee, *Advances in Fingerprint Technology* (p. 19). CRC Press.
- Maceo, A. (2009). Qualitative assessment of skin deformation: A pilot study. *Journal of Forensic Identification*, 59(4), 390 - 440.
- Maltoni, D., Maio, D., Jain, A., & Prabhakar, S. (2005). *Handbook of Fingerprint Recognition*. New York: Springer-Verlag.
- MathWorks. (2008, August 23). SPSS Statistics GradPack 17.0.
- Moenssens, A. (1971). *Fingerprint Techniques*. Radnor, PA: Chilton Book Company.
- National Academy of Sciences. (2009). *Strengthening Forensic Science in the United States*. National Academy of Sciences.

- National Research Council. (2009). *Strengthening Forensic Science in the United States: A Path Forward*. Washington DC: The National Academies Press.
- Neumann, C. (2007, March). *Validation and Implementation Challenges of the FSS Fingerprint Statistical Model*. Canberra: International Fingerprint Research Group.
- Neumann, C., Champod, C., Puch-Solis, R., Egli, N., Anthonioz, A., & Bromage-Griffiths, A. (2007). Computation of likelihood ratios in fingerprint identification for configurations of any number of minutiae. *Journal of Forensic Science*, 52(1), 54-64.
- Neumann, C., Champod, C., Puch-Solis, R., Egli, N., Anthonioz, A., Meuwly, D., et al. (2006). Computation of likelihood ratios in configurations of three minutiae. *Journal of Forensic Science*, 51(6), 1255-1266.
- Pankanti, S., Prabhakar, S., & Jain, A. (2002). On the individuality of fingerprints. *IEEE transactions on pattern analysis and machine intelligence*, 24(8), pp. 1010 - 1025.
- Polinski, J., Smith, J., & Garrett, R. (March, 2011). *The Report of the International Association for Identification, Standardization II Committee*. Retrieved February 19, 2012, from <https://www.ncjrs.gov/pdffiles1/nij/grants/233980.pdf>
- Scientific Working Group on Friction Ridge Analysis, S. a. (2011). *STANDARD TERMINOLOGY OF FRICTION RIDGE EXAMINATION*. Retrieved January 30, 2012, from http://www.swgfast.org/documents/terminology/110323_Standard-Terminology_3.0.pdf
- Stacey, R. B. (2005, January). *Report on the Erroneous Fingerprint Individualization in the Madrid Train Bombing Case*. Retrieved June 2011, from Forensic Science Communications:
http://www2.fbi.gov/hq/lab/fsc/backissu/jan2005/special_report/2005_special_report.htm
- Stoney, D. A. (2001). Measurement of Fingerprint Individuality. In H. C. Lee, & R. E. Gaensslen, *Advances in Fingerprint Technology second edition* (pp. 327-387). Boca Raton CRC Press.
- Tabachnick, B. E., & Fidell, L. S. (2001). *Using Multivariate Statistics*. (4th, Ed.) Allyn & Bacon.
- The Scottish Parliament. (n.d.). *SECTION 3: REVIEWS OF THE SCRO FINGERPRINT BUREAU*. Retrieved June 2011, from Justice 1 Committee Report - Inquiry into the Scottish Criminal Record Office and Scottish Fingerprint Service:
<http://www.scottish.parliament.uk/business/committees/justice1/reports-07/j1r07-03-vol1-03.htm>
- Tredoux, G. (2003, December). *Henry Faulds: the Invention of a Fingerprinter*. Retrieved May 2011, from <http://galton.org/>

- Tuthill, H. (1994). *Individualization: Principles and Procedures in Criminalistics*. Salem: Lightning Powder Company.
- Ulery, B. T., Hicklin, R. A., Buscaglia, J., & Roberts, M. A. (2011). *Accuracy and reliability of forensic latent fingerprint decisions*. Retrieved February 29, 2012, from <http://www.pnas.org/content/early/2011/04/18/1018707108.full.pdf>
- Vanderkolk, J. (1999). Forensic individualization of images using quality and quantity of information. *Journal of Forensic Identification*, 49(3), 246-256.
- Zabell, S. L. (2005). Fingerprint Evidence. *Journal of Law and Policy*, 13(1), 143 - 179.

7. Appendices

7.1 INI file

c:\test\camera_image_conversion.ini

Summary

The ini file existed as a repository for paths and constants used in scripts. The file is as follows:

```
[file_locations]
camera_output="C:\test_in"
V++_output="C:\test_out"
```

where to collect new images from camera
folder to move images to after renaming

```
[scale_factor]
sFact=1.4
```

factor to overcome foreshortening

7.2 V++ Scripts

7.2.1 Process images

Summary

This script opens two images; a target and a reference image. The reference image is affected by nonlinear distortion. Both images contain “flags” which mark locations in them that correspond in terms of the “same” locations. Opened images use the flags in the reference image and are corrected (using the warp function) geometrically, to match the target image flags. The process is to open the images, correct linear distortion in the Y direction (due to foreshortening) and then the non-linear distortion. The red component is extracted and the image inverted and rotated, then saved.

Flags in V++ are represented by a cross on the image and their location is defined by Cartesian coordinates. The function “getflags(image)” returns a $2 \times n$ array of values where the 1st column (0) contains the x values, the 2nd column (1) contains y values, and each row represents the flag (n). The flags are referenced in order from 0 to $n-1$.

```

button btn_text, 'process images';
var
  img, ref, distort;
  sFactor;
  Coeff ;
  SrcPts ;
  RefPts ;
const
  //DPIscaleFactor=0.2189;// 500DPI
  DPIscaleFactor=0.4378;// 1000DPI

begin
  sFactor:=val(ReadPrivateIniString( 'c:\test\camera_image_conversion.ini',
  'scale_factor', 'sFact') ) ;

  if not imageExists('C:\test\ref grid.tif' ) then OpenTodesktop(
  'C:\test\ref grid.tif' ) ;

  GetImage('ref grid.tif',ref); minimize(ref);
  if not imageExists('C:\test\resized mm grid.tif' ) then OpenTodesktop(
  'C:\test\resized mm grid.tif' );

  GetImage('resized mm grid.tif',distort); minimize(distort);

  RefPts := GetFlags( ref ) ;
  SrcPts:= getFlags(distort);

  GetFirstImage( Img ) ;
  while IsImage( Img ) do
    begin
      if (getname(img)<>'resized mm grid') and (getname(img)<>'ref grid')then
      begin
        img:=zoomby(img,1,sFactor);
        if isnull(SrcPts) then writeln('srcpts');
        if isnull(RefPts) then writeln('RefPts');
        Coeff := SolveWarp( SrcPts,RefPts,3 ) ;
        Img := Warp( Img,Coeff ) ;
        img := Rotate90( img,1 );
        img:=zoomto(img,integer(getxsize(img)*DPIscaleFactor),integer(getysize(i
mg)*DPIscaleFactor));

        img := Red( img ) ;
        img := not img ;
        SetDisplayMode( img,dm_Histogram ) ;
        ShowFullFrame( img ) ;

        save(img,'H:\masters\data collection\image data\within source
images\lateral forward\' +getname(img)+'.tif');
      end;
      free(img);
      GetNextImage( Img ) ;
    end;
  end
end

```

place a button on the toolbar
define variables for script

start of script

open distortion target image

open distortion reference image

get flag locations for the reference
get flag locations for the target

process each fingerprint image open

resize image in y dim by sFactor
check for presence of flags

correct non-linear distortion
rotate image 90 degrees

scale to 1000 DPI
extract red component only
tonally invert image
contrast image by histogram range
fit image to screen (display only)

save image

free the image variable for re-use

7.2.2 Get NAFIS sub images

Summary

This script takes a captured AFIS screen containing the result of a AFIS search. It contains two images; a search image and a candidate that the AFIS has nominated as possible being from the same source. The image is flipped horizontally as all images captured in this project are reversed, due to the image capture in the prism. Both images are extracted from the screen images, resized to 1000 DPI and saved.

```

button btn_text, 'get sub images';
var

    Img, Img1, Img2, copy ;

begin

    GetActiveImage(Img) ;                                get the active image
    copy:=img;                                           make a copy of the image
    copy := ZoomBy(copy, 1.97, 1.97 ) ;                 resize to 1000 DPI
    copy := Reflect( copy, ref_Horiz ) ;                mirror the image horizontally
    img1:= copy[179..1340, 251..1530] ;                 extract a section (candidate print)
    show(img1, getname(img)+ ' b' );
    save(img1, 'H:\masters\data collection\image data\between-source
images\searches based on comber scan\' + getname(img1) + '.tif');
                                                         save candidate image
    img2:= copy[1359..2520, 251..1530] ;                 extract a section (search print)
    show(img2, getname(img)+ ' w' );
    save(img2, 'H:\masters\data collection\image data\between-source
images\searches based on comber scan\' + getname(img2) + '.tif');
                                                         save search image
    delete(img);                                         delete images
    delete(img1);
    delete(img2);
    free(copy);
end

```

7.2.3 Create Distance Map

Summary

This script takes creates an image whose pixel values are derived from the order of all flags (0 to n-1) in an image. This is discussed in Chapter 3 and is shown in Figure 28. The script creates a square image of sides the size equal to the number of flags placed on the image. The script creates a temporary image “pointdist” that will contain all of the distances between each flag to all other flags. A row n in pointdist contains the distances from flag n to all other flags. Each row is extracted and sorted from smallest value to largest, thereby indicating which flags are closest to the flag in question. This row is assigned to a variable “sorted”. Another image “ordereddist” is created into which all the “sorted” rows are inserted. The left most value in each row of ordereddist contains the sequential number (0 to n-1) of the flags and the other values in the rows contain the other flags numbers in order of closest most distant. In V++, any functions or procedures exist before the start of the script.

```
button btn_text, 'create distance map';
```

```
var
img, copyimg;
flags;
i, j, p, f;
a1, a2;
pointdist, ordereddist, sorted;
temp, numpts;
ed;
```

```
procedure sortvalues(values);
```

```
var
mx, mn, a, b, mark;
begin
sorted:=byte(values-values);
mx:=maxof(values)+1;
for a:=0to getxsize(values)-1do
  begin
    mn:=mx;
    mark:=getxsize(values)-1;
    for b:=0to getxsize(values)-1do
      begin
        if values[b,0]<mn then
          begin
            mn:=values[b,0];
            mark:=b;
          end;
      end;
    end;
```

sort the distances for extracted row
define variables for procedure

conduct a bubble sort

```

end;
sorted[a,0]:=mark;
values[mark,0]:=mx;
end;
end;

begin start of script
f:=pi/180;
getactiveimage(img);

flags:=getflags(img);
if getysize(flags)<1 then halt('no flags marked');

pointdist:=Createimage( typ_single,getysize(flags) , getysize(flags) ) ;
create pointdist image
ordereddist:=CreateArray( typ_single,getysize(flags) , getysize(flags) ) ;
create ordereddist image

for j:=0to getysize(flags)-1do fill pointdist with distance values
begin
for i:=0to getysize(flags)-1do
begin
pointdist[j,i]:=sqrt(sqr(flags[0,j]-flags[0,i])+sqr(flags[1,j]-
flags[1,i]));
end;
end;

for i:=0to getysize(flags)-1do fill ordereddist with distance values
begin
writestatus('Sorting...' + str((getysize(flags)-1)-i) + ' to go');
temp:=pointdist[..,i]; extract row from pointdist
sortvalues(temp); order values
ordereddist[..,i]:=sorted; place ordered row into ordereddist
end;

show(ordereddist,'distances'); show ordereddist on desktop
free(pointdist);
free(ordereddist);
free(img);
free(copyimg);
end.

```


7.2.4 get 2 coords for 10 minutiae matlab output training data

Summary

This script generates training data from a reference image and a selection of images of fingerprints with induced distortion. Measurements are taken for D1, D2 and A for the reference image and then all other images. The order of the minutiae measured is determined by a distance map “distances” which needs to be generated from the reference image before running this script. The measurements are output to an “editor” which is a plain text window that can be edited, cut, copied and pasted to. The editor contents are finally copied to the Windows clipboard for pasting into Excel if required, and also saved as comma separated values. The CSV file is later opened by Matlab for the calculation of means and covariances.

```

button btn_text, 'get nearest 2 coords';

var
img, copyimg, ref;
flagsimg;
i, j;
ordereddist, orderedlist;
temp, numpts, nextPt;
ed;
D1, D2, A1, A2, Adiff;
intX, intY;
dist, new, closex, closey, flagnum;
meanx, meany;

procedure getCentroid;                                procedure to locate centroid x and y
    begin
        if getysize(img)>getxsize(img) then dist:=getysize(img) else
dist:=getxsize(img);
        for i:=0to getysize(flagsimg)-1do
            begin
                meanx:=meanx+flagsimg[0,i];
                meany:=meany+flagsimg[1,i];
            end;
        meanx:=integer(meanx/getysize(flagsimg));
        meany:=integer(meny/getysize(flagsimg));
    end;

procedure getNearestMinutia;                            procedure to locate central minutia
    begin
        for i:=0to getysize(flagsimg)-1do
            begin
                new:=sqrt(sqr(flagsimg[0,i]-meanx)+sqr(flagsimg[1,i]-meany));
                if new<dist then
                    begin

```

```

        dist:=new;
        flagnum:=i;
    end;
end;
writeln('Centroid minutia is ',+str(flagnum));
write centroid minutiae to text editor
end;

function getangle(x1,y1,x2,y2);
var
    retValue;
    dist1,dist2;
begin
    dist1:=single(abs(x1-x2)); if dist1=0 then dist1:=1;
    dist2:=single(abs(y1-y2));

    if ((x1=x2) and (y1>y2)) then
retValue:=arctan(dist2/dist1)/(pi/180)
    else
    if ((x1<x2) and (y1>y2)) then retValue:=arctan(dist2/dist1)/(pi/180)
    else
    if ((x1<x2) and (y1=y2)) then retValue:=arctan(dist2/dist1)/(pi/180)
    else
    if ((x1<x2) and (y1<y2)) then retValue:=360-
(arctan(dist2/dist1)/(pi/180))
    else
    if ((x1=x2) and (y1<y2)) then retValue:=360-
(arctan(dist2/dist1)/(pi/180))
    else
    if ((x1>x2) and (y1<y2)) then
retValue:=180+(arctan(dist2/dist1)/(pi/180))
    else
    if ((x1>x2) and (y1=y2)) then
retValue:=180+(arctan(dist2/dist1)/(pi/180))
    else
    if ((x1>x2) and (y1>y2)) then retValue:=180-
(arctan(dist2/dist1)/(pi/180))
    else
    if ((x1=x2) and (y1=y2)) then retValue:=0;
        getangle:=retValue;
    end;

procedure measure;
begin
    for j:=0 to 9 do
    begin
        D1:=integer(sqrt(sqr(flagsImg[0,orderedlist[j]]-
flagsimg[0,ordereddist[1,orderedlist[j]])+
sqr(flagsImg[1,orderedlist[j]]-
flagsimg[1,ordereddist[1,orderedlist[j]]]));
        write(ed,D1,',');

        D2:=integer(sqrt(sqr(flagsImg[0,orderedlist[j]]-
flagsimg[0,ordereddist[2,orderedlist[j]])+
sqr(flagsImg[1,orderedlist[j]]-
flagsimg[1,ordereddist[2,orderedlist[j]]]));
        write(ed,D2,',');

        A1:=integer(getangle(flagsImg[0,orderedlist[j]],

```

```

        flagsImg[1,orderedlist[j]],
        flagsimg[0,ordereddist[1,orderedlist[j]]],
        flagsimg[1,ordereddist[1,orderedlist[j]]]);
    A2:=integer(getangle(flagsImg[0,orderedlist[j]],
        flagsImg[1,orderedlist[j]],
        flagsimg[0,ordereddist[2,orderedlist[j]]],
        flagsimg[1,ordereddist[2,orderedlist[j]]]));
    ADiff:=abs(A1-A2);
    if ADiff>180then ADiff:=360-ADiff;
    write(ed,ADiff,',');
end;
    writeln(ed);

end;

begin_____start of script

selectimage('get reference image',img);           select reference image
flagsImg:=getflags(img);
getimage('distances',ordereddist);               get distances image

meanx:=0; meany:=0;
getCentroid;                                     determine centroid point

getNearestMinutia;                               get nearest minutia to centroid

orderedlist:=integer(ordereddist[0..9,flagnum]);

ed:=createEditor('training data for '+getname(img),800,0,1000,500);
                                                    create editor to receive values

for i:=1to10do
    begin                                         write text output header
        write(ed,'M'+str(i)+'D1',' ','M'+str(i)+'D2',' ','M'+str(i)+'A',' ');
    end;
    writeln(ed);

measure;                                         measure D1,D2 and A for reference
delete(img);
free(img);

    selectimage('get next image', Img );         select distorted image
while IsImage( Img ) do
begin
    writeln(getname(img));
    flagsImg:=getflags(img);
    measure;                                     measure D1,D2 and A for all images

    delete(img);                                delete selected image
    free(img);                                   free variable for re-use
    selectimage('get next image', Img );         select next distorted image
end;

copyToClipboard(ed);                             copy editor content to clipboard
writestatus('');
free(ordereddist);
free(img);

delete(orderedlist);

```

```
save(ed, 'C:\Documents and Settings\BC\Desktop\values2.csv');  
                                     save editor as csv file  
  
end.
```

7.2.5 get 2 coords for all minutiae matlab output training data2

Summary

This script generates data from a reference image to be tested against data from a compared candidate image. Measurements are taken for D1, D2 and A. The order of the minutiae measured is determined by a distance map “distances” which needs to be generated from the reference image before running this script. The measurements are output to an editor. The CSV file is later opened by Matlab for the calculation probability density that the compared images are from the same source.

```

button btn_text, 'get number coords training';

var
img, copyimg, ref;
flagsImg, numFlags;
i, j, k;
ordereddist, orderedlist;
temp, numpts, nextPt;
ed;
D1, D2, A1, A2, Adiff;
intX, intY;
dist, new, closex, closey, flagnum;
meanx, meany;
name;

procedure getCentroid;
    begin
        if getysize(img) > getxsize(img) then dist := getysize(img) else
dist := getxsize(img);
        for i := 0 to getysize(flagsimg) - 1 do
            begin
                meanx := meanx + flagsimg[0, i];
                meany := meany + flagsimg[1, i];
            end;
        meanx := integer(meanx / getysize(flagsimg));
        meany := integer(meany / getysize(flagsimg));
    end;

procedure getNearestMinutia;
    begin
        for i := 0 to getysize(flagsimg) - 1 do
            begin
                new := sqrt(sqr(flagsimg[0, i] - meanx) + sqr(flagsimg[1, i] -
meanx));
                if new < dist then
                    begin
                        dist := new;
                        flagnum := i;
                    end;
            end;
    end;

```

```

end;
    writeln('Centroid minutia is ',+str(flagnum));;
end;

function getangle(x1,y1,x2,y2);
    var
        retValue;
        dist1,dist2;
    begin
        dist1:=single(abs(x1-x2)); if dist1=0 then dist1:=1;
        dist2:=single(abs(y1-y2));

        if ((x1=x2) and (y1>y2)) then retValue:=arctan(dist2/dist1)/(pi/180)
        else
        if ((x1<x2) and (y1>y2)) then retValue:=arctan(dist2/dist1)/(pi/180)
        else
        if ((x1<x2) and (y1=y2)) then retValue:=arctan(dist2/dist1)/(pi/180)
        else
        if ((x1<x2) and (y1<y2)) then retValue:=360-
(arctan(dist2/dist1)/(pi/180))
        else
        if ((x1=x2) and (y1<y2)) then retValue:=360-
(arctan(dist2/dist1)/(pi/180))
        else
        if ((x1>x2) and (y1<y2)) then
retValue:=180+(arctan(dist2/dist1)/(pi/180))
        else
        if ((x1>x2) and (y1=y2)) then
retValue:=180+(arctan(dist2/dist1)/(pi/180))
        else
        if ((x1>x2) and (y1>y2)) then retValue:=180-
(arctan(dist2/dist1)/(pi/180))
        else
        if ((x1=x2) and (y1=y2)) then retValue:=0
getangle:=retValue;
    end;

procedure measure

    begin

        for j:=0to numpts-1do
        begin
            D1:=integer(sqrt(sqr(flagsImg[0,orderedlist[j]]-
flagsimg[0,ordereddist[1,orderedlist[j]]])+
                sqr(flagsImg[1,orderedlist[j]]-
flagsimg[1,ordereddist[1,orderedlist[j]]])));
            write(ed,D1,',');

            D2:=integer(sqrt(sqr(flagsImg[0,orderedlist[j]]-
flagsimg[0,ordereddist[2,orderedlist[j]]])+
                sqr(flagsImg[1,orderedlist[j]]-
flagsimg[1,ordereddist[2,orderedlist[j]]])));
            write(ed,D2,',');

            A1:=integer(getangle(flagsImg[0,orderedlist[j]],
                flagsImg[1,orderedlist[j]],
                flagsimg[0,ordereddist[1,orderedlist[j]]],
                flagsimg[1,ordereddist[1,orderedlist[j]]]));

```

```

        A2:=integer(getangle(flagsImg[0,orderedlist[j]],
                           flagsImg[1,orderedlist[j]],
                           flagsimg[0,ordereddist[2,orderedlist[j]]],
                           flagsimg[1,ordereddist[2,orderedlist[j]]]));
        ADiff:=abs(A1-A2);
        if ADiff>180 then ADiff:=360-ADiff;
        write(ed,ADiff,',');
    end;
    writeln(ed);
end;

begin
selectimage('get reference image',img);
name:=getname(img);
flagsImg:=getflags(img);
k:=getysize(flagsImg);

getimage('distances',ordereddist);
meanx:=0; meany:=0;
getCentroid;
getNearestMinutia;
orderedlist:=integer(ordereddist[0..k-1,flagnum]);

for numpts := 1 to k do
begin
ed:=createEditor('training data for '+getname(img)+' '+str(numpts)+'
minutiae',800,0,1000,500);
for i:=1 to numpts do
begin
write(ed,'M'+str(i)+'D1',',',',','M'+str(i)+'D2',',',',','M'+str(i)+'A',',',');
end;
writeln(ed);
measure;
save(ed,'C:\Documents and Settings\Administrator\Desktop\data\' +name+'
'+str(numpts)+' minutiae.csv');
delete(ed);
end;

end.

```

start of script

select known image to measure

get number of flags

get distance map

write text output header

measure and write D1,D2 and A

save editor as csv file

7.2.6 get 2 coords for all minutiae matlab output training data2 test case

Summary

This script generates data from a candidate image to be tested against data from a compared reference image. Measurements are taken for D1, D2 and A. The order of the minutiae measured is determined by the same distance map “distances” that was used in the measurement of the reference image. The measurements are output to an editor. The CSV file is later opened by Matlab for the calculation probability density that the compared images are from the same source.

```

button btn_text, 'get number coords test';

var
img,copyimg,ref;
flagsImg, numFlags;
i,j,k;
ordereddist, orderedlist;
temp, numpts, nextPt;
ed;
D1,D2,A1,A2,Adiff;
intX,intY;
dist, new, closex, closey, flagnum;
meanx, meany;
name;

procedure getCentroid;
    begin
        if getysize(img)>getxsize(img) then dist:=getysize(img) else
dist:=getxsize(img);
        for i:=0to getysize(flagsimg)-1do
            begin
                meanx:=meanx+flagsimg[0,i];
                meany:=meany+flagsimg[1,i];
            end;
            meanx:=integer(meanx/getysize(flagsimg));
            meany:=integer(meany/getysize(flagsimg));
        end;

procedure getNearestMinutia;
    begin
        for i:=0to getysize(flagsimg)-1do
            begin
                new:=sqrt(sqr(flagsimg[0,i]-meanx)+sqr(flagsimg[1,i]-
meany));
                if new<dist then
                    begin
                        dist:=new;
                        flagnum:=i;
                    end
            end
        end
    end

```



```

        end;
    end;
end;

function getangle(x1,y1,x2,y2);
var
    retValue;
    dist1,dist2;
begin
    dist1:=single(abs(x1-x2)); if dist1=0 then dist1:=1;
    dist2:=single(abs(y1-y2));

    if ((x1=x2) and (y1>y2)) then retValue:=arctan(dist2/dist1)/(pi/180)
    else
    if ((x1<x2) and (y1>y2)) then retValue:=arctan(dist2/dist1)/(pi/180)
    else
    if ((x1<x2) and (y1=y2)) then retValue:=arctan(dist2/dist1)/(pi/180)
    else
    if ((x1<x2) and (y1<y2)) then retValue:=360-
(arctan(dist2/dist1)/(pi/180))
    else
    if ((x1=x2) and (y1<y2)) then retValue:=360-
(arctan(dist2/dist1)/(pi/180))
    else
    if ((x1>x2) and (y1<y2)) then
retValue:=180+(arctan(dist2/dist1)/(pi/180))
    else
    if ((x1>x2) and (y1=y2)) then
retValue:=180+(arctan(dist2/dist1)/(pi/180))
    else
    if ((x1>x2) and (y1>y2)) then retValue:=180-
(arctan(dist2/dist1)/(pi/180))
    else
    if ((x1=x2) and (y1=y2)) then retValue:=0;
        getangle:=retValue;
    end;
end;

procedure measure;
begin
    for j:=0 to numpts-1 do
    begin
        D1:=integer(sqrt(sqr(flagsImg[0,orderedlist[j]]-
flagsimg[0,ordereddist[1,orderedlist[j]])+
sqr(flagsImg[1,orderedlist[j]]-
flagsimg[1,ordereddist[1,orderedlist[j]]))));
        write(ed,D1,',');

        D2:=integer(sqrt(sqr(flagsImg[0,orderedlist[j]]-
flagsimg[0,ordereddist[2,orderedlist[j]])+
sqr(flagsImg[1,orderedlist[j]]-
flagsimg[1,ordereddist[2,orderedlist[j]]))));
        write(ed,D2,',');

        A1:=integer(getangle(flagsImg[0,orderedlist[j]],
flagsImg[1,orderedlist[j]],
flagsimg[0,ordereddist[1,orderedlist[j]]],
flagsimg[1,ordereddist[1,orderedlist[j]]]));
        A2:=integer(getangle(flagsImg[0,orderedlist[j]],
flagsImg[1,orderedlist[j]],

```

```

        flagsimg[0,ordereddist[2,orderedlist[j]]],
        flagsimg[1,ordereddist[2,orderedlist[j]]]);
    ADiff:=abs(A1-A2);
    if ADiff>180then ADiff:=360-ADiff;
    write(ed,ADiff,',');
end;
    writeln(ed);
end;

begin_____start of script

selectimage('which image',img);           select candidate image to measure
flagsimg:=getflags(img);
numFlags:=getysize(flagsimg);
k:=numFlags;
getimage('distances',ordereddist);        get distance map
meanx:=0; meany:=0;
getnumber('Centroid minutia?',flagnum);   query user for centroid minutia
orderedlist:=integer(ordereddist[0..k-1,flagnum]);

for numpts := 1to k do                     write text output header
begin
ed:=createEditor('test case '+getname(img)+' '+str(numpts)+'
minutiae',800,0,1000,500);
for i:=1to numpts do
    begin
        write(ed,'M'+str(i)+'D1',',',',','M'+str(i)+'D2',',',',','M'+str(i)+'A',',',',');
    end;
    writeln(ed);
measure;                                  measure and write D1,D2 and A
save(ed,'C:\Documents and Settings\Administrator\Desktop\data\test case
'+getname(img)+' '+str(numpts)+' minutiae.csv');
save editor as csv file

delete(ed);
end;

end.

```

7.2.7 Draw numbers for flags

Summary

This script places a red number on an image where a flag is. The flags are numbered in the order that they have been placed; the first flag numbered 0 and the last numbered $n-1$.

Square_palette.tif is a 3x256 ramp image with values going from 0 to 255 representing the changes from black to white in the three RGB channels. This is used to create a false colour table for an RGB image. The first row has values 255,0,0 which creates the colour red for all pixels in an image to which the table is applied, that have the real value of 0. With the table applied, the numbers in the image appear red. The value of 1 is added to the image so that only the numbers will appear red. This has no impact on the data as the measurements are taken from the flag locations irrespective of the pixel values.

```

button btn_Text, 'draw numbers for flags' ;
var
img;
nf,nc;
flags,Pa11;
copy,temp,letter_img;

const
path='C:\Program Files\Digital Optics\V++\Executable\settings.ini';
chrx=16;                                x dimension of number image
chry=26;                                y dimension of number image

begin
getactiveimage(img);
if typeof(img)=typ_rgb then copy := Intensity( img,cm_XYZ ) ;
if isfloat(img) then                                convert image to 8 bit greyscale
begin
    copy:=img-minof(img);
    copy:=copy/maxof(copy);
    copy:=copy*255;
    converttype(copy,typ_byte);
end;
if isnull(copy) then copy:=img;
copy:=copy+1;

flags:=getflags(img);
if getysize(flags)=0then halt('no flags');

```

```

                                loop over all flags
for nf:=0to getysize(flags)-1do//number of flags
begin
                                build number image for flag
for nc:=1to length(str(nf)) do//number of characters in flag number
begin
    temp:=copy[flags[0,nf]+(chrx*(nc-1))..(flags[0,nf]+(chrx*(nc-
1)))+chrx-1,flags[1,nf]-12..(flags[1,nf]+chry-1)-12];
    Open( 'C:\Program Files\Digital
Optics\V++\scripts\CHARS\' +ExtractStr(str(nf),nc,1)+'.tif',letter_img) ;
    temp:=temp*(letter_img<128);

    copy[flags[0,nf]+(chrx*(nc-1))..(flags[0,nf]+(chrx*(nc-1)))+chrx-
1,flags[1,nf]-12..(flags[1,nf]+chry-1)-12]:=temp;
                                insert built number into the image
end;
end;

show(copy,'copy with flag number');
copy:=copy+1;
                                add the value of 1 to the image
Open( 'C:\Program Files\Digital
Optics\V++\Executable\square_palette.tif',Pall ) ;
SetPalette( copy,Pall ) ;
                                set palette to make numbers red
                                create a copy to save
createdisplayimage(copy);
Free( Pall ) ;
delete(copy);
end

```

7.2.8 Acquire image of finger for pressure test

Summary

This script processes images for friction ridge contact area measurement. The images are corrected for systemic distortion and then normalized by contrasting over the dynamic range for a byte image. The image is finally thresholded at the value of 127, making all values less than 127 black (value 0) and those equal to or above white (value 1) and making the image of a binary type. This type of image is suitable for object analysis.

```

var
  img, ref, distort;
  sFactor;
  Coeff ;
  SrcPts ;
  RefPts ;

const
  //DPIscaleFactor=0.2189;// 500DPI
  DPIscaleFactor=0.4378;// 1000DPI

begin
  sFactor:=val(ReadPrivateIniString( 'c:\test\camera_image_conversion.ini',
  'scale_factor', 'sFact') ) ;                               get scale factor value

  ifnot imageExists('C:\test\ref grid.tif' ) then OpenTodesktop( 'C:\test\ref
  grid.tif' ) ;                               open distortion target image

  GetImage('ref grid.tif',ref); minimize(ref);
  ifnot imageExists('C:\test\resized mm grid.tif' ) then OpenTodesktop(
  'C:\test\resized mm grid.tif' );                               open distortion reference image

  GetImage('resized mm grid.tif',distort); minimize(distort);

  RefPts := GetFlags( ref ) ;
  SrcPts:= getFlags(distort);

  GetFirstImage( Img ) ;                               process each fingerprint image open
while IsImage( Img ) do
begin
  if (getname(img)<>'resized mm grid') and (getname(img)<>'ref grid')then
  begin
    img:=zoomby(img,1,sFactor);
    if isnull(SrcPts) then writeln('srcpts');
    if isnull(RefPts) then writeln('RefPts');
    Coeff := SolveWarp( SrcPts,RefPts,3 ) ;
    Img := Warp( Img,Coeff ) ;                               correct non-linear distortion
    img := Rotate90( img,1 ) ;                               rotate image 90 degrees
    img:=zoomto(img,integer(getxsize(img)*DPIscaleFactor),integer(getysize(i
    mg)*DPIscaleFactor));
  end;
end;

```

```

img := Red( img ) ;
ShowFullFrame( img ) ;
img:=img-minof(img);
img:=img*(single(255)/maxof(img));
converttype(img,typ_byte);
SetDisplayMode( img,dm_Full ) ;
img := ( img >= 127 ) ;
save(img,'H:\masters\data collection\pressure\100 to 5600
1000DPI\' +getname(img)+'.tif');
end;
free(img);
GetNextImage( Img ) ;
end;

delete( ref );
delete( distort ) ;
writeinfo('Complete');
end

```

scale to 1000 DPI
 extract red component only

 contrast image over dynamic range

 threshold the image at value 127
 save image

 free the image variable for re-use

7.2.9 get finger contact area

Summary

This script takes a pre-processed image and calculates contact area. This is done by using the “AnalyzeImage” function, which makes many measurements of each white (in this case) object. One of these measurements is area. The area for each white object in the image is measured and a total area accumulated. As the white parts of the image constitute contact of the friction ridges, the summed area is representative of the contact area.

```

button btn_text, 'get area';
var
    Img, Obj ;
    i, j;
    area;
begin
    GetActiveImage( Img ) ;
    Obj := AnalyzeImage( Img, Img, obj_White ) ;
    area:=0;
    for i:=0 to getysize(obj)-1 do
        begin
            area:=area+obj[obj_area,i];
        end;
    writeln(getname(img), ' ', area);
end

```

measure all white objects in image

accumulate all object areas

output to text the total area

7.2.10 move random direction fixed amount

Summary

This script copies an image containing flags and repositions the flags up to a specified distance from their initial location. The user is queried for a change of distance and then the flags are reset in a “random” direction, according to a random value being generated. If the value generated is less than 0.5 for the xcoordinate, then the distance moved is subtracted from the x coordinate of the flag, otherwise the distance is added to the x coordinate value. The same is applied to the y coordinate. This script is used to generate an image that simulates a carelessly marked comparison, for the purpose of seeing what effect there is on the calculated probability density.

```

button btn_text, 'move flags random';
var
img, copy;
flags;
i;
x,y,dist;

begin
getactiveimage(img);
copy:=img;
getnumber('move flags by how much?',dist);

show(copy,getname(img)+' '+str(dist));
flags:=getflags(img);

for i:=0to getysize(flags)-1do
  begin
    x:=random;
    y:=random;

    if x>0.5then x:=flags[0,i]+dist else x:=flags[0,i]-dist;
    if y>0.5then y:=flags[1,i]+dist else y:=flags[1,i]-dist;
    setflag(copy,x,y);
  end;
end

```

duplicate image
query user – how much movement?

show duplicate of image and rename

loop over all flags

get random x movement value
get random y movement value

set the flag on the new image

7.2.11 move one flag

Summary

This script copies an image containing flags and repositions one flag up to a specified distance from its initial location. The direction of the movement is determined by the random number generated as per the previous script.

This script is used to generate an image that simulates a carelessly marked comparison, for the purpose of seeing the effect on the calculated probability density of one poorly marked minutia.

```

button btn_text, 'move one flag';
var
img, copy;
flags;
i, j;
x, y, num;

const
dist=10;                                flag movement is a set constant

begin
getactiveimage(img);
copy:=img;
flags:=getflags(img);
getnumber('which flag ('+str(getysize(flags))+')?', num);
                                                    user nominates which flag to move
show(copy, getname(img)+' '+str(num)+' '+str(dist));

for i:=0 to getysize(flags)-1 do
  begin
    x:=random;
    y:=random;
    if i=num then
      begin
        if x>0.5 then x:=flags[0,i]+dist else x:=flags[0,i]-dist;
        if y>0.5 then y:=flags[1,i]+dist else y:=flags[1,i]-dist;;
      end
    else
      begin
        x:=flags[0,i];
        y:=flags[1,i];
      end;
    setflag(copy, x, y);
  end;
end

```

7.2.12 swap two flags

Summary

This script copies an image containing flags and repositions two specified flags by swapping their x and y coordinates. This script is used to generate an image that simulates comparison where not all of the minutiae are marked in the same order, for the purpose of seeing what effect there is on the calculated probability density. In this instance only two minutiae have been marked in the wrong order.

```

button btn_text, 'swap two flags';
var
img, copy;
flags;
i, j;
x1, y1, x2, y2, num1, num2;

const
dist=10;

begin
getactiveimage(img);
copy:=img;
flags:=getflags(img);
getnumber('first flag?', num1);
getnumber('second flag?', num2);
x1:=flags[0, num1]; y1:=flags[1, num1]; x2:=flags[0, num2]; y2:=flags[1, num2];

show(copy, getname(img) + ' ' + str(num1) + ' swapped with ' + str(num2));

for i:=0 to getysize(flags)-1 do
begin
if i=num1 then
begin
setflag(copy, flags[0, num2], flags[1, num2]);
end
else
if i=num2 then
begin
setflag(copy, flags[0, num1], flags[1, num1]);
end
else
begin
end;

setflag(copy, flags[0, i], flags[1, i]);
end;
end

```

which 1st flag to swap
which 2nd flag to swap

if 1st flag then swap

if 2nd flag then swap

7.3 Matlab scripts

7.3.1 csv input from V++ 2 no abs_18 values

Summary

This script opens the CSV file for a finger containing measured reference and distorted image data. The values in the second to the last row are subtracted from the first row (reference data) to form an array containing the differences in the data between all distorted images and the reference image. The difference values are used to calculate and output as XLS files, the covariance, mean and difference of the values.

```

data=xlsread('BC_RI_ref.csv');           read csv file
% get differences between first and all other rows...then get the means
temp=data(1,:)-data(2,:);               assign differences to "temp"
diffData=temp;
for i=3 : 19
    temp=data(1,:)-data(i,:);           assign more differences to "temp"
    diffData=cat(1,diffData,temp);       accumulate differences in "diffData"
end
mu=mean(diffData)';% produces 30x1 mean  calculate mean vector

sigma=eye(30); % produces 30x30 cov matrix  create 30x30 identity matrix
for i=1:10;    % 10 steps of three
    a=(i*3)-2;    % eg: from 1 to 3, 4 to 6, etc
    b=i*3;
    % fill matrix with covariance values
    tempData=diffData(:,a:a+2);% fill the identity matrix diagonal values
    first
    tempCov=cov(tempData);    % for each diagonal group of 3x3
    sigma(a,a)=tempCov(1,1);
    sigma(a+1,a+1)=tempCov(2,2);
    sigma(a+2,a+2)=tempCov(3,3);

end
xlswrite('sigma 18',sigma)              save covariance matrix
xlswrite('mu 18',mu)                    save mean vector
xlswrite('diffData no abs 18',diffData) save difference data

```

7.3.2 all minutiae data input from max minutiae file 18

Summary

This script opens CSV files containing measured data from two images purporting to contain images from the same source. The names of the CSV files and the number of minutiae marked are entered into the script before running. A generic covariance matrix and a mean vector are then created for the number of minutiae marked. Differences between the data from the two opened CSV files are then calculated to form a test vector “diff”. The test vector is then tested against the generic mean vector and covariance matrix to calculate the probability density of the two images being from within-source.

```

numMin=17;% number of minutiae          enter the number of minutiae
case1name='section of 18 latent 17 minutiae.csv'% within source
                                           known print image CSV file
case2name='test case section of 18 17 minutiae.csv'% between-source
                                           candidate print image CSV file
                                           open both CSV files

case1=xlsread(case1name)';
case2=xlsread(case2name)';

for j=1:numMin                            loop for the number of minutiae
    c1=case1(1:j*3);
    c2=case2(1:j*3);
    sigma=eye(j*3);                      create an identity matrix to populate
    for i=1:j;
        a=(i*3)-2;
        temp=[19.43193 0 0; 0 19.43193 0; 0 0 52.69997];
        sigma(a,a)=temp(1,1);
        sigma(a+1,a+1)=temp(2,2);
        sigma(a+2,a+2)=temp(3,3);
    end
    m=[0;0;0];                            create a mean vector of zeros
    mu=m;
    for i=1 : (j)-1 % produces 30x1 mean
        mu=cat(1,mu,m);
    end

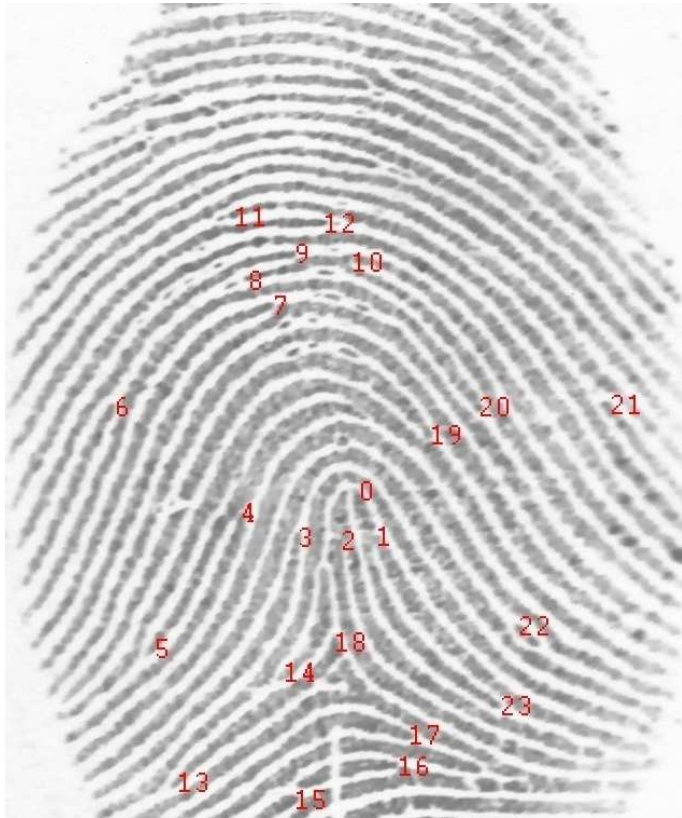
    diff=c1-c2;                            calculate the difference values

    %j
    psame=mvnpdf(diff,mu,sigma)            test difference values against generic mean and covariance
                                           “psame” = probability density of known and candidate images being
within-source
end

```

7.4.0 Data

7.4.1 Sample marked image and coordinate data collected



minutiae number	x coordinate	y coordinate
0	344	542
1	360	584
2	327	588
3	287	585
4	234	562
5	154	688
6	117	464
7	264	370
8	241	347
9	284	322
10	337	330
11	228	288
12	311	294
13	175	812
14	274	710
15	284	828
16	380	797
17	390	768
18	321	682
19	410	490
20	455	464
21	577	462
22	492	667
23	475	741

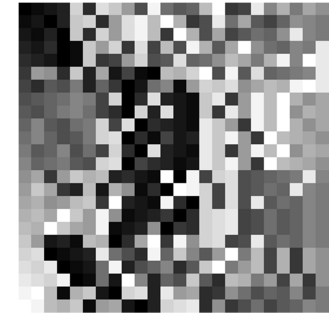
Left index reference image and the marked minutiae numbered. The marked minutiae are to the immediate left of the number.

Coordinates of the marked minutiae

The left index finger reference image with marked minutiae and the Cartesian coordinates of the minutiae as marked.

7.4.2 Sample distance map and values

Minutiae number	Nearest minutia in order of nearest to furthest																						
	1	2	3	4	5	6	7	8	9	10	11	12	13	14	15	16	17	18	19	20	21	22	23
0	1	2	3	19	4	20	18	14	7	22	10	8	9	17	23	5	6	21	12	16	11	15	13
1	2	0	3	18	19	4	14	20	22	17	23	16	5	7	21	10	15	8	6	9	13	12	11
2	1	3	0	18	4	19	14	20	22	17	5	23	16	7	15	6	8	10	9	13	21	12	11
3	2	4	0	1	18	14	19	5	20	6	17	7	22	16	8	15	23	13	10	9	12	11	21
4	3	2	0	1	18	5	6	14	19	7	8	20	9	10	13	17	15	11	16	22	12	23	21
5	14	13	4	18	3	15	2	6	1	0	17	16	19	23	7	22	8	20	9	10	11	12	21
6	4	8	7	11	3	9	5	0	2	10	12	1	14	19	18	20	13	15	17	16	22	23	21
7	8	9	10	12	11	6	19	0	4	20	3	2	1	18	21	5	14	22	17	23	16	13	15
8	7	9	11	12	10	6	4	0	19	3	20	2	1	18	5	21	14	22	17	23	13	16	15
9	12	8	7	10	11	19	6	20	0	4	3	2	1	21	18	14	5	22	17	23	16	13	15
10	12	9	7	8	11	19	20	0	4	1	6	2	3	21	18	22	14	5	23	17	16	15	13
11	8	9	12	7	10	6	19	4	0	20	3	2	1	21	18	5	14	22	17	23	13	16	15
12	9	10	11	8	7	19	20	0	6	4	3	1	2	21	18	22	14	5	23	17	16	15	13
13	15	5	14	18	16	17	3	4	2	1	23	0	22	6	19	20	7	8	9	10	11	21	12
14	18	15	5	3	17	2	16	13	1	4	0	23	22	19	6	20	7	8	10	9	21	12	11
15	16	13	14	17	18	5	23	3	2	1	22	4	0	19	6	20	7	21	8	10	9	12	11
16	17	15	23	18	14	22	13	1	2	3	5	0	4	19	20	21	6	7	10	8	9	12	11
17	16	23	18	15	14	22	1	2	3	13	0	5	4	19	20	21	6	7	10	8	9	12	11
18	14	2	3	1	17	16	0	4	15	23	5	22	13	19	20	6	7	21	8	10	9	12	11
19	20	0	1	2	3	21	10	7	4	22	9	18	12	8	14	23	11	17	6	16	5	15	13
20	19	21	0	1	2	10	22	3	7	9	12	4	8	18	23	11	14	17	6	16	5	15	13
21	20	19	22	0	1	10	2	23	12	3	9	7	18	8	4	17	16	11	14	6	15	5	13
22	23	17	1	16	18	2	0	19	20	3	21	14	15	4	5	13	10	7	9	8	12	6	11
23	22	17	16	18	1	14	15	2	0	3	19	20	21	4	13	5	7	10	6	8	9	12	11



Distance map values and image for the left index finger containing 23 marked minutiae. The values in the 1st column refer to each minutia in order of placement, hence the 1st column in the image being a ramp. The columns refer to the next nearest minutiae from left to right, with the right-most column containing the furthest.

7.4.3 Sample data extracted from a reference image and related movement images

Reference image		M1D1	M1D2	M1A	M2D1	M2D2	M2A	M3D1	M3D2	M3A	M4D1	M4D2	M4A	M5D1	M5D2	M5A	M6D1	M6D2	M6A	M7D1	M7D2	M7A	M8D1	M8D2	M8A	M9D1	M9D2	M9A	M10D1	M10D2	M10A
		32	33	120	32	42	63	33	44	76	40	42	46	44	49	41	35	54	61	57	96	8	64	70	77	51	64	133	29	35	114
Movement images	1	29	41	136	29	41	76	41	47	74	44	41	39	47	53	47	32	63	48	63	108	3	75	68	73	51	75	153	33	32	96
	2	29	44	144	29	34	75	44	44	75	39	34	46	44	54	53	33	65	46	68	107	3	74	68	72	51	74	158	28	33	98
	3	30	42	138	30	33	86	42	51	71	43	33	44	51	54	47	27	63	54	65	107	8	71	63	71	51	71	159	30	27	106
	4	36	27	133	36	42	65	27	36	85	43	42	51	36	43	39	33	57	55	58	101	3	67	68	74	61	67	127	35	33	112
	5	37	30	127	37	39	74	30	45	70	46	39	51	45	45	39	33	57	51	61	106	7	71	66	77	62	71	124	39	33	101
	6	33	29	121	33	41	63	29	35	83	40	41	48	35	43	41	35	59	55	60	100	5	69	67	78	66	69	121	34	35	101
	7	31	31	133	31	38	70	31	32	81	40	38	46	32	41	49	36	59	58	62	102	4	63	71	86	64	63	126	35	36	117
	8	29	35	132	29	36	72	35	33	73	39	36	45	33	41	56	35	61	48	61	99	5	64	75	90	63	64	127	41	35	103
	9	31	26	156	31	38	86	26	47	93	47	38	41	47	55	29	33	67	46	66	113	2	73	71	75	49	73	144	33	33	100
	10	36	31	122	36	40	68	31	45	72	43	40	52	45	46	39	34	65	48	60	102	7	65	67	80	55	65	142	36	34	104
	11	39	27	118	39	44	73	27	44	72	50	44	49	44	43	36	31	59	58	54	102	12	74	71	71	62	74	132	32	31	110
	12	39	33	106	39	43	58	33	48	59	40	43	57	48	42	43	33	60	49	62	101	5	71	70	75	61	71	136	35	33	102
	13	38	29	122	38	44	60	29	41	78	41	44	53	41	44	39	33	57	59	63	104	4	69	73	74	63	69	131	32	33	110
	14	36	31	114	36	41	67	31	47	65	43	41	51	47	44	40	32	59	53	60	101	8	67	66	79	62	67	130	32	32	106
	15	40	24	125	40	42	67	24	42	74	46	42	54	42	42	33	36	57	52	57	102	6	71	70	74	56	71	132	31	36	103
	16	38	24	133	38	41	78	24	42	72	50	41	48	42	41	34	35	62	51	61	110	8	65	69	79	57	65	130	36	35	101
	17	25	46	114	25	38	64	46	49	67	35	38	40	49	51	54	31	55	55	63	97	6	73	71	77	58	73	141	34	31	104
	18	25	41	122	25	36	71	41	48	73	37	36	40	48	53	47	30	60	47	66	101	9	72	67	79	52	72	152	34	30	104

Data extracted from reference image (1st row) of the left index finger and all movement images (subsequent rows) from that finger. The columns refer to the variables D1, D2 and A for each minutia 1 to 10

7.4.4 Sample of the difference data calculated from the reference and movement images

		M1D1	M1D2	M1A	M2D1	M2D2	M2A	M3D1	M3D2	M3A	M4D1	M4D2	M4A	M5D1	M5D2	M5A	M6D1	M6D2	M6A	M7D1	M7D2	M7A	M8D1	M8D2	M8A	M9D1	M9D2	M9A	M10D1	M10D2	M10A
Movement image data subtracted from reference image. Image number:	1	3	-8	-16	3	1	-13	-8	-3	2	-4	1	7	-3	-4	-6	3	-9	13	-6	-12	5	-11	2	4	0	-11	-20	-4	3	18
	2	3	-11	-24	3	8	-12	-11	0	1	1	8	0	0	-5	-12	2	-11	15	-11	-11	5	-10	2	5	0	-10	-25	1	2	16
	3	2	-9	-18	2	9	-23	-9	-7	5	-3	9	2	-7	-5	-6	8	-9	7	-8	-11	0	-7	7	6	0	-7	-26	-1	8	8
	4	-4	6	-13	-4	0	-2	6	8	-9	-3	0	-5	8	6	2	2	-3	6	-1	-5	5	-3	2	3	-10	-3	6	-6	2	2
	5	-5	3	-7	-5	3	-11	3	-1	6	-6	3	-5	-1	4	2	2	-3	10	-4	-10	1	-7	4	0	-11	-7	9	-10	2	13
	6	-1	4	-1	-1	1	0	4	9	-7	0	1	-2	9	6	0	0	-5	6	-3	-4	3	-5	3	-1	-15	-5	12	-5	0	13
	7	1	2	-13	1	4	-7	2	12	-5	0	4	0	12	8	-8	-1	-5	3	-5	-6	4	1	-1	-9	-13	1	7	-6	-1	-3
	8	3	-2	-12	3	6	-9	-2	11	3	1	6	1	11	8	-15	0	-7	13	-4	-3	3	0	-5	-13	-12	0	6	-12	0	11
	9	1	7	-36	1	4	-23	7	-3	-17	-7	4	5	-3	-6	12	2	-13	15	-9	-17	6	-9	-1	2	2	-9	-11	-4	2	14
	10	-4	2	-2	-4	2	-5	2	-1	4	-3	2	-6	-1	3	2	1	-11	13	-3	-6	1	-1	3	-3	-4	-1	-9	-7	1	10
	11	-7	6	2	-7	-2	-10	6	0	4	-10	-2	-3	0	6	5	4	-5	3	3	-6	-4	-10	-1	6	-11	-10	1	-3	4	4
	12	-7	0	14	-7	-1	5	0	-4	17	0	-1	-11	-4	7	-2	2	-6	12	-5	-5	3	-7	0	2	-10	-7	-3	-6	2	12
	13	-6	4	-2	-6	-2	3	4	3	-2	-1	-2	-7	3	5	2	2	-3	2	-6	-8	4	-5	-3	3	-12	-5	2	-3	2	4
	14	-4	2	6	-4	1	-4	2	-3	11	-3	1	-5	-3	5	1	3	-5	8	-3	-5	0	-3	4	-2	-11	-3	3	-3	3	8
	15	-8	9	-5	-8	0	-4	9	2	2	-6	0	-8	2	7	8	-1	-3	9	0	-6	2	-7	0	3	-5	-7	1	-2	-1	11
	16	-6	9	-13	-6	1	-15	9	2	4	-10	1	-2	2	8	7	0	-8	10	-4	-14	0	-1	1	-2	-6	-1	3	-7	0	13
	17	7	-13	6	7	4	-1	-13	-5	9	5	4	6	-5	-2	-13	4	-1	6	-6	-1	2	-9	-1	0	-7	-9	-8	-5	4	10
	18	7	-8	-2	7	6	-8	-8	-4	3	3	6	6	-4	-4	-6	5	-6	14	-9	-5	-1	-8	3	-2	-1	-8	-19	-5	5	10

Values for the differences for the left index finger images obtained by subtracting movement image data from reference image data.

7.4.5 Sample of covariance values returned from Matlab

	M1D1	M1D2	M1A	M2D1	M2D2	M2A	M3D1	M3D2	M3A	.	.	M10D1	M10D2	M10A
M1D1	23.78104 6	0	0	0	0	0	0	0	0	.	.	0	0	0
M1D2	0	49.32352 9	0	0	0	0	0	0	0	.	.	0	0	0
M1A	0	0	143.2026 1	0	0	0	0	0	0	.	.	0	0	0
M2D1	0	0	0	23.78104 6	0	0	0	0	0	.	.	0	0	0
M2D2	0	0	0	0	10.5	0	0	0	0	.	.	0	0	0
M2A	0	0	0	0	0	60.80065 4	0	0	0	.	.	0	0	0
M3D1	0	0	0	0	0	0	49.32352 9	0	0	.	.	0	0	0
M3D2	0	0	0	0	0	0	0	32.22222 2	0	.	.	0	0	0
M3A	0	0	0	0	0	0	0	0	60.09477 1	.	.	0	0	0
.	0	0	0
.	0	0	0
M10D1	0	0	0	0	0	0	0	0	0	0	0	9.398692 8	0	0
M10D2	0	0	0	0	0	0	0	0	0	0	0	0	5.045751 6	0
M10A	0	0	0	0	0	0	0	0	0	0	0	0	0	27.05882 4

Sample of covariance matrix for the difference values for the left index finger images, returned from the Matlab “cov” function. Note that the non-zero values are the variance values for each variable. The zero values represent the covariances, which in each finger’s instances, were insignificant and therefore assigned the zero value.

7.4.6 Sample of mean values returned from Matlab

M1D1	-1.38889
M1D2	0.166667
M1A	-7.55556
M2D1	-1.38889
M2D2	2.5
M2A	-7.72222
M3D1	0.166667
M3D2	0.888889
M3A	1.722222
M4D1	-2.55556
M4D2	2.5
M4A	-1.5
M5D1	0.888889
M5D2	2.611111
M5A	-1.5
M6D1	2.111111
M6D2	-6.27778
M6A	9.166667
M7D1	-4.66667
M7D2	-7.5
M7A	2.166667
M8D1	-5.66667
M8D2	1.055556
M8A	0.111111
M9D1	-7
M9D2	-5.66667
M9A	-3.94444
M10D1	-4.88889
M10D2	2.111111
M10A	9.666667

Average values for the difference values for the left index finger images, returned from the Matlab “mean” function.

7.4.7 Descriptive statistics on means and variances from finger data

		min	average	median	max
angles	mu	-7.72222	0.061111	-0.69444	9.666667
	sigma	6.617647	56.83758	42.5	143.2026
distances	mu	-7.5	-1.6	-0.61111	2.611111
	sigma	5.045752	20.04477	15.54248	49.32353

Descriptive statistics for the variances and means of the difference values as returned from Matlab, with reference to the left index finger. Note the actual mean/median values are close to zero, as they were assigned for probability density calculation.

7.4.8 Generic values for means and variances from finger data

		min	average	median	max
angles	mu	-9.92778	0.650556	1.1	10.17778
	sigma	6.864706	52.69997	43.4134	134.6144
distances	mu	-7.26667	-0.27	0.16667	6.244444
	sigma	4.927451	19.43193	14.4116	58.53072

Descriptive statistics for the variances and means of the difference values as returned from Matlab for all fingers. The values highlighted in red are those used in the generic covariance matrix.

7.4.9 Example of test within-source and another within-source image



Compared left index finger and a within-source candidate

7.4.10 Example of test within-source and other within-source data

	M1D1	M1D2	M1A	M2D1	M2D2	M2A	M3D1	M3D2	M3A
Reference image	40	42	41	29	40	72	29	42	67
Candidate image	39	42	44	31	39	74	31	42	62
	M4D1	M4D2	M4A	M5D1	M5D2	M5A	M6D1	M6D2	M6A
Reference image	53	86	166	56	102	123	53	119	154
Candidate image	64	87	161	71	72	125	64	115	178
	M7D1	M7D2	M7A	M8D1	M8D2	M8A	M9D1	M9D2	M9A
Reference image	56	115	117	31	86	135	73	142	30
Candidate image	71	86	117	30	95	147	66	146	30
	M10D1	M10D2	M10A	M11D1	M11D2	M11A	M12D1	M12D2	M12A
Reference image	39	47	158	31	123	52	73	86	125
Candidate image	40	59	149	30	107	71	66	95	129
	M13D1	M13D2	M13A	M14D1	M14D2	M14A	M15D1	M15D2	M15A
Reference image	59	47	77	39	83	54	115	108	78
Candidate image	50	59	81	40	91	50	86	112	78
	M16D1	M16D2	M16A	M17D1	M17D2	M17A	M18D1	M18D2	M18A
Reference image	124	125	68	174	210	15	59	67	43
Candidate image	113	149	55	140	166	16	50	71	55
	M19D1	M19D2	M19A	M20D1	M20D2	M20A			
Reference image	119	169	8	108	124	110			
Candidate image	115	180	1	112	113	119			

Example reference and test data for a within-source (candidate) comparison of 20 minutiae.

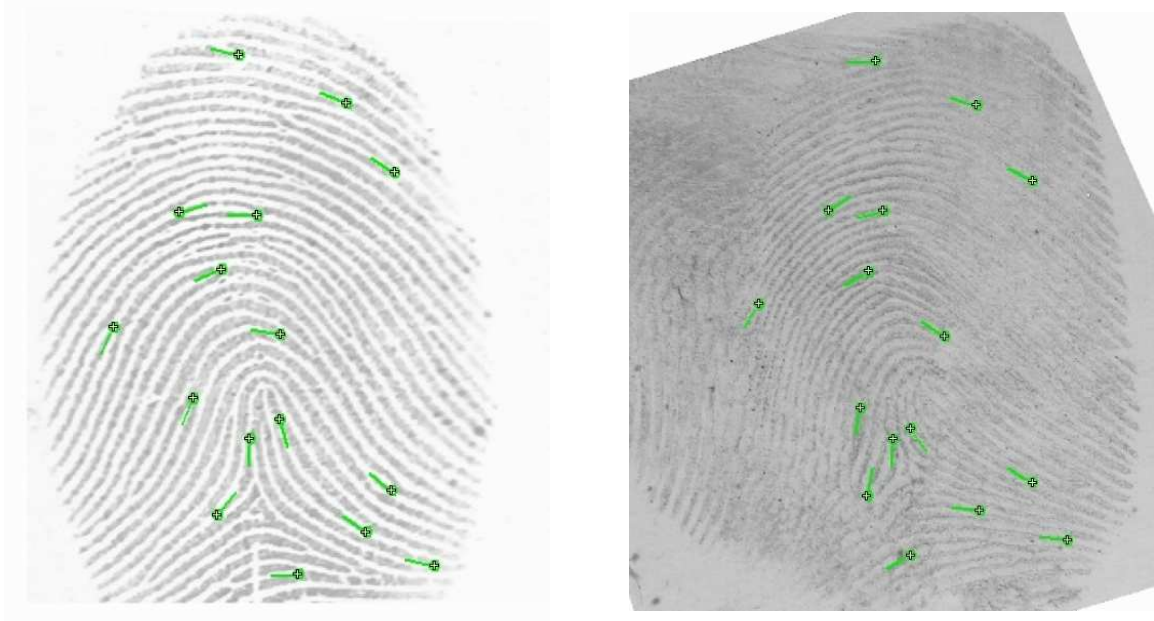
The values shown are the raw measurements taken for each variable. To calculate the probabilities, the data (above) is input into Matlab, the differences calculated, and then those differences compared against the generic mean and variances.

7.4.11 Example of probabilities calculated for a within-source comparison for varied numbers of minutiae

Number of minutiae	Probability density that samples are from the same source
1	4.03E-04
2	1.53E-07
3	4.92E-11
4	7.56E-16
5	8.79E-32
6	4.93E-39
7	2.72E-54
8	3.78E-59
9	3.19E-63
10	1.60E-68
11	3.14E-76
12	4.29E-81
13	5.07E-87
14	3.68E-91
15	4.39E-104
16	6.47E-116
17	8.09E-154
18	7.65E-159
19	6.37E-164
20	3.92E-169

The probabilities that the samples in Section 7.4.9 are from the same source, for an increasing number of minutiae. In this instance the compared images are from the same left index finger.

7.4.12 Example of test within-source and between-source images



Compared left index finger and an AFIS nominated between-source candidate

7.4.13 Example of test within-source and between-source data

	M1D1	M1D2	M1A	M2D1	M2D2	M2A	M3D1	M3D2	M3A
Reference image	118	121	137	48	118	123	90	98	69
Candidate image	142	145	110	29	142	141	91	106	47
	M4D1	M4D2	M4A	M5D1	M5D2	M5A	M6D1	M6D2	M6A
Reference image	96	123	21	48	96	112	90	108	59
Candidate image	65	78	21	29	65	106	91	80	76
	M7D1	M7D2	M7A	M8D1	M8D2	M8A	M9D1	M9D2	M9A
Reference image	98	108	52	147	169	70	115	139	103
Candidate image	106	80	57	212	166	62	91	108	118
	M10D1	M10D2	M10A	M11D1	M11D2	M11A	M12D1	M12D2	M12A
Reference image	68	120	61	117	199	73	68	105	85
Candidate image	87	98	93	136	221	65	87	135	47
	M13D1	M13D2	M13A	M14D1	M14D2	M14A	M15D1	M15D2	M15A
Reference image	117	164	149	110	139	111	105	120	34
Candidate image	136	160	150	119	108	93	135	98	40
	M16D1	M16D2	M16A						
Reference image	164	223	59						
Candidate image	160	218	64						

Example reference and test data for a between-source (candidate) comparison of 16 minutiae.

7.4.14 Example of probabilities calculated for a between-source comparison for varied numbers of minutiae

Number of minutiae	Probability density that samples are from the same source
1	5.97E-20
2	4.20E-35
3	3.60E-41
4	6.95E-78
5	3.75E-96
6	1.84E-109
7	2.18E-122
8	2.59E-173
9	9.21E-195
10	9.03E-212
11	7.99E-225
12	3.27E-248
13	8.93E-256
14	4.22E-272
15	4.62E-291
16	5.71E-295

The probabilities that the samples in 7.4.12 are from the same source, for an increasing number of minutiae. In this instance the compared images are from the left index finger and an AFIS nominated between-source candidate.

7.5 DVD contents

Note that images from persons not being the donor in this research have not been included. If there is a specific requirement for these images the author must be contacted to obtain permission and these images.

Folder	Contents
--------	----------

7.5.1 Data collection

- | | |
|---|---|
| <ul style="list-style-type: none"> • Comparisons <ul style="list-style-type: none"> ○ All minutiae comparison data ○ All minutiae comparison output ○ Test cases compared to slopes ○ Testing of sensitivity and moved minutiae | <p>Summaries of all within- and between-source probabilities for incrementing numbers of minutiae. See Excel spread sheets “all cases data (log) 18” and “all me (log) 18”. This data was the basis for the slopes for the mean probabilities.</p> <p>Probabilities for incrementing numbers of minutiae for each comparison, for within and between-source comparisons. “between-source 18” for between-source “ and “me 18” for within-source.</p> <p>Predicted mean slopes for within- and between-source cases and all test cases plotted against the slopes. See Excel spread sheet “predicted means for within & between-source 3”.</p> <p>Separate folders containing the experimentation for testing model sensitivity. This folder also contains test images, “17 at 1000 DPL.tif” and “section of 17 at 1000 DPL.tif” being a test latent image, and “17a” and “section of 17a” being the test reference image.</p> |
| <ul style="list-style-type: none"> • Image data <ul style="list-style-type: none"> ○ Reference images ○ Test latents | <p>All reference images used in the research.</p> <p>All latent images as used to test the model. These include AFIS nominated between-</p> |

source cases, further comparisons from the donor (within-source) and known error from www.onin.com

○ Within-source images

All test images from the donor. These are the images of each finger with induced distortion.

In each finger's folder, there are the distortion images, and various Excel spread sheets. The sheet titled "BC_LI_ref" (in this case for the Left Index finger) contains measurements for the reference image in the first row and all movement images in the subsequent rows.

7.5.2 Miscellaneous

- Best case probability density slope Test images and data for calculating the best case scenario (where there are no differences) in which an image is compared with a duplicate of itself. See the Excel spread sheet "best case scenario".
- Calibration image Sample ("resized mm grid.tif") image and target image ("ref grid.tif") for systemic distortion correction.
- Camera config Nikon camera configuration files
- Distance angle function Excel spread sheet showing the calculations for the effect on angle between three minutiae for varied distances between the minutiae.
- File copier Executable and VB source for the file copier/naming application.
- Grid error Excel spread sheet showing the potential error generated when using digital images as the basis for measurement.
- Pressure Images and data for calculating actual pressure on the surface of the skin.

- Test folder from C drive

Ini file for V++ and, reference and target images for systemic distortion correction.

7.5.3 Scripts

- Process 10

V++ scripts and Matlab scripts